Confinement of Non-neutral Plasmas in Stellarator Magnetic Surfaces

Paul Brenner

SUBMITTED IN PARTIAL FULFILLMENT OF THE

REQUIREMENTS FOR THE DEGREE

OF DOCTOR OF PHILOSOPHY

IN THE GRADUATE SCHOOL OF ARTS AND SCIENCES

Columbia University

2011

Abstract

Confinement of Non-neutral Plasmas in Stellarator Magnetic Surfaces

Paul Brenner

The Columbia Non-neutral Torus (CNT) is the first experiment designed to create and study small Debye length non-neutral plasmas confined by magnetic surfaces. This thesis describes experimental confinement studies of non-neutral plasmas on magnetic surfaces in CNT.

Open orbits exist in CNT resulting in electron loss rates that are much faster than initially predicted. For this reason a conforming boundary was designed and installed to address what is believed to be the primary cause of open orbits: the existence of a sizable mismatch between the electrostatic potential surfaces and the magnetic surfaces. After installation a record confinement time of 337 ms was measured, more than an order of magnitude improvement over the previous 20 ms record. This improvement was a combination of the predicted improvement in orbit quality, a reduced Debye length that resulted in decreased transport due to the perturbing insulated rods, and improved operating parameters not indicative of any new physics.

The perturbation caused by the insulated rods that hold emitters on axis in CNT is a source of electron transport and would provide a loss mechanism for positrons in future positron-electron plasma experiments. For these reasons an emitter capable of creating plasmas then being removed faster than the confinement time was built and installed. Measurements of plasma decay after emitter retraction indicate that ion accumulation reduces the length of time that plasmas are confined. Plasmas have been measured after retraction with decay times as long as 92 ms after the emitter has left the last closed flux surface.

Experimental observations show that obstructing one side of an emitting filament with a nearby insulator substantially improves confinement. As a result, experiments have been performed to determine whether a two stream instability affects confinement in CNT. Results indicate that the improvement is not caused by reducing a two stream instability. Instead, the improvement is a result of altering the sheath of the emitting filament which allows the plasma to reach an equilibrium state with improved confinement. These measurements agree with confinement times for plasmas created by unobstructed emission that are in the same

improved confinement state.

Contents

List of Figures

List of Tables

I would like to thank my advisor Thomas Pedersen and everyone that I worked on CNT with especially Xabier Sarasola, Benoit Durand de Gevigney, Mike Hahn, Jack Berkery, Quinn Marksteiner, Remi Lefrancois and all of the undergraduates who I put to work over the years especially Peter Traverso, Derek Hernandez, Seth Davidovits, Emma Cramer, Scott Massidda, Paul Ennever, Joanna Corby, Josh Narciso, and Dennis Boyd. I would also like to thank professors Michael Mauel and Gerald Navratil for their valuable suggestions and ideas as members of my committee. Many experiments described in this thesis would not have been possible without Xabi's long arms so I thank Spain for that. PhDs take a long time and I had further support from everyone in the plasma lab, my class in the APAM department, my family, Sixpoint brewery, five hour energy, and the internet.

Of course, I owe the most thanks of all to Mary Lee.

Chapter 1

Introduction

This thesis describes experimental confinement studies of non-neutral plasmas on magnetic surfaces in the Columbia Non-neutral Torus (CNT). CNT is a stellarator dedicated to systematic studies of non-neutral plasmas [80]. While magnetic surface configurations, such as the stellarator, have been used to confine quasi-neutral plasmas for over 50 years [91], they have not been used to study non-neutral plasmas until recently [44, 46, 80]. This thesis focuses on efforts to understand and reduce transport in CNT plasmas. In addition to gaining insight into the underlying physics, these efforts aimed at a specific application: laying the groundwork for an experiment capable of creating and studying electron-positron plasmas [80, 81]. The mass symmetry of electron-positron plasmas makes them simpler to study numerically and analytically than standard quasi-neutral plasmas. Electron-positron interactions have been observed experimentally [34] but confined electron-positron plasmas have not yet been studied. The studies of non-neutral plasmas confined on magnetic surfaces in CNT have laid the groundwork for the design of a new experiment that will use magnetic surfaces to confine electron-positron plasmas. The experiments described in this thesis have resulted in an a factor of 16 increase in confinement time for CNT (plasmas from 0.02 seconds to 0.337 seconds) and the creation of plasmas with 0.092 ms decay times after removal of internal objects.

Non-neutral plasmas have been studied for well over 30 years, primarily confined in Penning traps [22,65,77]. However, standard Penning traps are limited to confining particles of one sign of charge. Although nested Penning traps can simultaneously confine both signs

of charge [1, 29], they cannot confine many Debye lengths of positive and negative species simultaneously in the same volume [35]. The purely magnetic confinement of a stellarator can simultaneously confine many Debye lengths of both positive and negative particles. In CNT, magnetic surfaces confine plasmas of various degrees of neutralization, ranging from single species to quasineutral.

Theory predicts that these non-neutral plasmas confined on magnetic surfaces will exhibit fundamentally different equilibrium, stability, and transport than non-neutral plasmas confined in Penning or pure toroidal field traps [80, 82]. The quality of magnetic surfaces in CNT has been verified [84], however the magnetic field configuration is not optimized to prevent trapped particle orbits. Long confinement times are still predicted in these plasmas as a result of the large space charge electric field [6, 80]. The $\mathbf{E} \times \mathbf{B}$ drift resulting from the strong electric field closes trapped particle orbits and reduces the neoclassical transport that would otherwise dominate in an un-optimized stellarator. Similarly, quasi-neutral plasmas in stellarators can benefit from a radial electric field [28]. While the ambipolar electrostatic potential that develops in quasineutral plasmas is on the order of T_e/e, the non-neutral plasmas in CNT are a demonstration of the extreme electric field ($e\Delta\phi/T_e \gg 1$) case for this effect [79]. For a typical experiment, the electrostatic potential, ϕ, in CNT ranges from -200 V on axis to 0 V at the plasma edge and the electron temperature, T_e, is between 2-7 eV resulting in $e\Delta\phi/T_e$ in the range 30 - 100.

First studies of the stability [67] and equilibrium [38] of non-neutral plasmas were performed in CNT prior to this thesis. This thesis focuses on three specific questions pertaining to the confinement of non-neutral plasmas on magnetic surfaces:

- **Can confinement be improved by reducing the mismatch between equipotential and magnetic surfaces?** Simulations predict that a mismatch between equipotential and magnetic surfaces will result in cross field transport [24]. A reduction in the mismatch is predicted when the last closed magnetic flux surface is an equipotential [58]. A conducting boundary designed to conform to the last closed magnetic flux surface was installed to study this effect experimentally. A factor of two reduction in neutral driven transport was measured and is attributed improved orbit quality through greater match between equipotential and magnetic surfaces. These

experiments are presented in chapter 3.

- **How do transient plasmas behave after the emitter and all other internal objects have been removed?** The insulated rods that hold emitters on axis for steady state plasma creation are perturbative. These rods charge negatively and drive transport via $E \times B$ drift along the rods. Furthermore the negatively charged rods would act as sinks for positrons. A retractable emitter capable of creating steady state plasmas and then being removed faster than the confinement time was used to study plasmas unperturbed by internal objects. Confinement times after emitter retraction were measured to be shorter than for steady state plasmas as a result of ion accumulation in the confining region. The longest confinement time without internal objects was 92 ms. These experiments are presented in chapter 4.

- **Is a two stream instability responsible for the observed decrease in confinement time when emitting with unobstructed bare filaments?** Plasmas are regularly created in CNT by heated biased filaments capable of emitting in both directions along a field line. Measured confinement times increased by as much as a factor of four when blocking emission in one direction. This observation led to studies evaluating whether a two stream instability could be responsible for the change in confinement. Results indicate that the improvement is not related to a two stream instability. Instead, the difference results from the perturbation caused by the blocker when it is located near the emissive filament. We believe that the blocker perturbs the filaments sheath allowing the plasma to reach a stable equilibrium with improved confinement. Multiple confinement states have been observed previously in CNT [37]. Experiments investigating improved confinement with obstructed emission are presented in chapter 5.

The layout of this thesis is as follows. Chapter 2 describes the Columbia Non-neutral Torus and provides relevant background information. Chapters 3, 4, and 5 present experimental results as described above. Chapter 6 summarizes the conclusions presented in this thesis. Finally, possible future experiments are suggested in chapter 7.

Chapter 2

The CNT Experiment

This chapter will present a basic overview of background information relevant to this thesis. Previous experiments studying non-neutral plasmas will be described followed by the characteristics specific to non-neutral plasmas confined by magnetic surfaces. Properties of the CNT experiment will be detailed and a description of diagnostic techniques will be presented.

2.1 Non-Neutral Plasma Physics

The study of non-neutral plasmas is not a new field. Child studied the behavior of electrons flowing from heated biased filaments in the beginning of the 20th century [20], Langmuir looked at how electrodes are effected by space charge soon afterward in 1923 [57], and Brillouin realized the limits on electron density for radially confined equilibriums in a magnetic field before 1950 [16]. In the second half of the 20th century, modern plasma theory and advances in experimental equipment were used to demonstrate that many of the equilibrium, stability, and collective behaviors studied in quasi-neutral plasmas have direct analogs in non-neutral plasmas [22].

While magnetic surfaces are a familiar method to confine quasi-neutral plasmas the majority of non-neutral plasma research has studied plasmas confined in Penning traps [22, 65, 77]. A penning trap is a cylindrical device that uses the open field lines of an axial magnetic field to radially confine charged particles. An electric field is enforced at each end

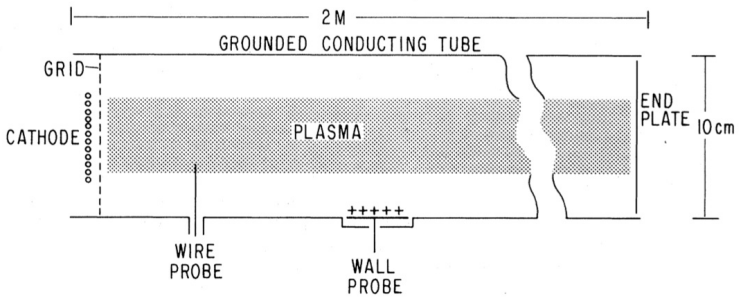

Figure 2.1: A schematic of a penning trap taken from the physical review letters article by Malmberg. [65].

of the device to prevent particle losses along the field lines. A schematic of the penning trap used by Malmberg is shown in figure 2.1 [65]. As the figure shows, pure electron plasmas are created by emission from a heated spiral filament (labeled "cathode") positioned behind a grid. When the trap is full, the bias on the grid can be quickly made more negative to isolate the cathode and confine the plasma. Penning traps benefit from conserved canonical angular momentum as a result of the traps cylindrical symmetry. This conservation allows for confinement times that are very long relative to any of the time scales considered in this thesis [4, 22, 66, 78]. For example, the Penning trap studied by Amoretti has measured confinement times of several minutes for pure electron plamas [2]. Penning trap plasmas also benefit from a wide array of diagnostic techniques. Plasma can be collected on an end plate by quickly reducing the confining bias at one of the ends. This destructive diagnostic technique provides two dimensional temperature and density measurements [66, 75]. Wall probes provide a non-destructive diagnostic by measuring the image charge induced in a plate positioned outside of the plasma [36, 65].

Interest in the behavior of non-neutral plasmas in other magnetic configurations has resulted in their study in more complex magnetic fields. Pure-toroidal traps can be operated as a complete torus or a partial torus with bias plates capping the ends [5, 21, 69, 92, 99]. Pure-toroidal traps have successfully employed many of the plasma creation and diagnostic techniques used in Penning traps [92,93]. Confinement times longer than 1 second have been measured in such toroidal configurations. Dipoles have also been used to confine and study non-neutral plasmas [87, 88, 98]. Plasmas are created with an electron gun positioned at the

plasma edge. An electron gun accelerates electrons from a heated biased filament through a hole in a grounded cap that surrounds the filament.

2.2 Non-Neutral Plasmas on Magnetic Surfaces

The Columbia Non-neutral Torus is the first experiment designed to create and study small Debye length non-neutral plasmas confined by magnetic surfaces. However, there are earlier experiments that investigated the behavior of electrons on magnetic surfaces. Stellarators use external coils to create vacuum magnetic surfaces [11,12,91,97]. However, without careful optimization of the magnetic surfaces confinement will be limited by neoclassical losses [12, 30]. Numerical codes are used extensively for the design of stellarator experiments that will be robust against neoclassical losses [11,12]. These codes can be used to study the predicted quality of magnetic surfaces and neoclassical transport for a given configuration. However, accounting for error fields and coil misalignments can be challenging. Thus theoretical and numberical predications need to be experimentally verified.

The "stellarator diode method" is one such method used to experimentally study magnetic surfaces [26]. It has been used on various experiments for surface mapping including the Auburn Torsatron [31], Heliotron-E [40, 94], Uragan-2M and Uragan-3M [60, 61], and the H-1 Heliac [90]. This method involves emitting electrons from a source positioned on the magnetic surfaces. If electrons are perfectly confined then they will collect on a surface until their space charge is large enough to stop further emission from the source. In practice electrons are not perfectly confined and their transport can be related to the emission current. This provides a quantitative measure of the quality of a specific surface. Efforts were made to better understand the electron transport observed in stellarator diode experiments [63,71,76]. However, it was not until CNT that electron plasmas confined on mangetic surfaces with small Debye length were studied [80].

Since then interest has grown in the use of magnetic surfaces as a confinement method for non-neutral plasmas [44, 46]. Magnetic surfaces provide a significant benefit not offered by Penning traps. Pennning traps can provide long confinement times for particles of like charge. However, their reliance on a potential well for trapping limits their ability to confine positive and negative charges simultaneously without nested traps. In experiments like CNT,

magnetic surfaces confine plasmas of various neutralizations, ranging from single species to quasineutral. In a stellarator, no externally applied electric field is required for confinement (a requirement of Penning traps) and plasma current is not required to create magnetic surfaces (significant plasma current is a requirement of tokamaks). Thus plasmas of arbitrary neutrality can be studied. The first experiments continuously scanning the range from pure electron to quasineutral plasmas have been performed in CNT by Xabier Sarasola [70].

2.2.1 Transport

Fast losses are expected for a stellarator confined quasineutral plasma that has not been optimized to reduce helical ripple. These losses are due to the ∇B and magnetic curvature drifts of ripple trapped particles [11, 12]. However, the large space charge inherent in non-neutral plasmas results in a strong electric field that can limit such losses. $E\times B$ drift resulting from the electric field causes poloidal movement of ripple trapped particles. This keeps the particles close to magnetic surfaces. Thus the relevant confinement time for non-neutral plasmas on magnetic surfaces is not the neoclassical confinement time for an unoptimized stellarator:

$$\tau_d \approx \frac{a}{\mathbf{v}_{\nabla B} + \mathbf{v}_R} \approx \frac{ea^2 B}{T_e} \tag{2.1}$$

where $\mathbf{v}_{\nabla B}$ and $\mathbf{v}_R$ are the the ∇B and curvature drift velocities. Measurements and simulations have confirmed confinement times much longer than this neoclassical drift time [8, 24]. Instead Berkery and Boozer consider the radial electric field as the primary drive for electron transport [6]. They assume that the step size will depend on the variation of electric potential on a surface such that $\delta \approx T_e/(ed\Phi_0/d\psi)$. This results in a cross field flux of

$$\Gamma_T = \nu_c n \frac{T}{e(d\Phi_0/d\psi)} \frac{dV}{d\psi} \tag{2.2}$$

Here ν_c is the dominant collision frequency, ϕ_0 is the portion of the electric potential that remains constant on along a surface, and $\frac{dV}{d\psi}$ is the derivative of the volume enclosed by a constant ψ surface. From this particle confinement time is predicted to be

$$\tau \approx \frac{e\Delta\Phi}{T_e \nu_c} \approx \left(\frac{a}{\lambda_d}\right)^2 \frac{1}{\nu_c} \tag{2.3}$$

2.2.2 Transport In CNT

In CNT, two distinct transport mechanisms have been measured. Transport is driven by the insulated rods used to hold emitters in the plasma and by electron interaction with background neutral gas particles. It is believed that the rods cause transport due to the electrostatic perturbation that they create inside the plasma. These rods charge negatively and create $E \times B$ convection in a region around the rod. A simple model of this process yields reasonable agreement with experimental results [8].

The dominant collisions in typical CNT plasmas are electron-neutral collisions. For these collisions

$$\nu_{e\text{-}n} = n_n \sigma_{e\text{-}n} v_e \tag{2.4}$$

The electron neutral cross section can be found in the literature [47]. The resulting time scale for a typical CNT plasma at 2 nTorr is $\tau_{e\text{-}n} \approx 0.2$s. While equation 2.3 suggests that electrons should be confined on the order of one hundred electron neutral collisions, measurements have found electrons are confined for a time on the order of one collision [8]. Particle trajectory simulations suggest that these fast losses are the result of poorly confined orbits in CNT's phase space [24].

2.3 The CNT Experiment

CNT utilizes a simple four planar coil design to create magnetic surfaces, Fig. 2.2 [82]. Two interlocking coils are positioned inside of the vacuum chamber two poloidal field coils are positioned outside of the chamber. Steady state pure electron plasmas are created by thermionic emission from a heated and biased tungsten filament held near the magnetic axis by an insulating ceramic rod 2.3. Parallel transport fills the axis in microseconds and the remaining surfaces are filled by cross surface transport. Experiments have also been performed investigating the use of an electron gun to create plasmas in CNT. This allows for emission from the plasma edge but results in higher electron temperatures [39].

In CNT, magnetic surfaces are labelled by the coordinate ψ such that $\psi = 0$ at the axis and $\psi = 1$ at the last closed flux surface (LCFS). ψ is defined by convention at the midpoint of the thin cross section where $\phi = 0$ as

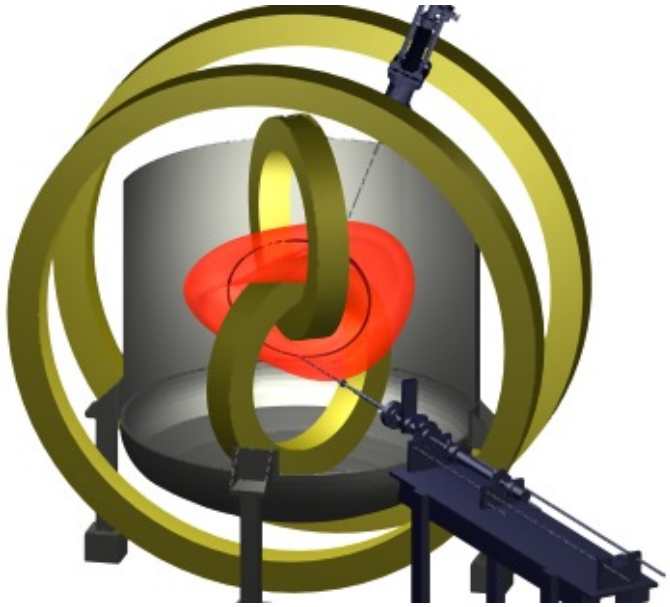

Figure 2.2: A drawing of CNT illustrates the confining volume in red, four planar coils in gold, and two filaments held on the magnetic axis by ceramic rods. The four probe array is represented on the bottom while the retractable emitter inserts from the top.

$$\psi = \frac{R - R_{Axis}}{R_{LCFS} - R_{Axis}} \tag{2.5}$$

Magnetic surfaces were mapped using field line visualizations as described in 3.2.1 and studied in detail using phosphor rod visualizations [84].

2.3.1 Ion Accumulation

An instability resulting from the accumulation of ions in CNT plasmas has been observed when $n_i/n_e > 10\%$ [67, 89]. Ions are continuously created in CNT from energetic electrons ionizing neutral gas molecules. The rate of ionization could neutralize plasmas in 450 ms at 2×10^{-8} Torr neutral pressure if unbalanced [7]. However, for steady state plasmas ions do not continuously accumulate over time [8]. Instead, the insulating rods allow for recombination and act as a sink for ions. The ion content reaches a steady state determined by the balance of ionization and recombination.

The steady state ion densities were directly measured by Jason Kremer [7, 55]. He found that n_i is linearly dependent on p_n and a linear fit to measured results indicates that $n_i = 2.1 \times 10^{17} m^{-3} Torr^{-1} \cdot p_n$. Thus for $p_n = 2 \times 10^{-8}$ Torr and $n_e \approx 10^{12} m^{-3}$, $n_i/n_e \approx 0.5\%$. Estimates made by balancing ion accumulation and recombination rates predict an ion fraction of $n_i/n_e \approx 0.1\% - 1\%$ which is consistent with measurements [55]. Furthermore, simulations by Quinn Marksteiner indicate that inserting a second insulating rod into the plasma results in a factor of two reduction in the lifetime of untrapped ions [67, 68]. This demonstrates the importance of the insulating rods for limiting ion accumulation.

2.3.2 Diagnostics

The same tungsten filaments used for plasma emission have also been successfully employed as diagnostics. A probe array with four individually wired filaments is positioned so that its inner most filament intersects the axis in the $\phi = 0$ cross section as shown in figure 2.2. A similar probe array (not shown) with eight filaments is inserted parallel to the first but from the opposite side of the chamber. These two probe arrays will be referred to simply as the "four probe array" and the "eight probe array". Figure 2.2 also shows the retractable

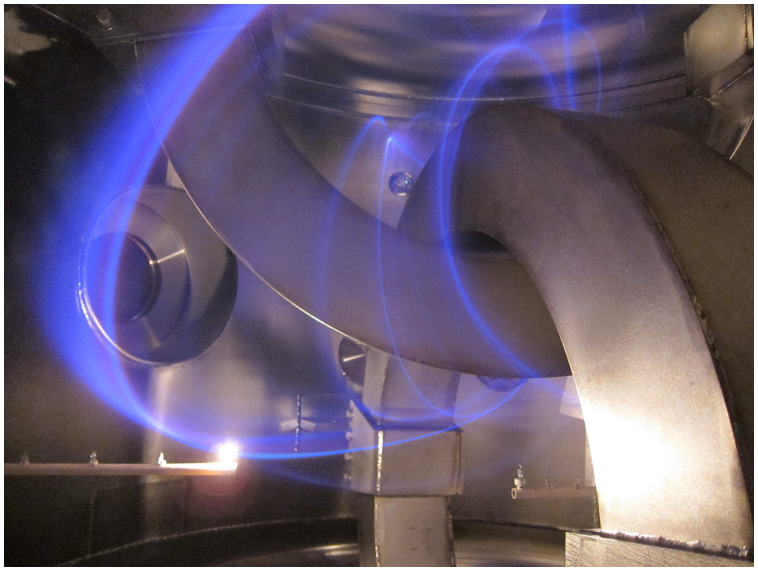

Figure 2.3: Plasmas are created and diagnosed with heated biased filaments held on the magnetic surfaces by insulated ceramic rods. Here a filament is used to visualize a magnetic field line near to the last closed flux surface.

emitter which is described in detail in chapter 4. These probes were aligned to the axis using phosphor rod visualizations [84]. Connection to the vacuum chamber via bellows allows probe positions to be adjusted in one linear dimension then returned to proper alignment without the need to repeat phosphor rod visualizations (figure 2.4). The position distance from the axis was then measured in centimeters. Where possible ψ values were measured for those positions and are reported.

Confinement times for CNT plasmas have been measured by three independent methods:

- **Method I - Steady State Emission:** The emission current used to create on-axis plasmas is measured. In steady state the electron injection rate must be equal to the electron loss rate. Thus $\tau = \frac{eN}{I_e}$ where N is the electron inventory and I_e is the injection rate. Electron density has been measured both directly [54, 56] and by measuring the potential profile then reconstructing the density using a Poisson-Boltzmann solver to generate a full 3D equilibrium reconstruction [58]. The reconstruction method was used by Mike Hahn to find all electron inventory results reported here [39].

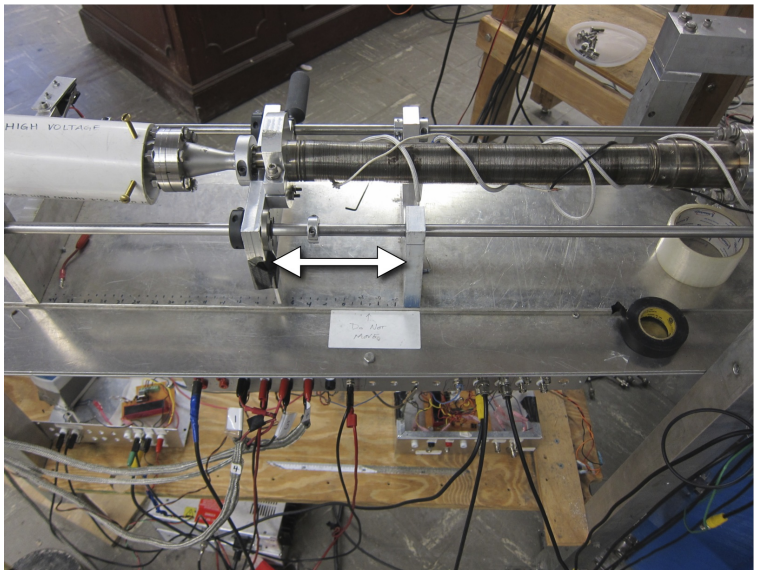

Figure 2.4: After alignment to the axis probe positions can be adjusted in one linear dimension then returned to proper alignment. The distance from the axis can be measured in centimeters as demonstrated by the white arrow.

- **Method II - Fixed Current Probe:** A probe measures the potential outside the last closed flux surface by measuring the voltage required to maintain a small emission current. The decay of potential indicates confinement time after on-axis emission has been stopped.

- **Method III - Fixed Voltage Probe:** A probe measures the potential outside the last closed flux surface by measuring whether a heated filament is emitting. The probe is set more negative than the local potential so it will not emit. Then when on-axis emission has been stopped the time required until the probe begins emitting is measured. Multiple shots can be used to reconstruct the plasma decay time.

Method I was used for all previous CNT confinement experiments. Methods II and III were developed so that plasmas could be studied non-perturbatively after emitter retraction and are described in detail in section 4.2.

The fixed current probe was also used to measure the plasma potential within the confining region. This could then be compared to the plasma potential measured using the

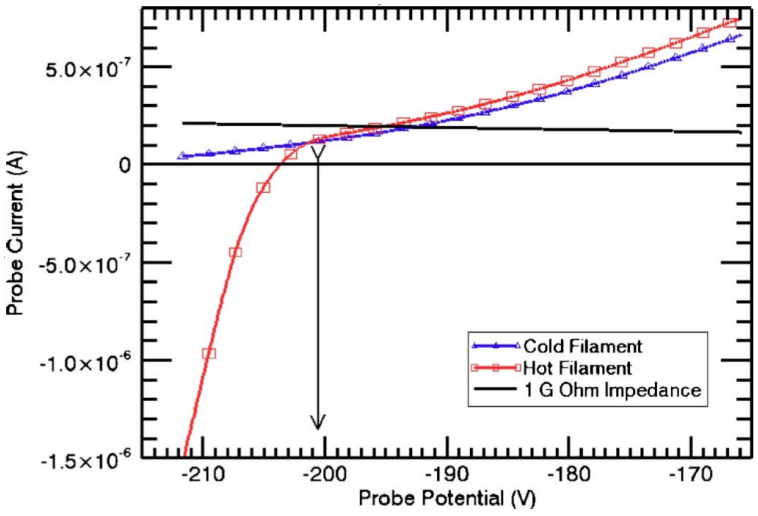

Figure 2.5: This figure by Kremer demonstrates the deviation potential measurement [54].

deviation potential method as described by Jason Kremer [54]. The deviation potential is found by comparing I-V characteristics for a heated (emissive) filament and cold (Langmuir probe) filaments. When the filaments are less negative than the plasma potential they will only be collecting electrons and their I-V characteristics should be in agreement. The cold filament cannot emit, so the I-V characteristic will only show fewer electrons collected. Once the heated filament is more negative than the plasma potential it will begin to emit and its I-V characteristic will differ from the cold emitter's I-V characteristic(see figure 2.5). The point where the two curves differ is the deviation potential and indicates the plasma potential within 0.5 V accuracy [39]. The deviation potential is a robust and trusted method and was used where possible. However, the deviation potential commonly requires at least 10 seconds for a measurement and in some cases can perturb the plasma. When these limitations created an issue the fixed current probe could be used as discussed in section 4.2.1.

With the plasma potential known, the electron temperature can then be measured following the method described by Jason Kremer et al. [54]. A plot of $ln(I_{probe})$ and $V_{probe} - \Phi_p$ shows three regions as shown in figure 2.6. If ions were present the region with very negative probe potentials (dashed line at left of the figure) would measure ion saturation current. In pure electron plasmas almost no current is collected. Electron saturation occurs when the probe voltage is near Φ_p (dashed line at the right of figure 2.6). In this region the surface the

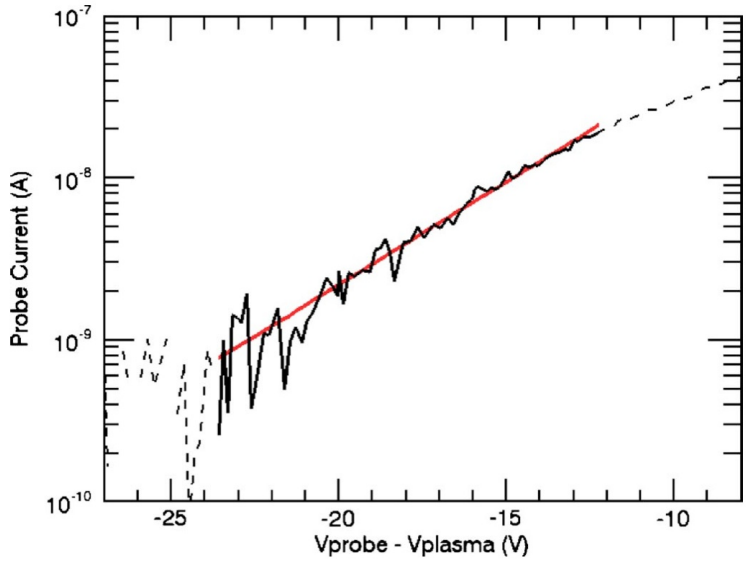

Figure 2.6: This figure by Kremer demonstrates how Langmuir probe IV traces can be used to find electron temperature [54].

probe is collecting on will begin to be depleted and the amount of current collected is dependent on cross field transport. Between these two regions the current collected by the probe depends on the number of electrons with enough thermal energy to overcome the probe's bias. Thus this region (solid line in the figure) can be used to find electron temperature. The current to the probe in this region is

$$I_{probe} = \frac{1}{4} e n_e \overline{v}_e A exp\left(\frac{V_{probe} - \Phi_p}{T_e}\right) \tag{2.6}$$

Where $\overline{v}_e$ is the mean speed and for a Maxwellian distribution and equals $\sqrt{2T_e/\pi m_e}$. The electron temperature is then found in electron volts from the inverse of the slope shown in figure 2.6. This process was greatly aided by the use of analysis codes written by Mike Hahn [39]

2.3.3 Typical Experimental Parameters

Plasmas can be studied in CNT with up to 0.2 T on-axis magnetic field strength and $> 1 \times 10^{-9}$ Torr neutral pressures. However for the majority of experiments the magnetic field

strength is set below 0.1 T to reduce the time needed between shots for the water cooled copper coils to cool. Throughout this thesis pressures are reported in nTorr and background neutral gas is dominated by nitrogen unless otherwise noted. This is because the lowest base pressure regularly achievable was 1 nTorr while at neutral pressures over 100 nTorr the ion content begins to effect confinement and stability. The range above 100 nTorr was studied by Quinn Markstiener first [67], and now by Xabier Sarasola [70].

The Larmor radius, $r_l = \frac{mv_\perp}{|q|B}$, is typically on the order of 0.1 mm for the plasmas studied in this thesis. For CNT the average plasma minor radius is $\bar{a} \approx 0.15$ m. Thus the larmor radius is very small compared to the size of the plasma and the gradient scale length of the magnetic field. So the guiding center approximation is valid and the electrons are magnetized. Unlike quasi-neutral plasmas where the Larmor radius is typically much larger than the Debye length, $\lambda_d \approx 15mm$ for CNT plasmas so $r_l < \lambda_d$ [8, 27].

During the course of this thesis a conducting boundary was installed and eventually removed as described in chapter 3. The magnetic geometry was also changed. The simple four coil design allows the angle between the interlocking coils to be changed between three title angles. This allows for the study of three different magnetic geometries in one experimental device. Experiments described in this thesis were performed at the 32° tilt angle with the conducting boundary installed or at the 39° tilt angle with no conducting boundary. After each major change the quality of magnetic surfaces was confirmed by the mapping techniques cited above.

Chapter 3

Confinement Effects Of A Conducting Boundary

Transport driven by electron-neutral collisions in CNT results in electron loss rates that are much faster than initially predicted [6, 80]. Neoclassical diffusion predicts that electrons will be lost after hundreds of collisions. However, measurements indicate that electrons are lost after only one to two electron-neutral collisions [8]. We interpret these results to indicate that there are open orbits in CNT. Numerical simulations by Benoit Durand de Gevigney confirm the existence of open orbits for a large part of the electron phase space [24]. These simulations predict that the installation of a grounded electrostatic boundary that conforms to the the last closed flux surface will reduce these fast losses.

Open orbits exist in CNT for several reasons. The conforming boundary is designed to address what is believed to be the primary reason: the existence of a sizable mismatch between the electrostatic potential surfaces and the magnetic surfaces [58]. Without a conforming boundary, electrostatic boundary conditions are set by the grounded vacuum chamber and interlocking coil vacuum jackets. We estimate that equipotential surfaces in this configuration deviated from magnetic surfaces by as much as Ψ=0.2 [23, 59]. With a perfectly conforming equipotential boundary the deviations are predicted to be on the order of Ψ=0.02 (Ψ is a coordinate to label magnetic surfaces that ranges from 0 on the magnetic axis to 1 at the last closed flux surface).

For experiments in this chapter, a conducting boundary was installed and operated in

CNT. The boundary was designed to improve surface mismatch as described and also to be used as an external diagnostic. After installation a new record confinement time of 323 ms was measured, more than an order of magnitude improvement over the previous 20 ms record. However, challenges aligning the boundary to the last closed flux surface limited the improvement to the equipotential to magnetic surface mismatch. In this chapter the installation, alignment, and operation of the conformal conducting boundary will be described in section 3.2, including the application of visualization techniques for aligning to magnetic surfaces will be described (section 3.2.1). Results demonstrating improved confinement despite misalignments of the conducting boundary will be presented and discussed (section 3.3). It will be shown that the confinement improvement results from a combination of sources. First, an increase in magnetic field strength and a decrease in neutral pressure improved confinement time by an amount that was expected. A factor of four reduction in rod driven transport was observed which we conclude results from a decreased Debye length. Finally, results indicate that a decrease in neutral driven transport is the result of improvements to the equipotential surface agreement with magnetic surfaces.

An even longer 337 ms confinement time was measured when emitting from an obstructed filament with the conducting boundary installed. The same improvements to rod driven and neutral driven transport detailed above aided in the record 337 ms confinement time. However, for simplicity, details of that result are presented in section 5.2.1 and only plasmas created with bare filaments are considered in this chapter.

3.1 Introduction

A conducting boundary was designed and constructed by Remi Lefrancois with the help of undergraduate students Mark Kendall, Charles Biddle-Snead, Andrew Coppock, and Elliot Kaplan [59]. The boundary was intended to reduce the mismatch between equipotential surfaces and magnetic surfaces. Figure 3.1 is a simulation performed by Lefrancois. This simulation predicts the equipotential and magnetic surfaces when the electrostatic boundary condition is set by the grounded vacuum chamber and magnetic coil vacuum jackets.

The mismatch is largest near the last closed flux surface, while close alignment is observed on inner surfaces. The alignment on inner surface is the result of Debye screening

where many Debye lengths of plasma can shield out the electrostatic perturbation. In the plasma electron density decreases to screen out negative potentials and increases to screen out positive potentials. Debye screening was studied in detail for CNT plasmas by Benoit Durand de Gevigney [23, 25]. The non-zero electron temperature and low electron density on outer surfaces limit the ability of the plasma to screen perturbations, resulting in the observed mismatch near the edge. Simulations by Lefrancois demonstrate that the match of equipotential and magnetic surfaces is improved when the Debye length is shortened by a decrease in electron temperature [58].

Figure 3.2 shows the resulting improvement in alignment between potential and magnetic surfaces when an ideal conducting boundary enforces an equipotential on the last closed flux surface [58]. The mismatch without a conforming boundary results in increased cross field transport. Electrons in CNT can $E{\times}B$ drift along equipotential surfaces as well as free stream along magnetic surfaces. If there is a mismatch between equipotential and magnetic surfaces, electrons are able to move from one to the other to quickly exit the plasma. Simulations show that electrons can leave on sub-millisecond time scales by this method [24].

The boundary is composed of 13 copper mesh sectors, completely enclosing the confined volume, and shaped to conform to the outermost magnetic surface shape. Each sector is composed of semi-rigid copper mesh wrapped around copper tubing. Figure 3.3 shows an example of one such sector attached to neighboring sectors by ceramic spacers. The ceramic spacers electrically isolate each sector. This allows sectors to be independently biased and diagnosed. The mesh was divided into four toroidal segments. Three of the toroidal segments were divided into three poloidal segments each, accounting for nine of the thirteen segments. The remaining toroidal segment was divided into four poloidal segments. These divisions were made for both spatial resolution and to aid installation.

Capacitive probes have previously been successfully used in CNT [67]. In those experiments capacitive probes were simply conducting plates placed outside of the last closed flux surface. Fluctuations in the induced charge on those plates were used to diagnose oscillations in the plasma from outside the last closed flux surface. Capacitive probes that surround the entire plasma have been used in other non-neutral plasma experiments to study equilibrium [21, 36, 65, 93], stability [21, 52, 87, 93], and confinement [52, 86, 87, 93]. These methods all involve either measuring the image charge induced on the probes or the directly collected

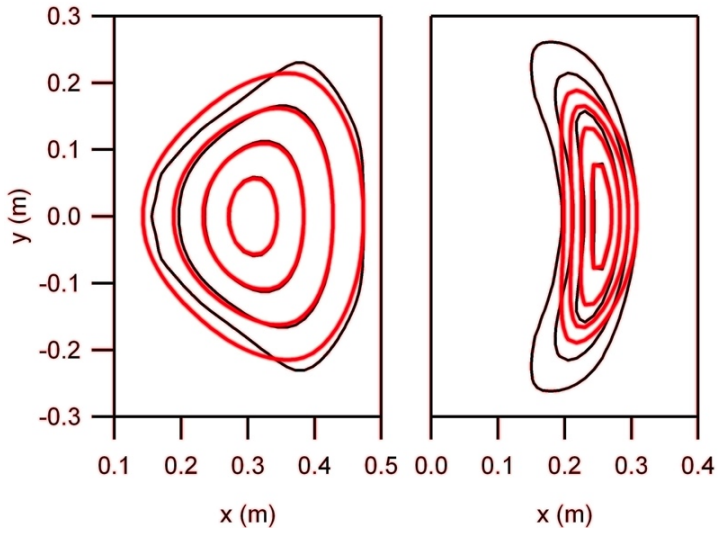

Figure 3.1: This simulation by Lefrancois shows the mismatch between equipotential (red) and magnetic (black) surfaces when the electrostatic boundary condition is defined by ground at the vacuum vessel and the magnetic coils' vacuum jacket.

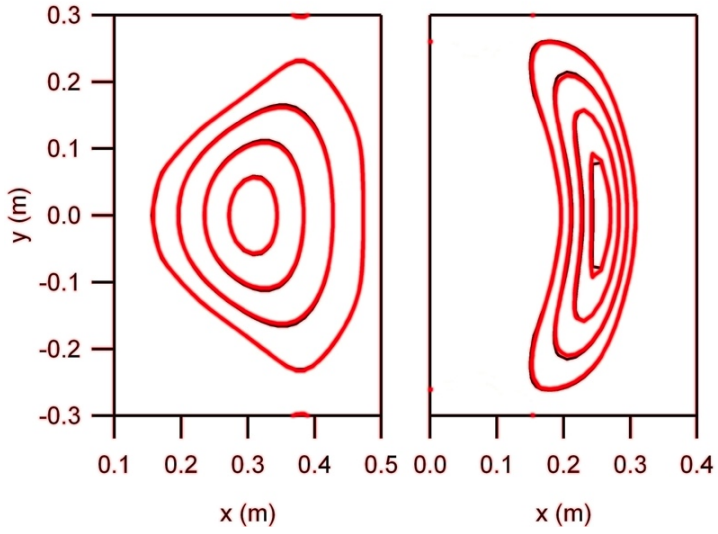

Figure 3.2: This simulation by Lefrancois shows the improved match between equipotential (red) and magnetic (black) surfaces when the last closed flux surface is an equipotential.

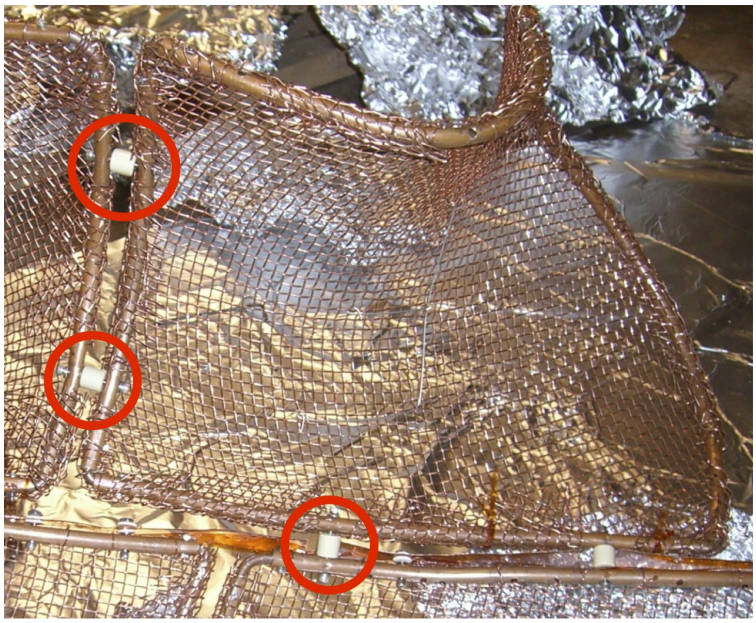

Figure 3.3: This photograph shows one sector of the conducting boundary before installation. It is attached to neighboring sectors by ceramic spacers (circled in red).

current. Equilibrium can be further studied by applying constant [10, 73, 74] or oscillating [3, 36] perturbations on one sector and measuring plasma response with other sectors. Thus the conducting boundary was intended to both improve confinement as well as provide new external diagnostics. Unfortunately misalignment of the conducting boundary limited its diagnostic capabilities. Measurements during the course of this thesis indicate that all segments collected current with steady state plasmas present, complicating image charge measurements. Decay measurements were abandoned when more accurate techniques were discovered as discussed in section 4.2.

3.2 Installation and Alignment

The conducting boundary was supported inside CNT by resting on the interlocking coils as can be seen in figures 3.7 and 3.8. The conducting boundary was electrically isolated from the grounded coils by a thin sheet of kapton film. This made for a relatively straight forward installation of the mesh. However, alignment of the three dimensional conducting boundary

to the magnetic surfaces in CNT quickly proved to be a challenge. Three methods were used to correct alignment errors:

- **Comparison to CAD Drawings:** A CAD drawing that indicates the proper position of the conducting boundary relative to tangible objects in CNT was used for gross alignments. Measurements of the location of features on the boundary, relative to points on the vacuum chamber, could be compared to lengths found in the CAD drawing. This was the only alignment method that could be used while the top of the chamber was open and the boundary was easily accessible. The use of more sophisticated metrology techniques, such as a roamer arm, would have substantially improved this method.

- **Magnetic Field Line Visualizations:** With the chamber under vacuum, visualizations of magnetic field lines proved to be a useful indicator of misalignments between the conducting boundary and magnetic surfaces. This method is described in detail in section 3.2.1 and was published in Transactions on Plasma Science [15].

- **Copper Excitation:** After magnetic field line visualization was used to locate large misalignments, an additional method was identified. Energetic electrons are capable of exciting copper to emit a green glow [53]. The location where a field line intersected a the conducting boundary could thus be identified by a green glow on the boundary. This allowed for further identification of misalignments.

Each of these methods was used to identify where misalignments occurred. Phosphor rod magnetic surface mapping was then used to evaluate the extent that boundary was cutting off good magnetic surfaces. Adjustments to the shape and location of the conducting boundary were made using structural wires to improve alignment. These wires were attached to the vacuum vessel in convenient locations then connected to metal tensioners. The tensioners were attached to the mesh via insulated wires to maintain electrical isolation (see figure 3.4).

The primary problem with the conducting boundary resulted from its lack of structural rigidity. The insulated ceramic spacers that held individual mesh segments together were too fragile to be tightly connected to the segments. This allowed the entire boundary to deform upon installation. Over time the boundary continued to sag under its own weight resulting

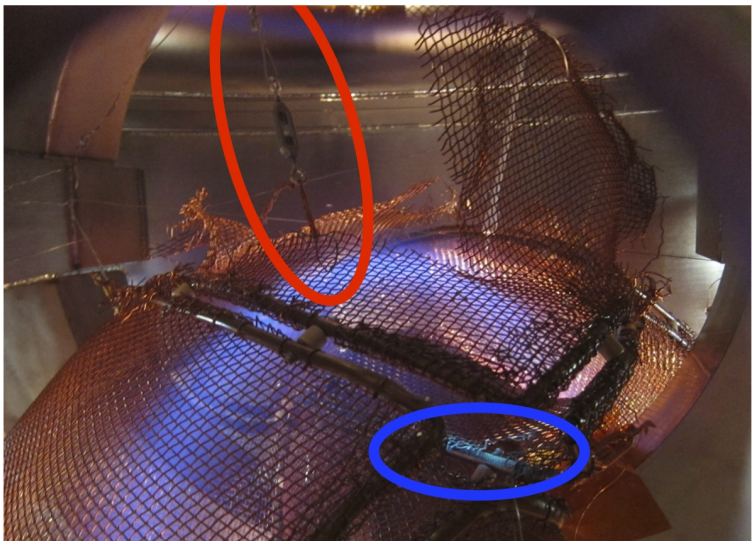

Figure 3.4: Adjustments were made to the conducting boundary using structural wires and metal tensioners (circled in red). The green glow (circled in blue) results from an electron beam intersecting the conducting boundary.

in further misalignment. In some cases segments were so misaligned that the only possible solution was to remove pieces of copper mesh. The top segment especially was pulled too low by the weight of the structure. As a result the mesh on the top segment was almost completely removed as can be seen in figure 3.4.

3.2.1 Visualizations

Magnetic field line visualizations have proven to be a valuable tool in CNT. Before magnetic surface topology was confirmed [83] using the electron beam-fluorescent rod technique [49], electron gun visualizations demonstrated CNT's magnetic surfaces. These visualizations resulted in impressive images of the shape of CNT's magnetic surfaces and have been used extensively to aid in describing the magnetic geometry. Figure 3.5 shows one such image taken by Thomas Pedersen. Recently electron gun visualizations were also used to demonstrate magnetic islands in a new magnetic configuration as can be seen in figure 3.6.

Pure electron plasmas in CNT are usually studied with pressures in the 10^{-9} Torr range to minimize the effect of electron-neutral collisions. However, by backfilling to a pressure

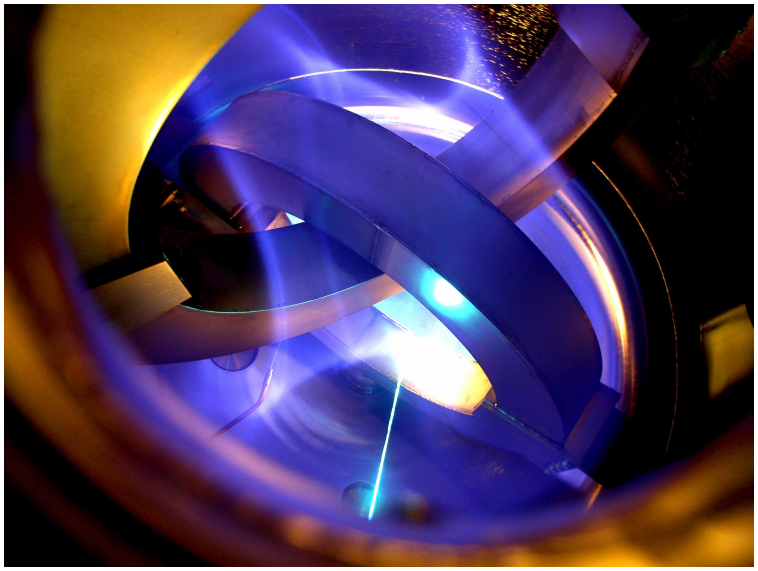

Figure 3.5: A photograph of a surface visualization made using an electron gun taken on an Olympus C-8080 digital camera (15 second exposure) taken by Thomas Pedersen.

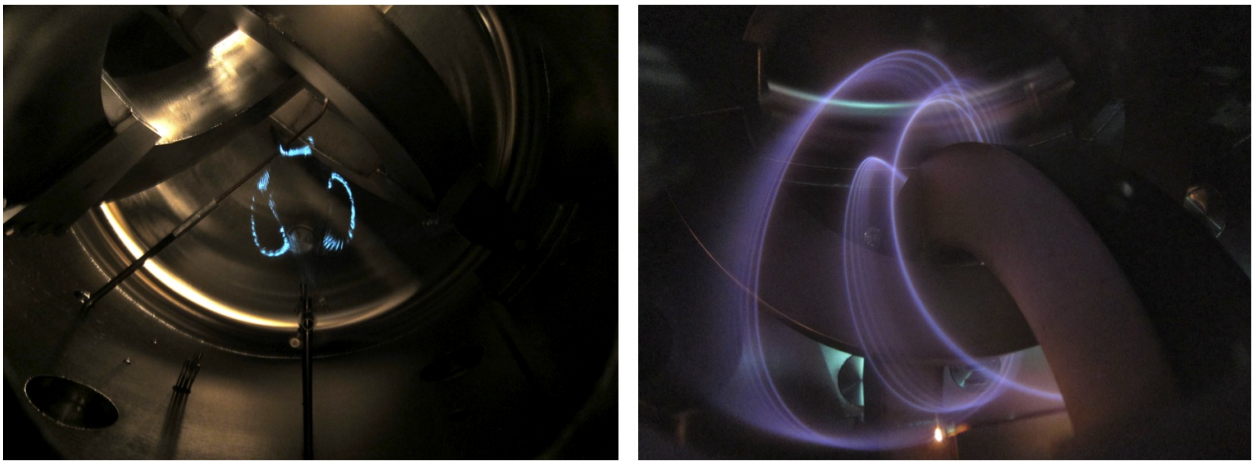

Figure 3.6: On the left phosphor rods are used to map magnetic islands at the 39° tilt angle with a 3.0 current ratio. On the right a photograph shows a visualization of the islands.

above 10^{-5} Torr and emitting a beam of electrons from an electron gun it is possible to visualize the complete three-dimensional shape of the magnetic surfaces. The electron gun is a heated-biased filament surrounded by a grounded metal cap with a hole in the end. Emitted electrons are accelerated out of the cap and travel along the magnetic surface with enough energy to excite and the neutral background gas which then emits visible light. Luminance increases with background pressure at the cost of reduced electron beam path length. Changing backfill gas results primarily in different color visualizations, although inert gases also allow for longer filament life.

Visualizations created with the electron gun provide a good example of the difference between luminance and brightness. Luminance is an absolute measure of how much light is emitted in a given area. Brightness describes the perception of relative light. Current emitted by the electron gun can be collected by the grounded cap that surrounds the filament. This results in visualizations with less luminance than if the full emission current could escape the cap. The visualization are still visible to the naked eye because the cap on the electron gun also blocks much of the light produced by the heated filament. Thus, other than the visualization, there is very little light in the vacuum chamber. The result is low luminance visualizations that appear bright in the vacuum chamber's low ambient light. Long exposure photography successfully captures these visualizations.

The bare filaments regularly used for plasma emission were successfully used to create visualizations after the installation of the conducting boundary. In this case, there is no grounded cap and all emitted electrons are available to travel along the surface. The increase in electrons travelling along a given field line results in visualizations with higher luminance than electron gun visualizations. However the bare filament also produces a significant increase in background light in the vacuum chamber. This reduces the perceived brightness of bare filament visualizations. This is demonstrated in figure 3.7. A heated filament outside of the image is used to create the visualization. The filament produces significant background light as well as a high luminance visualization. The result is still quite visible with the naked eye and can be captured on a camera without long exposures. A view from the other side of the chamber shows that bare filament visualizations are quite bright when the interlocking coils obstruct some of the background light produced by the bare filament (figure 3.8).

Bare filament visualizations have provided a valuable method for aligning many of the

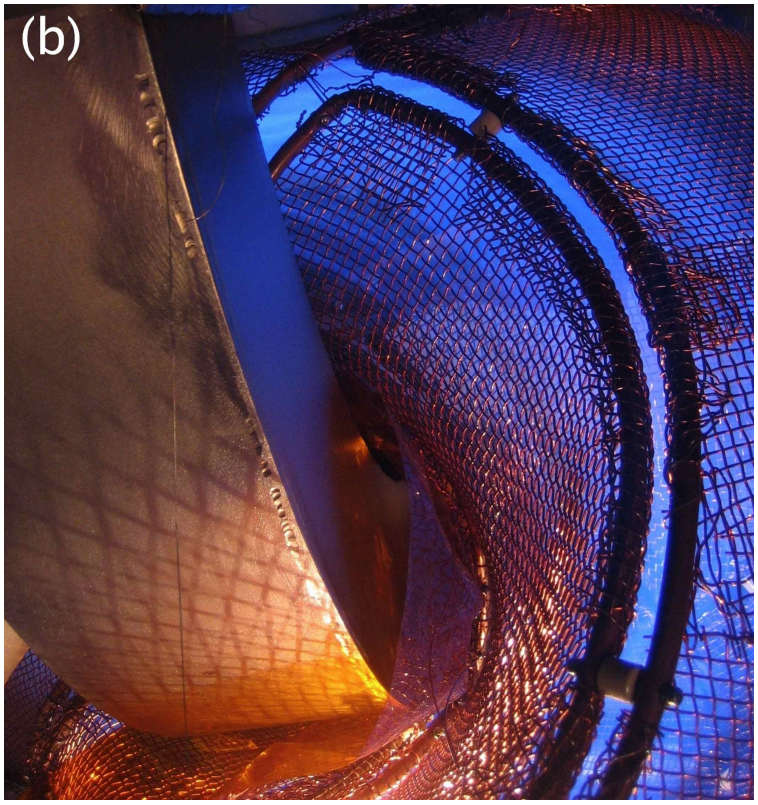

Figure 3.7: A photograph of a surface visualization made using a bare filament inside the conducting boundary. This photograph was taken on a Canon S200 digital camera (0.125 second exposure).

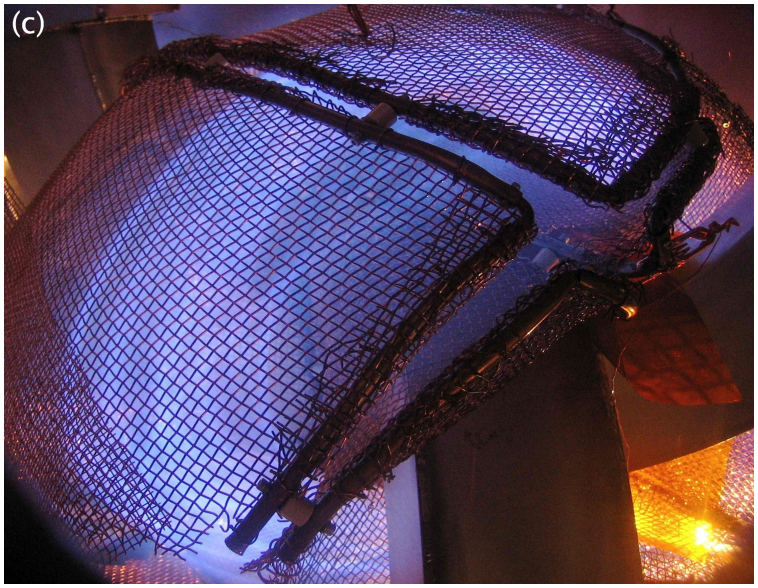

Figure 3.8: A different perspective of the visualization in figure 3.7 clearly shows details of individual magnetic field lines.

probes described in later sections to magnetic surfaces. When investigating the distribution function for the presence of beams a Langmuir probe was aligned to the same field line as an emitter using visualizations. Figure 5.12 shows this alignment with a glowing field line connecting the probe and emitter. When metal plates were installed at the plasma edge to ground the field lines connect to the fixed current probe visualizations were necessary for alignment (figure 4.8). Similarly, when a bias-able plate needed to be aligned with the magnetic axis visualizations were used (figure 5.22).

Visualizations were especially helpful when aligning the conducting boundary. Figure 3.9 demonstrates how the visualizations were used. A field line from a closed magnetic surface visibly passing through the mesh before alignment is completely inside the mesh after alignment. Without visualizations even gross misalignments such as the one shown in figure 3.9 would have been extremely challenging to identify. Photographs of visualizations could also be overlaid ontop of photographs of adjustments to the conducting boundary before bringing the chamber under vacuum. This provided a valuable reference for adjustments and reduced the number of times the chamber needed to be evacuated to evaluate improvements. These methods were necessary to bring the conducting boundary into an alignment that was

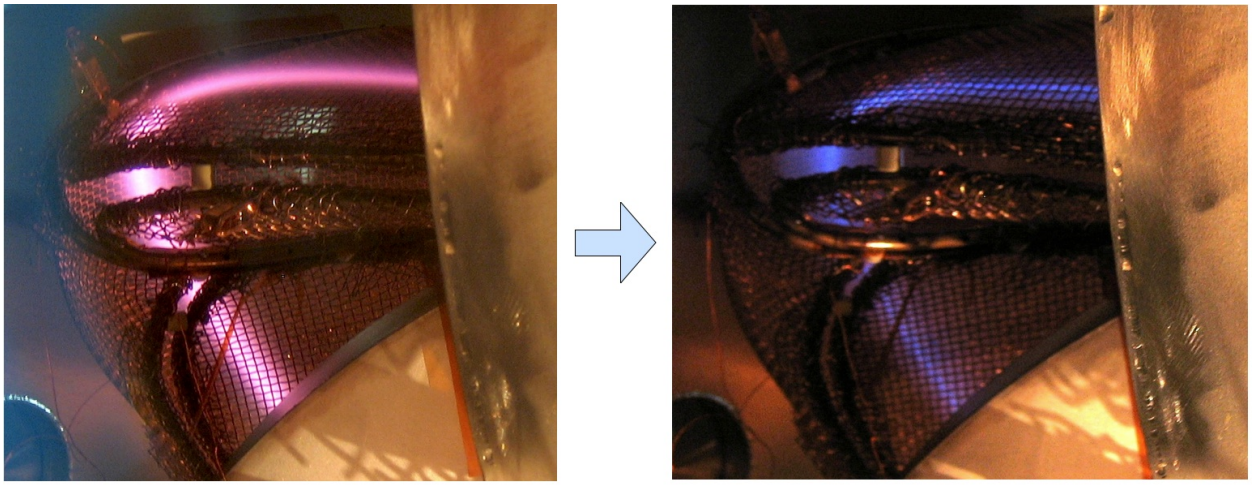

Figure 3.9: This figure shows a fieldline passing through the CB before alignment and the improvement afterwards. The change in color is the result of different background neutral gases that were present at the time of the visualization.

accurate enough to perform the experiments reported below.

3.3 Confinement Results With A Conforming Boundary

Unfortunately, complete alignment was never achieved. Figure 3.10 shows the emission current from a heated biased filament emitting as it is moved from positions near the axis to the edge of the plasma. Even with alignment based on CAD drawings, visualizations, and copper excitation, emission at $\psi \geq 0.7$ is large indicating poor confinement on those surfaces. This result is supported by phosphor rod magnetic surface mapping which indicates that surfaces larger than $\psi = 0.7$ were being intersected by the conducting boundary. This not only limits the size of the confining volume but also reduces the expected match improvement for equipotential and magnetic surfaces. Despite these limitations, improvements to the confinement time were measured. After installation of the conducting boundary the record measured confinement time increased by an order of magnitude from 20 ms to 323 ms. A comparison of confinement times measured before and after the installation of the conducting

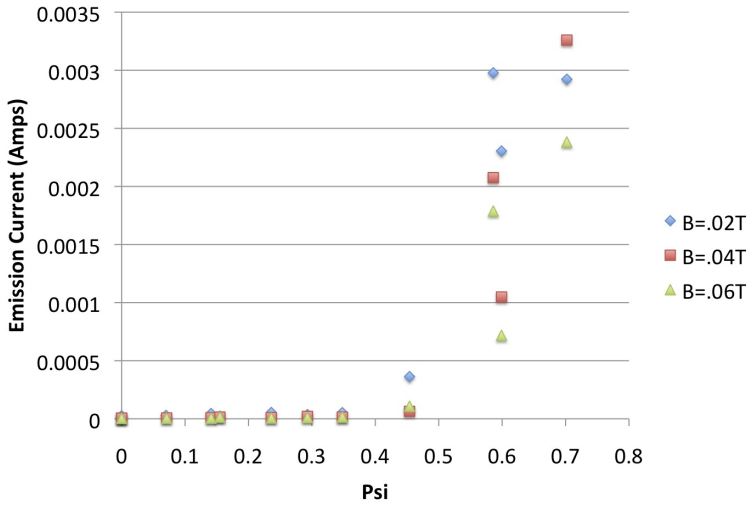

Figure 3.10: Even after careful alignment it was found that the conducting boundary was intersecting surfaces larger than $\psi = 0.7$. This data was collected by Mike Hahn.

boundary is shown in figure 3.11. These results are were measured at a neutral pressure of 20 nTorr to allow for comparison to results before the installation of the conducting boundary. Record confinement times measured at the best achievable neutral pressure after the installation of the conducting boundary (1.1 nTorr) are shown later in figure 5.5.

Experimentally, two dominant sources of transport have been identified in CNT. These confinement improvements resulted from reductions in both. The two sources of transport are introduced here and will be examined in detail in this section.

- **Electron-Neutral Driven Transport:** Results indicating a reduction in neutral driven transport can be interpreted as resulting from an improvement to the mismatch between equipotential and magnetic surfaces.

- **Rod Driven Transport:** Results indicating a reduction in rod driven transport can be interpreted as resulting from a decrease in Debye length.

Plasmas are created in CNT by emitting electrons from filaments attached to ceramic rods inserted into the magnetic surfaces. However, these rods are perturbative and drive cross field transport. At the low base pressures achievable in CNT, insulating rods account for the majority of transport.

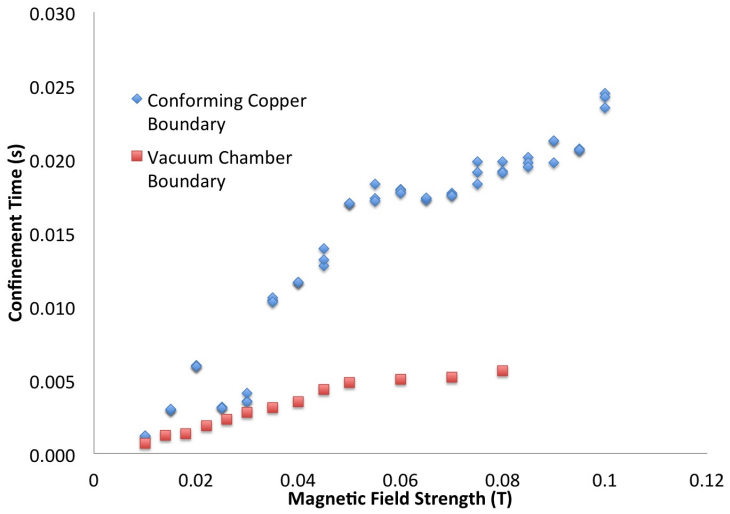

Figure 3.11: Improved confinement time after the installation of the conducting boundary is shown. These results are for plasmas created with a -200 V emission bias at 20nTorr neutral pressure. Record confinement measurements are shown later in figure 5.5.

The insulated rods cause transport due to the electrostatic perturbation that they create inside the plasma. These rods charge up negatively and create $E \times B$ convection in a region around the rod. This process is illustrated schematically in figure 3.12 taken from the paper by Berkery et al. [8]. A simple model of this process yields reasonable agreement with experimental results [8]. Results indicate that the ceramic rods are charged very negatively relative to the plasma potential, on the order of 60 V more negative than the -200 V on axis plasma potential. This voltage, although not very large relative to the difference between the plasma and the vacuum chamber, is very large in dimensionless units $e\phi/T_e \approx -15$. For a quasineutral plasma, one generically observes $|e\phi|/T_e < 5$.

The rate of rod driven transport is obtained by first measuring the total loss rate as a function of neutral pressure. Neutral pressure is controlled by varying the neutral gas injection rate through a leak valve, and also by varying the pumping speed. Plotting those results produces a plot like the one shown in figure 3.13. Extrapolating to zero neutral pressure yields the losses that are unrelated to neutrals. The losses not due to neutrals are attributed to the rods because doubling the number of rods very nearly doubles the loss rate at low neutral pressure [56].

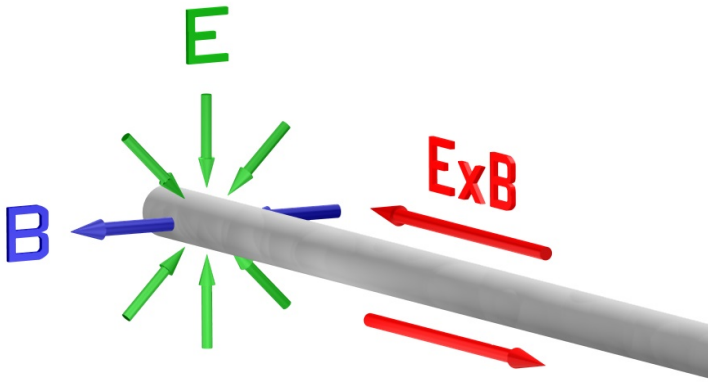

Figure 3.12: This figure from the paper by Berkery shows a schematic of rod driven transport [8]. The confining magnetic field and the electric field from the negatively charged rods causes $E \times B$ drift along the rods. This drift results in net transport of electrons from higher density regions on the inner surfaces to lower density regions further out.

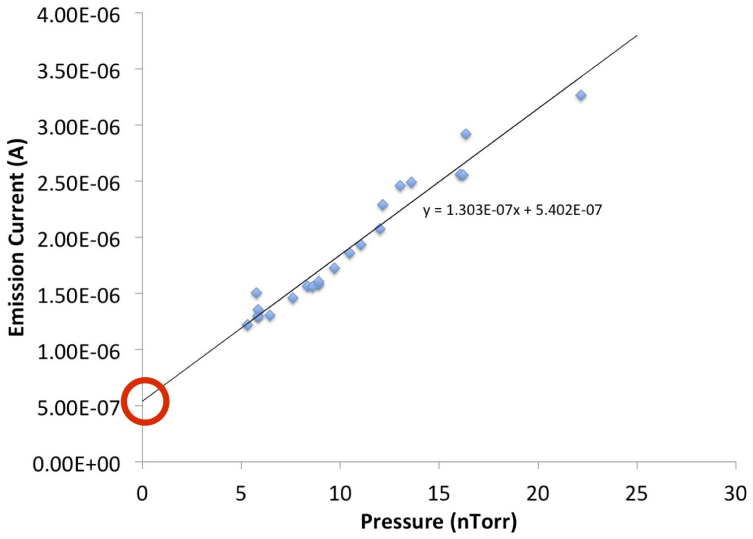

Figure 3.13: This figure demonstrates the method used to measure rod driven transport. Extrapolating to zero pressure gives the rate of transport attributed to pressure independent effects. Previous studies indicate that the pressure independent losses are is primarily due to the perturbation of the rods. These results are for a 0.055 T magnetic field and -200 V emission bias.

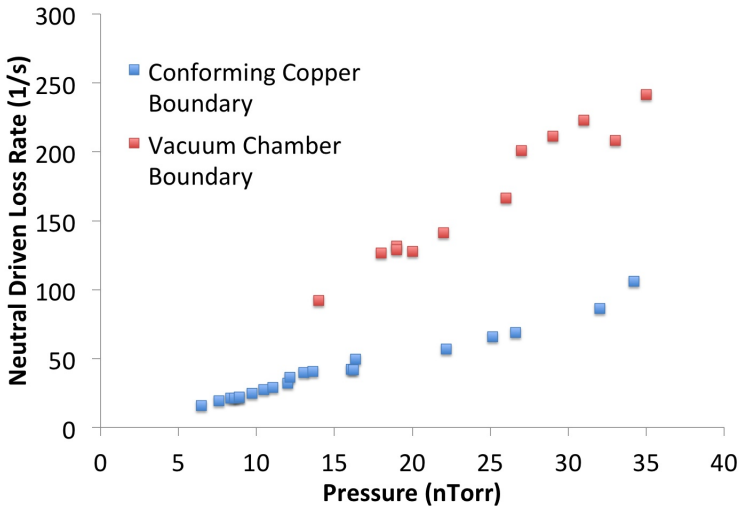

Figure 3.14: A comparison of the pressure dependent loss rate before and after the installation of the conducting boundary demonstrates smaller than anticipated improvement with the conducting boundary installed, as a result of misalignment of the conducting boundary. These results are for a 0.055 T magnetic field and -200 V emission bias.

After installation of the conducting boundary, confinement improved, although not exactly as expected. It was expected that the most significant effect of the conducting boundary would be an improvement in the match between equipotential and magnetic surfaces. In that case the neutral driven transport would be much reduced, given the improved orbit quality. Figure 3.14 shows the neutral driven loss rate versus neutral pressure. The rod driven loss rate was subtracted from the total loss rate each point to find this data. Only a modest factor of two reduction is seen in the neutral driven (collisional) transport. This improvement alone is not enough to account for the observed increase in confinement time.

Table 3.1 shows a comparison of the transport losses before and after installation of the conducting boundary. These measurements suggest that a reduction in rod driven transport is responsible for much of the large improvement in confinement measured at low pressures. The rod driven transport was reduced by roughly a factor of four. A fit of the rod driven transport results with the mesh installed indicates a $\sim B^{-1.8}$ scaling (figure 3.16). This is in contrast to the B^{-1} scaling that was observed before the installation of the conducting

	w/o Boundary	w/ Boundary
Electron Inventory	1×10^{11}	3×10^{11}
Total Loss Rate	135 s^{-1}	38 s^{-1}
Rod Driven	111 s^{-1}	27 s^{-1}
Neutral Driven	24 s^{-1}	11 s^{-1}
Confinement Time	7 ms	26 ms

Table 3.1: Installation of a conducting boundary conforming to the last closed magnetic surface has improved confinement, primarily a result of decreased rod driven transport, while the neutral driven transport remains significant. These are projected results for a 0.055 T magnetic field, 5 nTorr base pressure, and -200 V emission bias.

boundary [8]. These scalings were compared to simulation by Benoit Durand de Gevigney and results with the conducting boundary were found to be in good agreement [23, 25].

We interpret the factor of 16 improvement in confinement time obtained for steady state plasmas during this thesis as a combined result of four distinct means of transport reduction:

- **Conducting Boundary Related Improvements:** Two of the improvements resulted from the installation of the conducting boundary
  - **Neutral Driven Transport Improvement:** The results presented in this chapter indicate that for a fixed electron-neutral collision frequency, electron-neutral transport has decreased by roughly a factor of two after installation of the conducting boundary. This confirms the hypothesis that a conducting boundary conforming to the outermost magnetic surface should improve orbit quality and therefore confinement significantly. The hypothesis was based on the numerical and theoretical predictions that a large class of open orbits existed in CNT, before the installation of the conducting boundary, due to the large mismatch between magnetic and equipotential surfaces. The measured factor of two improvement is much less than what was expected from numerical simulations, which predict more than a factor of ten improvement [24]. The lack of quantitative agreement is

likely due to the experimentally verified fact that the conducting boundary intersects a significant volume of the outer magnetic surfaces ($\psi > 0.7$). Therefore, the boundary reduces the confined volume and does not properly establish an equipotential at the last closed flux surface. Despite the observed misalignments, it is clear that the mismatch is reduced and a corresponding factor of two reduction in neutral driven transport is observed.

  - **Rod Driven Transport Improvement:** The experiments and analysis in this chapter shows that the rod-driven transport rate was reduced by a factor of approximately 3-4 after installation of the conducting boundary. This is now understood as resulting from a decrease in Debye length, which implies that the Debye sheath around the rod is smaller, and therefore the rod transport, which occurs primarily in the rod sheath, is smaller. The Debye length decreased because, for the same central plasma potential, the plasma density is 3 times higher than without the mesh, whereas the temperatures is largely unchanged. The decrease in rod driven transport is shown in figure 3.15 and scales with magnetic field strength as predicted by theory [25].

- **Machine Parameter Related Improvements:** The remaining two improvements were the result of operation at improved machine parameters.

  - **Decreased Neutral Pressure:** Improvements to the vacuum in CNT resulted in a reduction of about a factor of four in base pressure, and therefore a factor of four reduction in collisional transport. The vacuum improvement was achieved through a dedicated effort of identification and elimination of leaks, while adhering to ultrahigh vacuum practices. This improvement was an important technical achievement but was independent of the conducting boundary installation and does not involve new plasma physics.
  - **Increased Magnetic Field Strength:** A doubling of the magnetic field strength from 0.1 to 0.2 T reduced overall transport. This was an expected improvement, not indicative of any new physics, or new physics insights.

These improvements resulted in a measured confinement time of 323 ms.

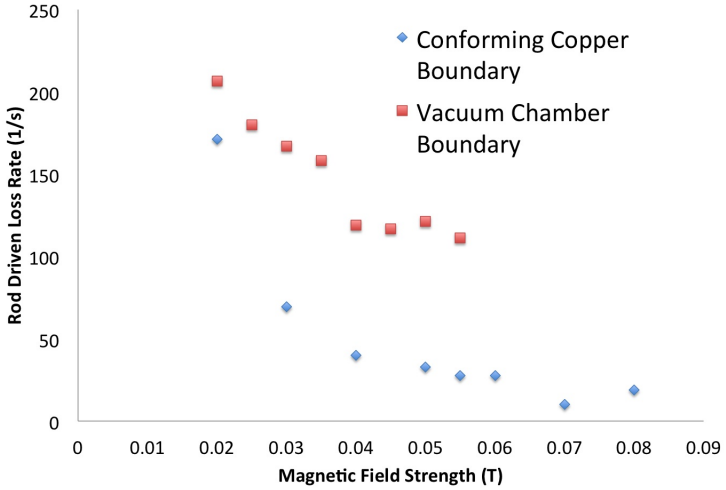

Figure 3.15: This figure shows a comparison of rod driven transport before and after the installation of the conducting boundary. These results are for a -200 V emitter bias.

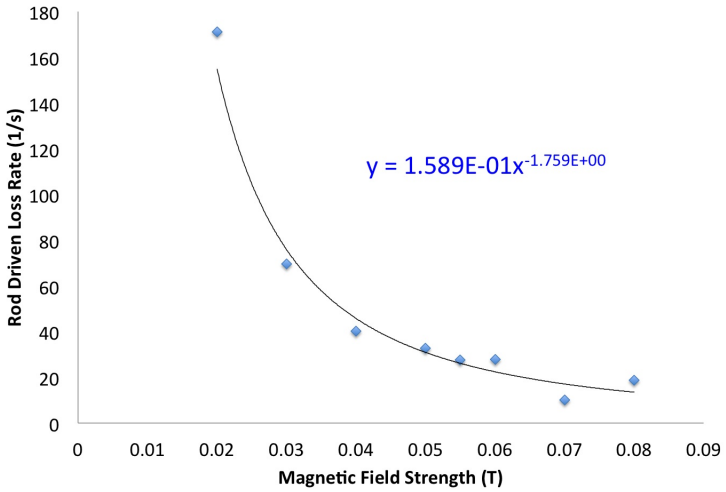

Figure 3.16: This figure shows the $\sim B^{-1.8}$ measured for rod driven transport. This scaling agrees well with the $B^{-1.9}$ scaling predicted by simulations [23, 25].

3.4 Conclusions

Two primary sources of transport have previously been identified in CNT: rod driven transport and neutral driven transport [8]. The installation of a conducting boundary in CNT successfully reduced the transport due to both of these sources. With the boundary installed a smaller Debye length was measured resulting in a reduction in rod driven transport. The boundary was installed to improve the match between equipotential and magnetic surfaces. Measured reductions in neutral driven transport are interpreted as an indication that the match was improved. However challenges aligning the boundary limited the improvement to less than numerically predicted values.

Installation required the development of techniques to align the boundary to the complex geometry of the magnetic surfaces. Alignment was achieved using comparisons to CAD drawings, field line visualizations, and the light emitted by the copper boundary when excited by energetic electrons. Field line visualization was the most used technique for aligning the conducting boundary as a result of its ability to quickly provide information about the three dimensional shape of the magnetic surfaces. These field line visualizations have since been regularly used when aligning probes in the magnetic surfaces.

Although the conducting boundary improved confinement time it was never properly aligned to conform to the last closed magnetic flux surface. The boundary intersected and grounded surfaces at $\psi > 0.7$ resulting in a reduced confining volume. The conducting boundary was not properly aligned because it deformed after installation. Ceramic insulators that were used to hold sectors together were too fragile and not structurally rigid enough to support the weight of the boundary. Furthermore, the large size of the top sector caused it to deform under its own weight. Portions of the top sector were removed to limit the amount that sectors intersected good magnetic surfaces. As a result of these deformations and misalignments the conducting boundary was never properly conforming. A factor of two reduction in neutral driven transport has been measured and is attributed to the improvement in equipotential and magnetic surface match. A measurement of the improvement from a very well conforming boundary was not achieved.

Nonetheless, the fundamental hypothesis that reduction of this mismatch should lead to significant confinement improvements was confirmed. Future experiments are expected to

see similar or even larger benefits when operating with a conducting boundary in place. A few design improvements were identified for future conducting boundaries. A next generation conducting boundary should include structurally rigid methods to connect segments while maintaining electrical isolation and methods to easily adjust boundary segments without removing the segments from the chamber. Also, a design that allows the conducting boundary to be larger than the last closed flux surface would provide space for a limiter and assure that good surfaces are not cut off. Finally the use of a roamer arm during installation would provide accurate measurement of the boundary location relative to predicted magnetic surface location. This should significantly simplify the alignment process. With these improvements a properly conforming conducting boundary should be able to provide a full test of the improvement from well matched equipotential and magnetic surfaces as well as the full diagnostic capabilities previously described for capacitive sector probes.

Chapter 4

Confinement of Plasmas After Emitter Retraction

At the 1 nTorr neutral pressure achievable in CNT the perturbation caused by the insulated rods that hold emitters on axis is a major source of transport [8, 13, 14, 56]. Furthermore, operation without internal rods is necessary for confinement of positron-electron plasmas. For these reasons an emitter capable of creating plasmas then being removed faster than the confinement time was built and installed [9]. This retractable emitter was designed to be a simple way to study long lived plasmas not limited by rod driven transport. Initial expectations were that after retraction the remaining plasma would decay on a time scale longer than the steady state rod perturbed confinement time [8, 9].

Measurements of decay time after retraction will be shown in this chapter. Contrary to prediction, these measurements indicate that plasmas without internal objects have shorter confinement times than steady state plasmas over the range of conditions achievable in CNT. Experiments presented here indicate that plasmas without internal objects are limited by a build up of ions in the plasma after retraction. The longest measured decay time after the retractable emitter has left the last closed flux surface was 92 ms.

In this chapter results are presented exploring plasmas without internal objects. The development and use of diagnostics created to study plasmas without internal probes will be described. Results of experiments without internal objects will be presented and evidence that ion accumulation limits decay time will be presented. These results and their

implications will be discussed.

4.1 Introduction

Confinement of steady state pure electron plasmas is primarily limited by two sources of transport in CNT: transport driven by neutral gas collisions and transport driven by the insulating rods [8]. The method used to measure neutral driven and rod driven transport was described in section 3.3 and illustrated in figure 3.13. Under normal operating conditions, losses that scale linearly with neutral gas pressure dominate for neutral pressures above 10 nTorr. At neutral pressures below 10 nTorr the neutral driven transport can be less than rod driven transport as was shown in table 3.1. CNT is routinely capable of operating at neutral pressures as low as 1 nTorr where the insulating rod that holds the emitter on axis creates a dominant source of transport. This motivated the creation of a retractable emitter so that plasmas that are not limited by rod driven transport could be studied [9].

Operation without internal rods not only removes a major source of transport but is also necessary for confinement of positron-electron plasmas. The negatively charged rods currently act as a sink for ions in steady state plasmas, and this limits ion accumulation in the confining region [7, 8]. Injected positrons would be similarly attracted to the rods introducing a large loss mechanism as positrons annihilate on the rods. Thus positrons would be lost faster than the time required for a positron to fully explore a surface [82]

$$\tau_p = \frac{2\pi R_0}{i\sqrt{T_p/m_p}} \approx 10\mu s \tag{4.1}$$

This assumes that plasmas can be made with cold positrons such that $T_e \approx T_p \approx 4eV$, a plasma major radius $R_0 = 30$ cm, and a rotational transform $i \approx 0.1$.

The majority of other pure electron plasma experiments emit from outside the plasma either using electron guns [43,45,46,86,88] or by first filling the confining region with electrons before negatively biasing a grid in front of the emitter to isolate the plasma from the emitter [65, 69, 78]. To study rod-free plasmas, an emitter capable of pneumatically retracting in 20 ms has been installed and is now routinely operated [9]. Plasmas are created by emission on the axis and can be confined for 337 ms (more than 10 times longer than the retraction time) as shown in section 5.2. It was expected that the absence of rods would significantly

improve confinement since the rod driven transport is dominant at low neutral pressures. Surprisingly, early measurements indicated that plasmas disappear during retraction (Section 4.3). This puzzling and disappointing result hindered progress until the reasons behind the short lived plasmas were discovered. As described in detail in section 4.3.2, we interpret the following observations as indication that the short decay times measured after retraction are the result of ion buildup in the confining region:

- **Neutral Gas Dependence:** Plasmas measured after retraction are more strongly pressure dependent than steady state plasmas. Decay times are only long enough to be measured at neutral pressures below 10 nTorr of nitrogen. Measured decay times after retraction are longer when the dominant neutral gas is helium as opposed to nitrogen at similar total neutral gas pressure.

- **Emitter Bias Dependence:** Short decay times are measured for emitter biases more negative than -40 v. For biases less negative than -40 v an abrupt increase in decay time is observed.

4.1.1 The Retractable Emitter

The retractable emitter uses a pneumatic system to pull a filament from the magnetic axis to outside the last closed flux surface within 20 ms. It was designed and constructed by Jack Berkery [9] and is shown installed on CNT in figure 4.1. The filament is held on axis in the thin cross section by a stainless steel tube insulated with alumina. Figure 4.2 shows the retractable emitter inside of the chamber and fully retracted while a visualization is created from an emitter outside of the image. The location of the retractable emitter was chosen to be in the thin cross section of the plasmas to minimize the physical distance between the axis and last closed flux surface thereby minimizing retraction time. Unless otherwise noted for the experiments reported in this chapter the retractable emitter was operated as described in the paper by Berkery et al. [9] with a driving gas of 40 psig helium and neutral gas dominated by nitrogen. A steady state plasma was created with the retractable emitter positioned on the magnetic axis. Then the filament was retracted to outside the last closed flux surface while emitting. The bias voltage on the filament was then slowly brought to

zero many seconds later.

4.2 External Probes

Confinement times measured from the steady state emission current (labeled "method I" in section 2.3.2) have been used successfully for all steady state confinement studies in CNT. However, new measurement techniques must be developed to study plasmas unperturbed by insulating rods. These techniques needed to be capable of measuring plasma properties from outside the plasma. The low densities found in CNT eliminate the possibility of using many probing methods used for quasi-neutral plasmas. Four diagnostics were evaluated and are summarized below:

- **Fixed Current Probe:** A filament forced to always emit a small current (20 nA) using a current source can measure the local potential created by CNTs large space charge. After retraction the local potential will decay as electrons are lost. The fixed current probe can measure voltages that change as fast as 10V/ms and is thus capable of measuring the decay of plasmas after retraction. This probe was also successfully used as a plasma potential diagnostic providing good agreement with deviation potential measurements. The fixed current probe was labeled "method II" of measuring confinement in section 2.3.2.

- **Fixed Voltage Probe:** A filament held in the plasma at a fixed voltage that is less negative than the local potential does not produce net electron emission. When the plasma is terminated the plasma potential will decay and the time when emission begins indicates the time required for the local potential to drop below the probe potential. This method was successfully used to measure the confinement times of steady state plasmas. However, the challenges presented for use with plasmas after retraction and the large number of shots required for one confinement time measurement made this method less practical for confinement time measurements than the fixed current probe. The fixed voltage probe was labeled "method III" of measuring confinement in section 2.3.2.

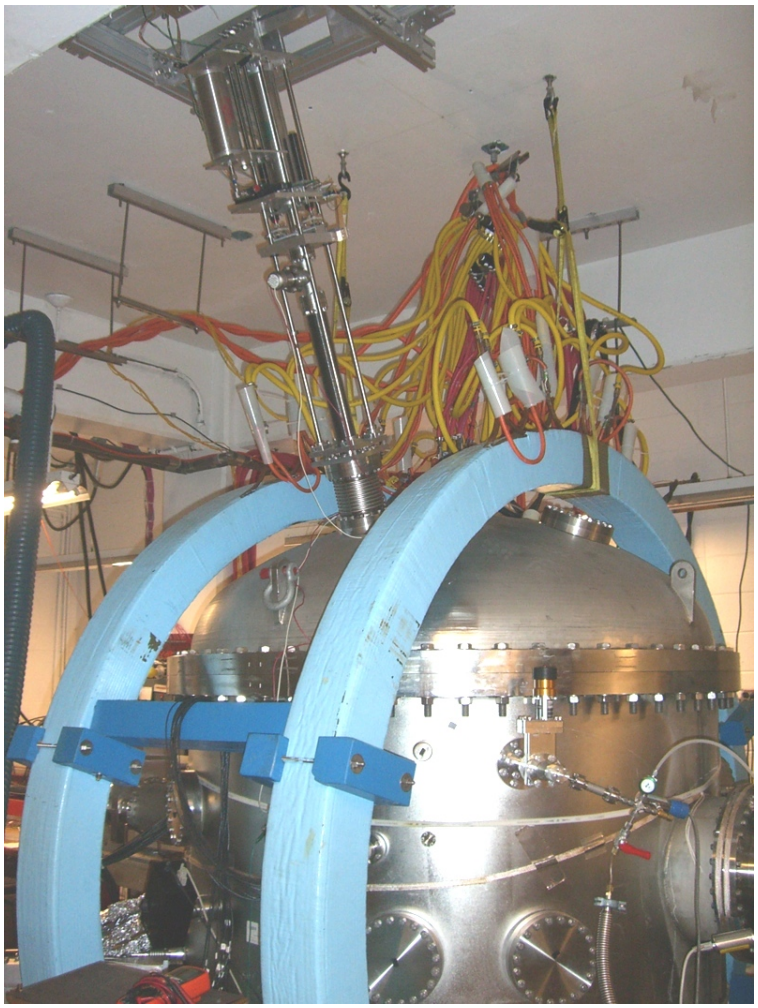

Figure 4.1: This photograph shows the retractable emitter installed on CNT. It is attached to the ceiling and connects to the vacuum chamber via a flexible bellows that allows for position adjustments.

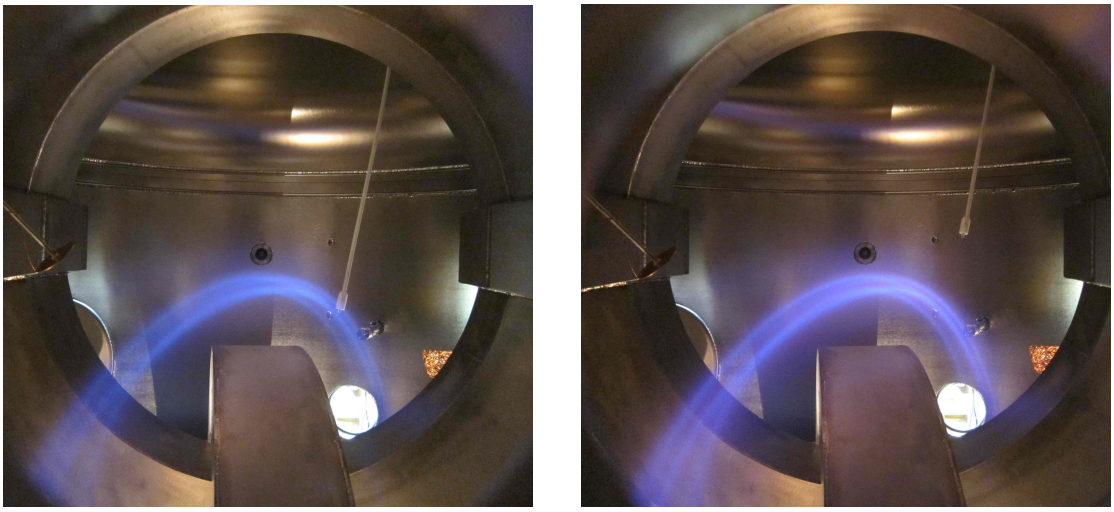

On Axis Retracted

Figure 4.2: A picture inside the chamber looking through the top interlocking coil is shown with the retractable emitter positioned on axis and fully retracted out of the magnetic surfaces. A visualization is created with an emitter positioned out of the image.

- **Conducting Boundary Sector Probes:** Sectors of the conducting boundary provide multiple methods to diagnose plasmas externally. Image charge is induced in the sectors by the large space charge of the plasma. A proper measurement of the image charge decay after the emitter has been removed can be used to find confinement time. Also, biasing one sector should result in a change in image charge on other sectors that depends on the presence of the plasma. Attempts to use these methods to study plasmas after retraction were unsuccessful due to the large amount of current collected by the sectors. To properly use these methods a limiter sufficient to collect plasma electrons before they intersect the conducting boundary should be installed. Electrons emitted by the retractable emitter after it leaves the last closed flux surface create a similar problem when they are intersect the conducting boundary.

- **Limiter Probe:** A limiter probe designed to collect electrons as they reach outer flux surfaces can provide another measure of confinement time. As electrons are lost after retraction the flux of electrons collected by a limiter probe should provide an indicator of the number of electrons reaching outer surfaces. However, the limiter probe designed

for use in CNT with the conducting boundary was removed when misalignments in the conducting boundary caused the limiter to cut off surfaces too deep in the plasma. Later attempts to use sectors of the conducting boundary that were known to intersect surfaces were again unsuccessful. This was due to the interference of electrons emitted by the retractable emitter after it left the last closed flux surface. Furthermore, it was found that all segments of the conducting boundary collected current in steady state. This indicates that even a properly aligned single limiter could miss a significant portion of electrons as they are quickly lost on outer surfaces.

The two most successful methods (fixed current probe and fixed voltage probe) will be described in more detail in the sections below. The fixed current probe (method II) was found to be the most precise and efficient external probing method. As a result the fixed current probe was used for all experiments reporting confinement time after retraction. The fixed voltage probe (method III) was used primarily to confirm the results of the fixed current probe.

4.2.1 Fixed Current Probe

The fixed current probe provides an effective diagnostic for non-perturbatively measuring confinement time. It is comprised of an emissive filament and a current source circuit. The current source is designed to adjust the voltage of the filament so that it always emits a constant 20 nA current. This small emission requires that the voltage on the probe be slightly more negative than the local floating potential. Voltage measurements with the fixed current probe show agreement with deviation potential measurements as shown in figure 4.3.

The fixed current probe is well suited for measuring the decay of plasmas after the retractable emitter has been removed because of its ability to measure local potentials in real time. Vacuum tests showed that the probe is fast enough to measure 200 V potential changes from a biased plate as fast as 1 ms. First, a simple test of the fixed current probe was performed. The probe was placed at the edge of the plasma. Transient plasmas were created at the axis with a non-retractable emitter. Emission was stopped by opening a high speed relay to quickly float the emitter. When on-axis emission is terminated, the plasma decays resulting in a corresponding decay in the potential. This decay is measured at the edge of

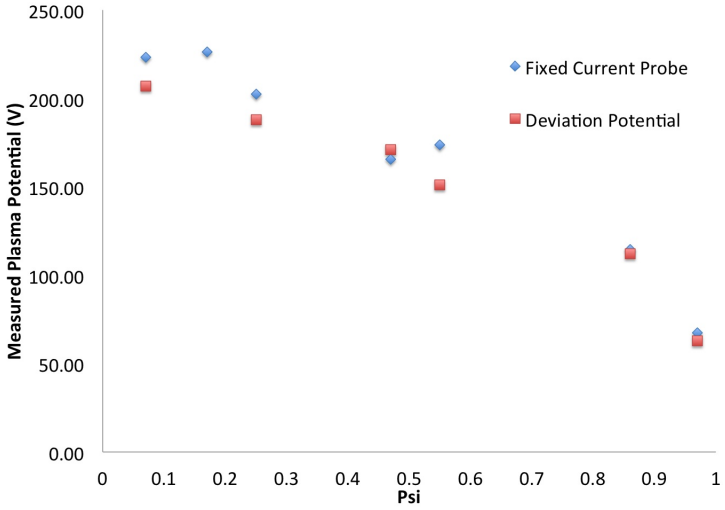

Figure 4.3: A comparison of local potential measured by the fixed current probe to plasma potential measured by deviation potential shows acceptable agreement. The deviation potential at $\psi = 0.13$ could not be measured due to confinement jumps as described in section 4.2.1.

the plasma by the fixed current probe. Figure 4.4 shows the results of such an experiment. When the relay closes, the heated filament on axis is connected to a -200 V bias and begins emitting. This causes the filament to begin emitting and the voltage measured at the edge to become more negative. One issue with this experiment is: Emission current decays but does not stop completely when the relay is opened. This is the result of the capacitance to ground for the wired filaments used in CNT measured to be 2×10^{-10} F. The capacitances results from the meter of in vacuum wiring surrounded by metal feedthrough and bellows. An estimate of the charge stored by this capacitance can be made with $Q = CV$. For the -200 V emitter biases commonly used in CNT this results in a stored charge of 2.5×10^{11}. This indicates that the capacitance is capable of storing a charge comparable to the 3×10^{11} total electron inventory in the plasma and cannot be avoided without a relay inserted inside the ceramic rods near the filaments. Thus the plasma decays supported by a decaying emission from the heated filament.

The decay of the edge voltage is measured using the fixed current probe. This decay is fit with an exponential as shown in figure 4.5 resulting in a 7 ms confinement time for this case. This is in close agreement with the steady state confinement time (method I) of 6.5 ms

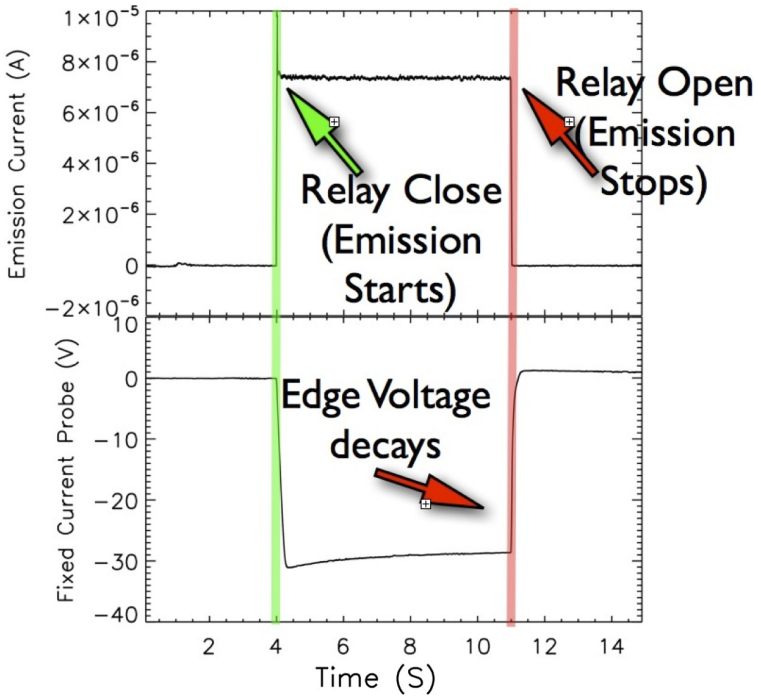

Figure 4.4: A demonstration of how the fixed current probe can be used to measure confinement time. At 4 s a plasma is created by biasing an on axis heated filament. At 11 s a relay is opened causing that filament to floated and the plasma is allowed to decay. The fixed current probe measures the evolution of the edge potential. This data has been smoothed for demonstrative purposes. A close up of the data behind the red bar is shown in figure 4.5.

measured in this shot from on-axis emission current. Figure 4.6 shows agreement between confinement times measured from the on axis emission current to times measured with the fixed current probe despite the non-zero on axis emission during decay.

One major weakness of this method was discovered and is shown in figure 4.7. Results indicate that the small emission currents used by the fixed current probe to measure the local potential are capable of maintaining plasmas in the magnetic surfaces. This was only observed when the probe was placed on surfaces near the last closed flux surface. Potential measurements in steady state plasmas indicate that there is a stronger electric field in this region. In this figure surfaces at 27 cm and larger were intersected by the grounded conducting boundary allowing for good measurements. Thus it was found that the fixed

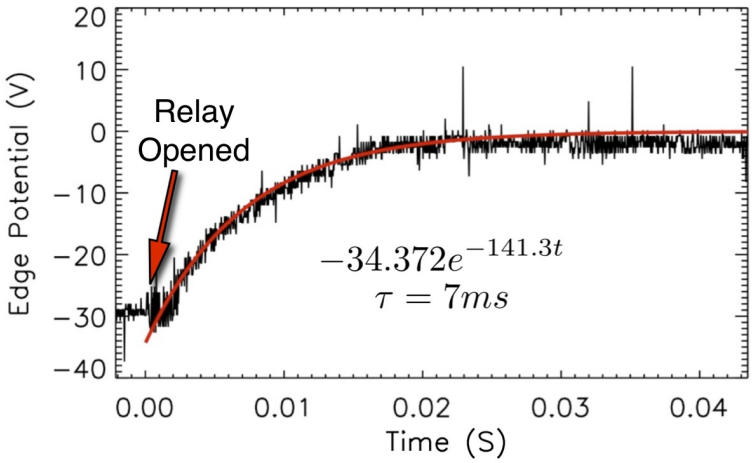

Figure 4.5: On-axis plasma emission is halted at time zero. An exponential (red) is fit to the data resulting in a measured confinement time of $\tau = 7$ ms. These results are for a 0.02 T magnetic field, -200 V emission bias, and neutral gas pressure of 6 nTorr.

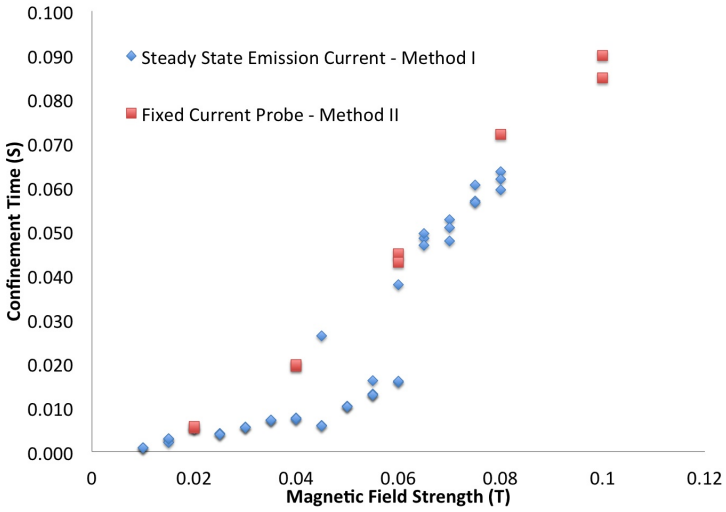

Figure 4.6: Confinement times measured from the emission current and the fixed current probe are in good agreement.

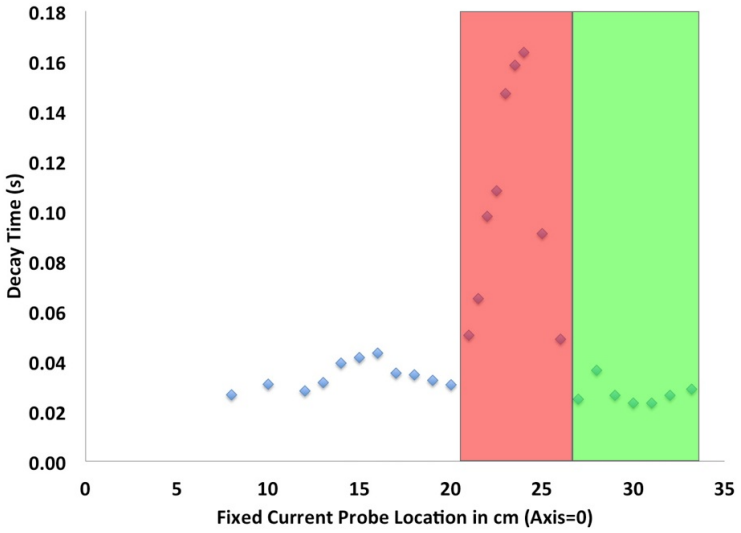

Figure 4.7: The 20 nA emission current emitted by the current source probe results in slow plasma decays when the probe is placed on a surface near the plasma edge. Here the conducting boundary sets the potential to zero on the surfaces at 27 cm and larger (green). The region between 21 cm and 27cm (red) connects the bulk plasma on inner surfaces to grounded conducting boundary at the edge. There is a stronger electric field in this region as the very negative potential on inner surfaces changes to ground over this short distance.

current probe measures confinement times in best agreement with emission current times when placed on a field line that is grounded on both sides. After the boundary was removed free standing plates were installed and aligned to a field line outside of the last closed flux surface as shown in figure 4.8. This setup allowed for accurate confinement time measurements without allowing the probe to create or extend the lifetime of confined plasmas. The final iteration of the fixed current probe used a grounded copper rod to hold the filament. The rod and filament were surrounded by a concentric copper cylinder 15 cm in diameter to ground the field lines that intersect the filament. This entire setup was affixed to a port on the vacuum chamber so that the probe was always available to measure confinement times when needed.

The fixed current probe not only allows for measurements of transient plasmas but also offers a fast potential diagnostic for steady state plasmas. The probe can be set to emit

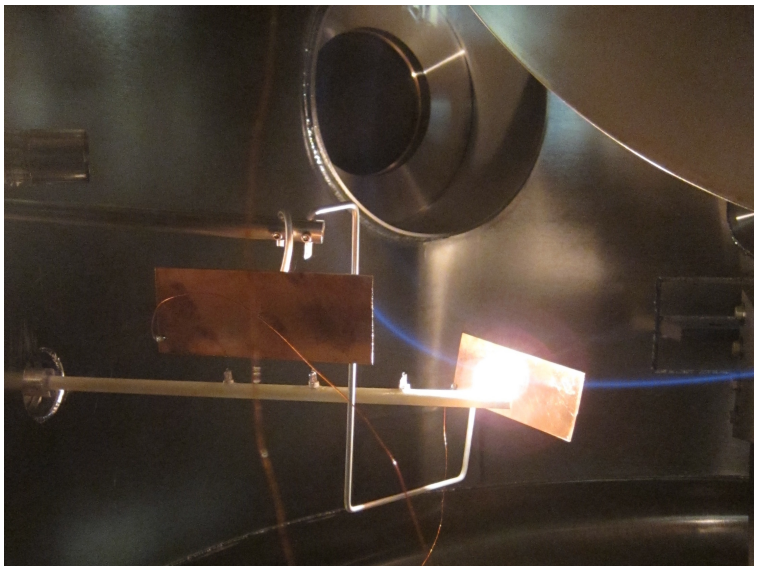

Figure 4.8: Here the grounded metal plate on the left has already been well aligned and the blocker on the right will be adjusted to cut off the field line. These blocking plates improved the quality of measurements made with the fixed current probe and ensured that the probe would not sustain plasmas with the small emission current it produces.

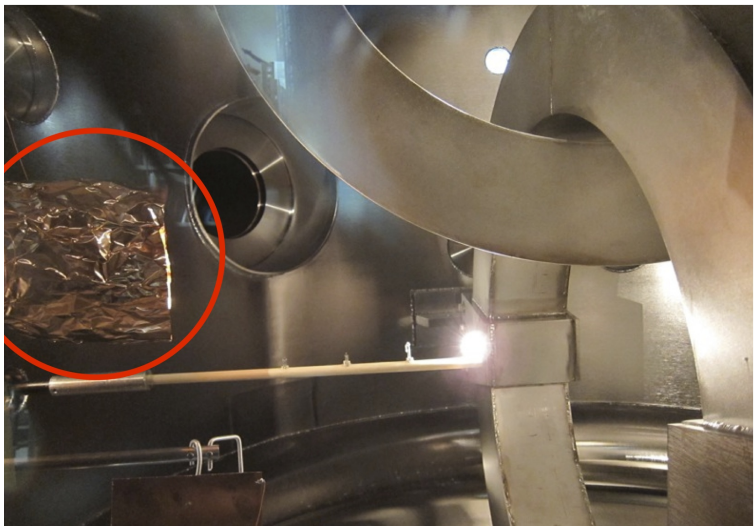

Figure 4.9: This picture shows the final location of the fixed current probe attached to a port on the vacuum chamber. It is away from the interlocking coils and on axis emissive filament and surrounded by a grounded copper cylinder that provides the same blocking as the metal plates shown in figure 4.8.

20 nA. This current creates only a small perturbation in CNT plasmas which typically have more than 1μA on axis emission current. The measurements agree with deviation potential measurements as was shown in figure 4.3 but take substantially less time. The fixed current probe also provides a solution for measurements when the plasma easily switches between two confinement states. In such situations the small perturbation necessary for a deviation potential measurement can cause the plasma to jump between confinement states as the probe voltage is varied. This can makes deviation potential measurements quite challenging as the probe current varies between confinement states. The fixed current probe does not have any similar problem.

4.2.2 Fixed Voltage Probe

A probe utilizing a fixed voltage was also investigated as a method to measure confinement times from the plasma edge. This probe consists of a heated filament set at a constant voltage and a circuit to measure emitted current. The method operates on the principle

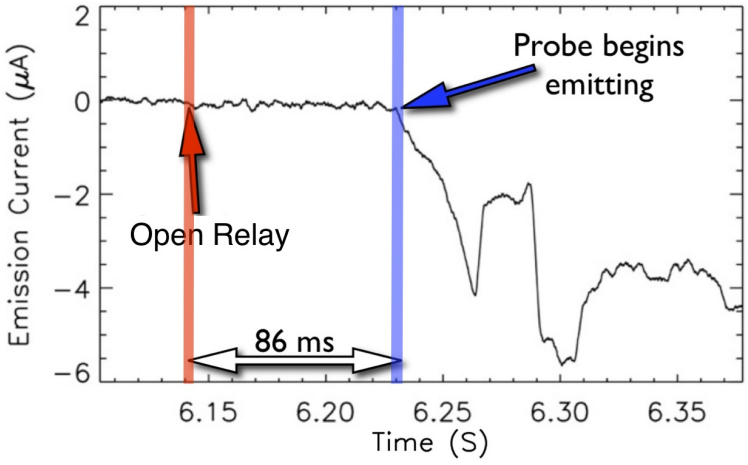

Figure 4.10: A demonstration of the fixed voltage probe. Emission at the axis is stopped (red arrow) and the -25 V probe does not start emitting at the edge until 86 ms later (blue arrow). This provides a single local potential versus time data point that is later used in plots like the one showed in figure 4.11.

that this filament will produce no net emission when the local potential is more negative than the probe potential. The probe will quickly begin emitting once the local potential is less negative than the probe potential. Collected current is negligible because the probe is operated near or outside of the last closed flux surface where density is low.

Plasmas are created by on axis emission and the fixed voltage probe is placed inside the last closed flux surface. When the on axis emitter is suddenly floated the plasma potential will begin to decrease as electrons are lost. The time until the fixed voltage probe begins emitting indicates the time required for the local potential to drop below the fixed voltage set on the probe. This technique is demonstrated in figure 4.10. Individual potential versus time data points are collected by repeating this procedure at various fixed probe voltages. The results are fit with an exponential as shown in figure 4.11 to find a decay time. The data obtained in this way agrees well with confinement times derived from steady state emission measurements (figure 4.12).

Although the fixed voltage probe provides a straightforward method to measure confinement times in steady state from the plasma edge it was not successfully used with the retractable emitter. Attempts to measure voltage versus time data points using the fixed

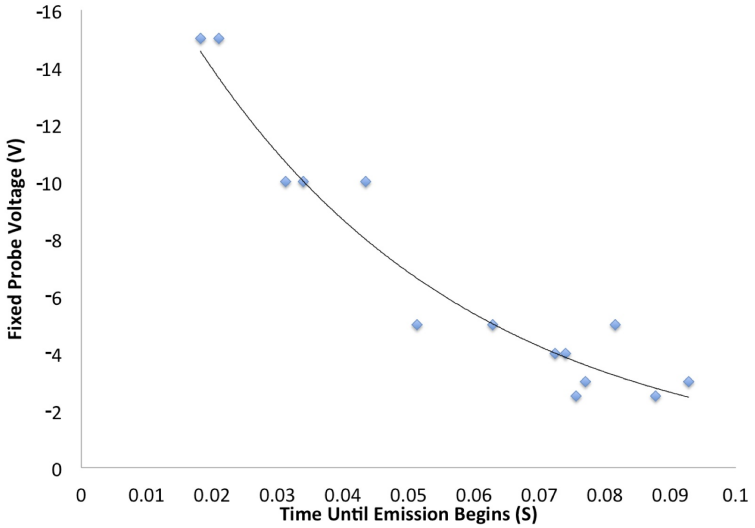

Figure 4.11: An exponential fitted to the points measured by the fixed voltage probe provides a confinement time. In this example at 0.04 T and 3 nTorr the confinement time was found to be 40 ms by this method.

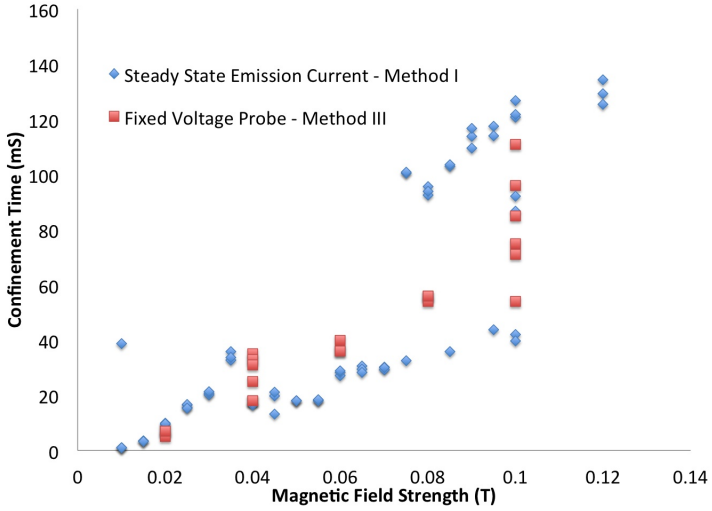

Figure 4.12: Confinement times measured by the fixed voltage probe are similar to times measured from emission current. Multiple confinement states are evident in this data which make measurements with the fixed voltage probe challenging. This challenge as well as the need to take multiple shots to measure one confinement time resulted in the fixed current probe being used more extensively than the fixed voltage probe.

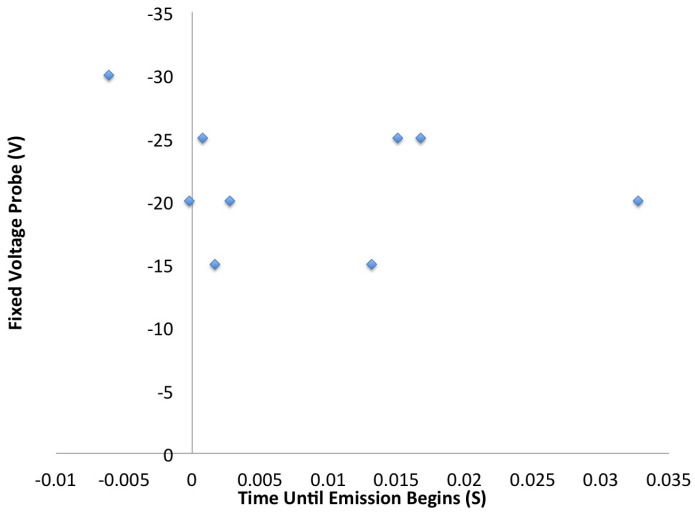

Figure 4.13: Measurements made with the fixed voltage probe after emitter retraction varied substantially from shot to shot and could not be used to successfully calculate a confinement time.

voltage probe produced erratic results after retraction. Figure 4.13 shows that it was even possible to measure probe emission before the retractable emitter had left the plasma. As will be explained in section 4.2.3, measurements with the retractable emitter present new challenges. The retractable emitter can create a measurable potential perturbation as it is retracted which causes the fixed voltage probe to begin emitting at times unrelated to the decay of the plasma. Instead, methods to measure confinement times after retraction focused on the fixed current probe which does not require multiple shots to measure one confinement time.

4.2.3 Measuring Confinement After Retraction

Additional challenges needed to be overcome to measure confinement times after retracting the retractable emitter. Section 4.2.2 already describes how the fixed voltage probe was unable to measure confinement with the retractable emitter. Instead, the use of the fixed current probe for retractable emitter experiments was explored extensively. The main challenges were the perturbation created by the retractable emitter and the unexpected behavior of plasmas after retraction. The challenges are summarized here:

- **Pressure Dependence:** Measured decay times after retraction change 10 times faster with changing neutral pressure than confinement times for comparable steady state plasmas. During experiments a small vacuum leak increased the neutral pressure to 13 nTorr. Although this decreased steady state confinement times to 50 ms it decreased confinement times after retraction to less than 1 ms which is too short to be measured by the fixed current probe.

- **Retractable Emitter Perturbation:** The retractable emitter's negatively biased emissive filament create a perturbation in the signal measured by the fixed current probe. This substantially reduced the amount of signal that could be used to find confinement times. This effect was reduced by installing metal blockers attached to the conducting boundary to shield probe filament. Dropping the bias voltage on the retractable emitter to zero during retraction removes this perturbation.

Attempts to measure the confinement time after retraction were unsuccessful until these challenges were understood and overcome. The pressure was improved by closing the vacuum leak. The decrease to neutral pressures near 1 nTorr resulted in plasmas that decayed slowly enough to be measured by the fixed current probe. A typical experiment measuring the potential with the fixed current probe after retractable emitter retraction is shown in figure 4.14. This experiment demonstrates the substantial perturbation to the potential measured by the fixed current probe.

The combined effect of installing metal plates on the conducting boundary to ground the field lines intersecting the fixed current probe as described in section 4.2.1 and decreasing the neutral pressure resulted in substantially clearer decay measurements as shown in figure 4.15. Fitting an exponential to the decay of potential measured at the edge results in the in the clear scaling with neutral pressure shown in figure 4.16. This method for measuring confinement time was used for all remaining confinement measurements reported in this chapter.

After the removal of the conducting boundary, perturbations to the the fixed current probe signal were still large even with blockers installed. To address this problem, experiments were performed where the bias on the retractable emitter was dropped to ground during retraction. Dropping the potential before retraction resulted in the emitter collecting

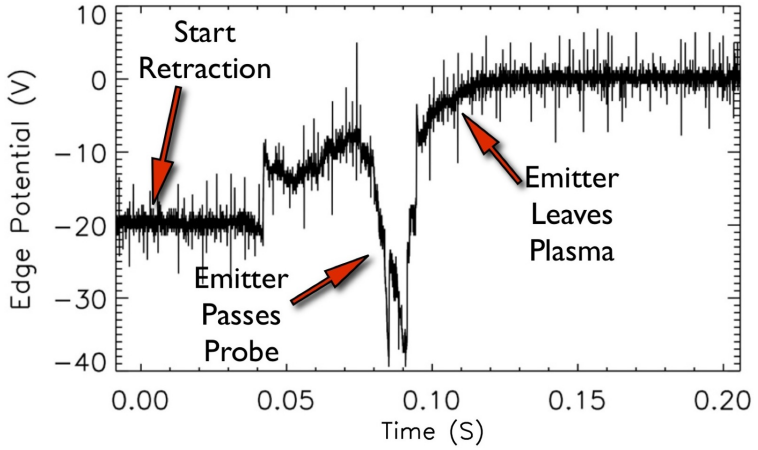

Figure 4.14: Measurements made at the edge of the plasma with the fixed current probe on ungrounded field lines are perturbed by the retractable emitter as it is removed from the plasma.

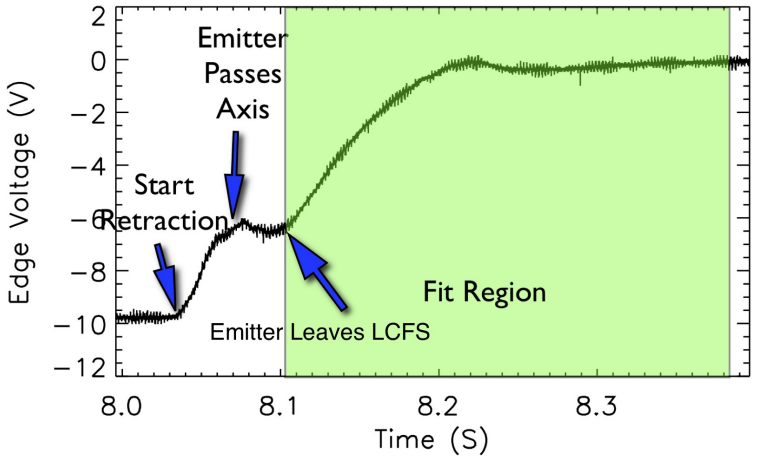

Figure 4.15: With blockers installed the retractable emitter no long creates such a significant perturbation to the voltage signal and a clear fit region is found. This shot was measured at a 0.055 T magnetic field strength, 1.3 nTorr base pressure, and -200V emitter bias.

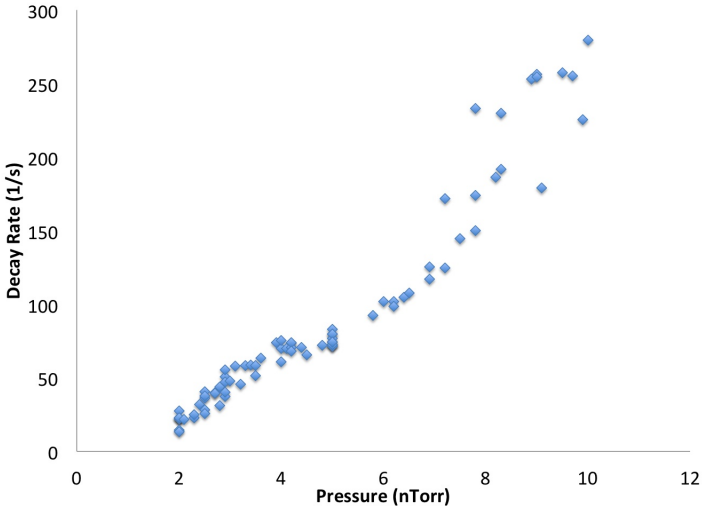

Figure 4.16: Measurements at low pressures (achievable after a vacuum leak was closed) and without the perturbation caused by the retractable emitter show an approximately linear scaling of the decay rate with pressure. Here the inverse of measured confinement time is plotted to show the approximately linear behavior at low pressure. At pressures above 7 nTorr confinement times are below 5 ms and are less repeatable than at lower pressures. At pressures above 10 nTorr confinement times are too small to be effectively measured with the fixed current probe.

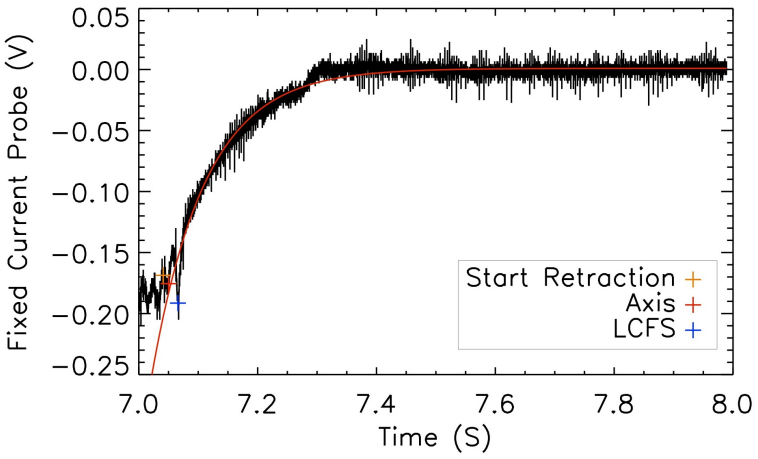

Figure 4.17: In this shot the bias on the retractable emitter is decreased to zero during retraction. This reduces the perturbation measured by the fixed current probe signal. The colored crosses in this figure determine the location of the retractable emitter during retraction.

some plasma as it retracted. However, timing the potential drop to correspond with retraction resulted in nearly unperturbed decays as shown in figure 4.17. Results when the bias is dropped during retraction are in agreement with results for constant bias during retraction (figure 4.18). We interpret this to mean that bias on the retractable emitter does not perturb the well confined bulk plasma during retraction.

4.3 Results After Retraction

Measurement of the confinement time after retracting the emitter revealed unexpected results. Plasmas unperturbed by the presence of an emitter behave differently than the steady state plasmas that were studied previously in CNT. In this section confinement results for plasmas unperturbed by internal objects are presented with an empirical scaling formula, evidence that short decay times result from ion accumulation is presented and the effect of leaving a heated filament in the plasma is discussed.

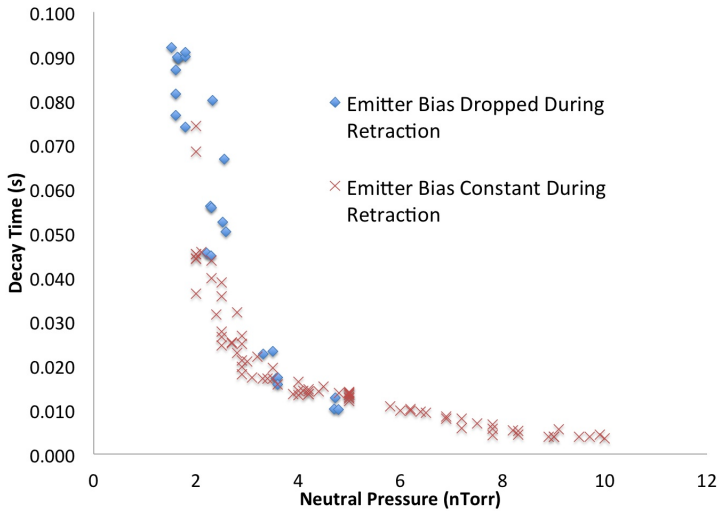

Figure 4.18: Although dropping the bias on the retractable emitter during retraction removes the perturbation to the fixed current probe it does not result in substantially changed confinement times. The longest measured decay time after retraction was 92 ms as shown here.

4.3.1 Results Without Internal Objects

Plasmas measured after the removal of the retractable emitter were originally expected to behave similar to steady state plasmas. The expectation was that removing the insulating rods would remove rod driven transport and result in longer confinement times. Instead the confinement times were shorter than the times for steady state plasmas under similar conditions as shown in figure 4.19. The plasmas measured after retraction still exhibit essentially linear pressure dependence, however decay times after retraction change with pressure 10 times faster than steady state plasma confinement times. Empirical formulas were found for neutral pressure and magnetic field strength scalings by fitting to collected data. A $B^{-1.5}$ scaling was enforced for these fits. This scaling was chosen because it agrees with observed neutral driven magnetic field dependent transport [8]. Also, a theory for anomalous transport in Penning-Malmberg traps predicts a $B^{-1.5}$ or B^{-2} scaling [50, 51]. This is based on an asymmetry-induced transport mechanism when an imposed potential or magnetic asymmetry causes axial particle trapping. The resulting particle loss via the scattering of particles into open orbits may be comparable to losses due to the mismatch in

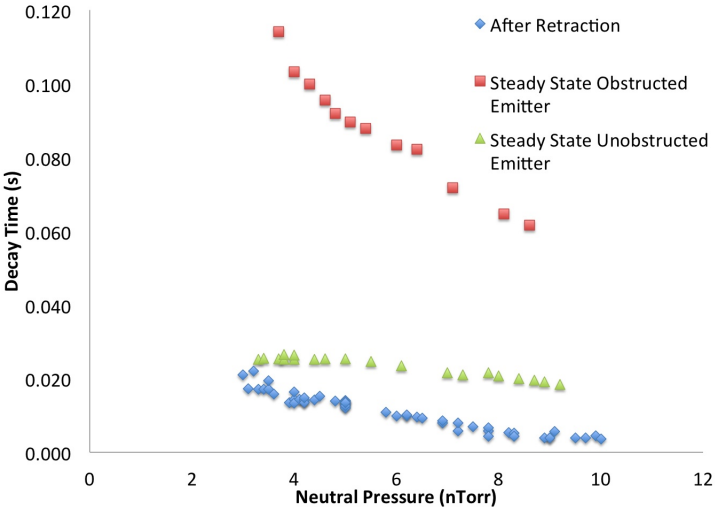

Figure 4.19: This figure shows reduced confinement times for plasmas measured after emitter retraction as opposed to steady state plasmas. These results were measured with the conducting boundary installed, a 0.08T magnetic field strength, -200V emitter bias, and 32° tilt angle. The difference between steady state plasmas emitted with and without obstruction is explained in detail in chapter 5.

magnetic and equipotential surfaces described in section 3.1. The best fit for the coefficients of $B^{-1.5}$ and P_n in an empirical formula for decay rate $(1/\tau)$ was found to be:

$$R = \frac{B^{-1.5}}{3} + 19.6 \times P_n - 27.7 \tag{4.2}$$

Where R is the decay rate in s^{-1}, B is the magnetic field strength in Tesla, and P_n is the neutral pressure of nitrogen in nTorr. This formula can be used to predict confinement times over the range of parameters studied as shown in figures 4.20 and 4.21. Although the $B^{-1.5}$ fits the data well, using other exponents can also result in good fits. This limits the usefulness of this equation to predicting and extrapolating confinement times. This formula has limited benefits for understanding the underlying physics of these plasmas because the exponent can not be confidently determined.

The retractable emitter was designed to emit electrons in steady state at a position past the magnetic axis until retraction begins. Then, as the filament moved through the magnetic surfaces it would fill them with electrons. This would allow the emitter to gain speed before

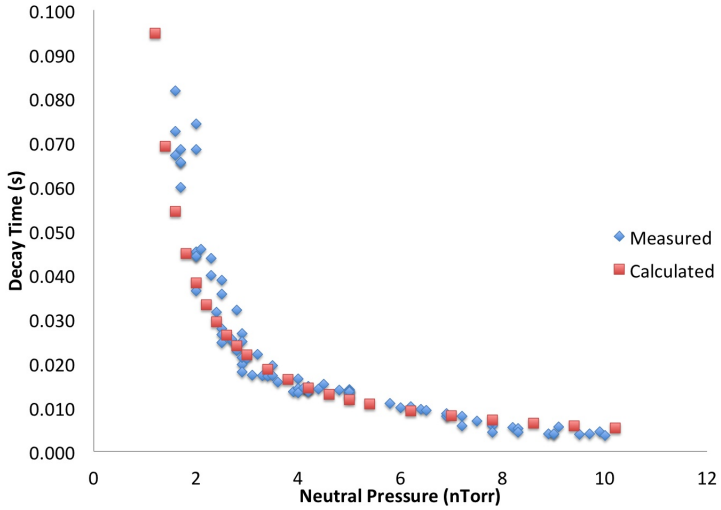

Figure 4.20: Measured pressure trends compared to predictions from empirical formula. These results were measured with the conducting boundary installed, a 0.08T magnetic field strength, -200V emitter bias, and 32° tilt angle.

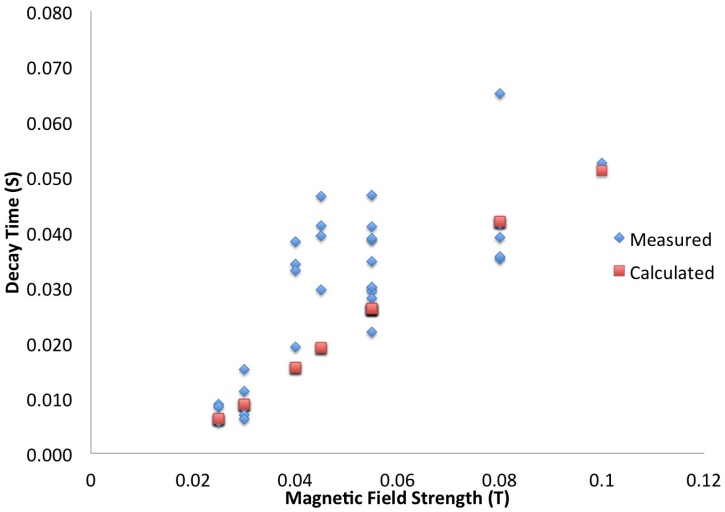

Figure 4.21: Measured B field trends compared to predictions from empirical formula. These results were measured under conditions similar to figure above and a base pressure of 2 nTorr.

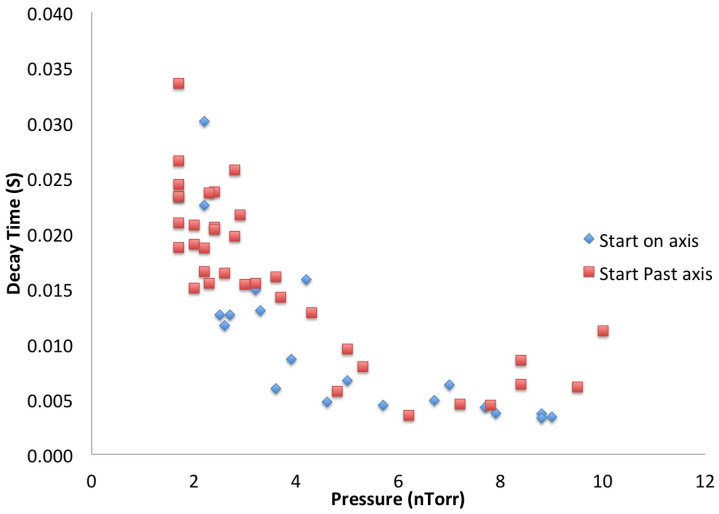

Figure 4.22: The retractable emitter was designed to start past the magnetic axis. This would allow it to gain speed before reaching the axis and thus spend less time between the axis and the last closed flux surface. However, results indicate no large differences in confinement time when starting the retractable emitter on axis or 3 cm past the axis.

reaching the axis and spend less time retracting from the axis to outside the last closed flux surface. However, as shown in figure 4.22 starting the retractable emitter 3 cm past the axis does not substantially change confinement time compared to starting on the axis. A study of the effect of the time required for the retractable emitter to exit the surfaces was also performed. The speed of retraction was varied by changing the pressure of helium used to drive the retractable emitter. Measured confinement times do not indicate a strong dependence on the speed of the retractable emitter. Both of these experiments suggest that transport created by the perturbation from the retractable emitter rod during retraction is small relative to what causes the plasma to decay after retraction.

4.3.2 Why Are Plasmas Short Lived After Retraction?

Multiple possible explanations were considered to explain why plasmas are short lived after retraction. Below is a list of some of the theories that were tested as well as the experiments performed. Each experiment involves a slight modification of the standard retractable emit-

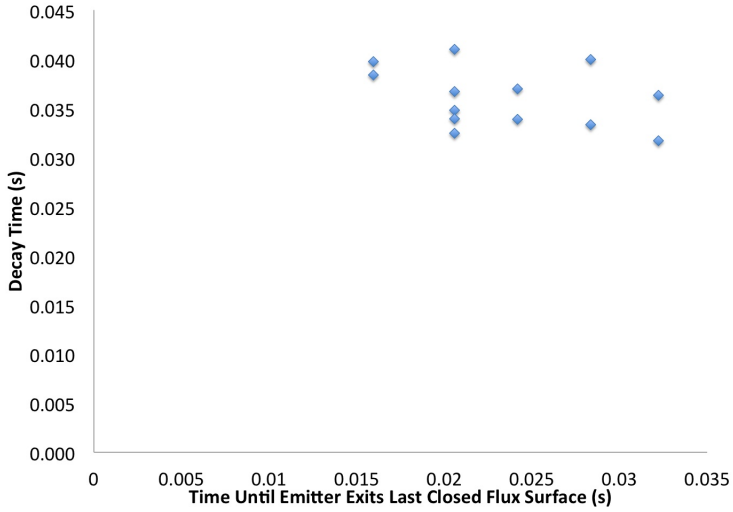

Figure 4.23: Experiments do not indicate a strong effect from the time taken for the retractable emitter to travel between the axis and last closed flux surface.

ter experiment used to collect the results reported in section 4.3.1. In those experiments the filament of the retractable emitter is positioned on the magnetic axis. The filament is biased negatively and then heated, resulting in emission and the formation of a steady state plasma. The filament is then quickly retracted while emitting. After leaving the last closed flux surface the filament is floated and allowed to cool.

- **Theory - Retraction Causes Plasma Collapse:** The negatively biased filament or the negatively charged rod perturb the plasma and moving that perturbation across surfaces could damage confinement.

  - Dropping the bias on retractable emitter filament during retraction still results in relatively short lived plasmas after retraction (Figur 4.18. **Conclusion:** The perturbation from the negatively biased filament is not responsible for short lived plasmas.

  - A plasma created by emitting on axis with the four probe array does not show evidence of increased transport when the retractable emitter is retracted during the shot. **Conclusion:** The potential perturbation caused by moving the negatively charged retractable emitter rod across the magnetic surfaces does not hurt

confinement and is not responsible for short lived plasmas.

- **Theory - Ceramic Rods Prevent Plasma Collapse:** Energetic electrons that collide with the insulated rods result in secondary electron emission that could have a cooling effect which helps maintain the plasma. The negative charge the insulated rods collect also make them a sink for ions which could limit potential ion instabilities.

  – When an additional ceramic rod is positioned within the magnetic surfaces retractable emitter experiments still result in short lived plasmas after retraction (Figure 4.27). **Conclusion:** The removal of the insulated ceramic rod used to hold emitters on axis is not responsible for short lived plasmas.

- **Theory - Filaments Prevent Plasma Collapse:** Heated filaments are capable of affecting the distribution function (presumably cooling the plasma) and their ability to affect plasma equilibrium is demonstrated in section 5.6. Cold filaments are not expected to effect equilibrium.

  – A cold floating filament positioned within the magnetic surfaces during retractable emitter experiments still results in short lived plasmas after retraction (Figure 4.27).
  Conclusion: Cold filaments do not effect the confinement time of plasmas after retraction.

  - A heated filament positioned within the magnetic surfaces during retractable emitter experiments result in long lived plasmas after retraction (Figure 4.27).
  Result: The capacitance to ground for wired filaments in CNT allows emission when the filament is otherwise floating. This emission current is enough to sustain a decaying plasma. However, the heated filament may also affect plasma equilibrium.

- **Theory - Ions Cause Plasma Neutralization:** Ion buildup in the confining region is responsible for short decay times after emitter retraction.

  + Longer confinement times are measured after retraction when the neutral background gas is predominately helium as opposed to nitrogen (Figure 4.24).

Result: Helium's higher ionization energy results in a slower build up of ions resulting in longer decay times than when nitrogen is the dominant background gas.

+ Longer confinement times are measured after retraction when the emitter bias is less negative than -40 V(Figure 4.25).
Result: At low emitter bias electrons are not able to gain energy necessary for the ionization process that results in the rapid production of ions.

These experiments lead us to conclude that a build up of ions in the confining region is responsible for the short decay times measured after retraction. We suggest that these fast decays occur when a self enhancing ionization process quickly increases the ion content in the plasma resulting in ion driven instabilities. This is explained bellow.

Calculations by Jack Berkery indicate that, at 2 nTorr neutral pressure and 4 eV electron temperature in the bulk plasma, complete plasma neutralization would occur in steady state CNT plasmas after 4.5 seconds without a sink for ions [7]. An ion instability has been studied in CNT beginning when the ion content is as low as 10% of electron inventory. Thus if the bulk plasma electron temperature were to remain 4 eV after retraction the ion instability would not be predicted to occur for 450ms. Measurements indicate that decay occurs an order of magnitude faster.

One possible explanation for the faster collapse is a self enhancing ionization process: Ions are created by ionization from energetic tail electrons. As ions accumulate, the plasma potential becomes less negative. Electrons are accelerated to the less negative plasma potential and gain energy. The increase in energy also increases the ionization cross section resulting in a faster ionization rate and closing the cycle. A similar process has been studied by Xabier Sarasola indicating that the plasma potential abruptly decouples from emitter bias as neutral pressure is increased above 1×10^{-6} Torr of nitrogen. His experiments indicate that when the dominant gas is helium, abrupt decoupling does not occur until the neutral pressure is increased above 5×10^{-5} Torr [70].

Figure 4.24 shows a comparison of decay times when the background gas is dominated by nitrogen or helium. Longer decay times are measured for the background neutral gas with higher first ionization energy (24.5 eV for helium) than for the background gas with lower

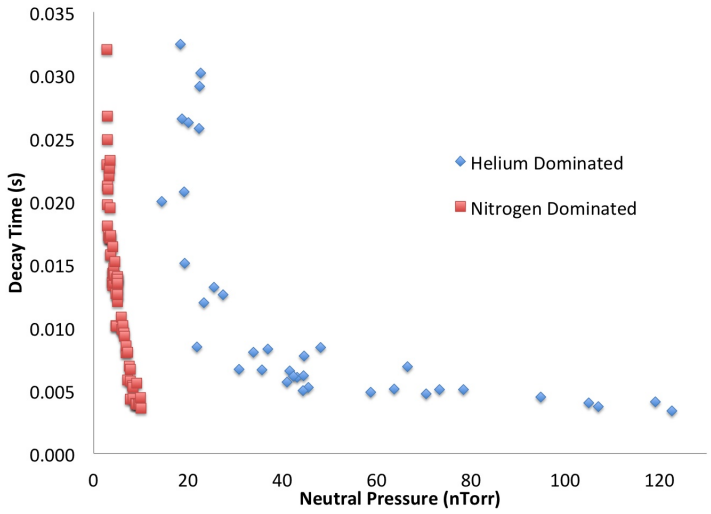

Figure 4.24: Longer decay times are measured when the neutral background gas is dominated by helium than when it is dominated by nitrogen.

first ionization (14.5 eV for nitrogen). At pressures over 10 nTorr of nitrogen the decay time is already at the limit measurable by the fixed current probe. Similar 30 ms confinement times are measured for 2 ntorr of nitrogen and 18 nTorr of helium. Helium dominant results at lower pressures could not be studied due to a leak in the vacuum chamber.

Further results supporting the conclusion that ion buildup results in short confinement time are shown in figure 4.25. A significant increase in confinement time is measured for emitter bias voltages less negative than -40 V. Figure 4.26 shows that the increase in decay times at low emitter bias occurs across magnetic field strengths. Similarly, results by Xabier Sarasola show that, at less negative emitter biases, the neutral pressure where plasma potential abruptly decouples from emitter bias increases. For example, while abrupt decoupling occurs at 2×10^{-6} Torr for a -200 V emitter bias, no abrupt decoupling is measured at neutral pressures up to $5 \times 10^{-}5$ Torr when emitting at -50V [70].

4.3.3 Results With A Heated Filament

The presence of a heated filament within the confining region results in increased decay time as shown in figure 4.27. This figure shows a comparison of confinement times after retraction

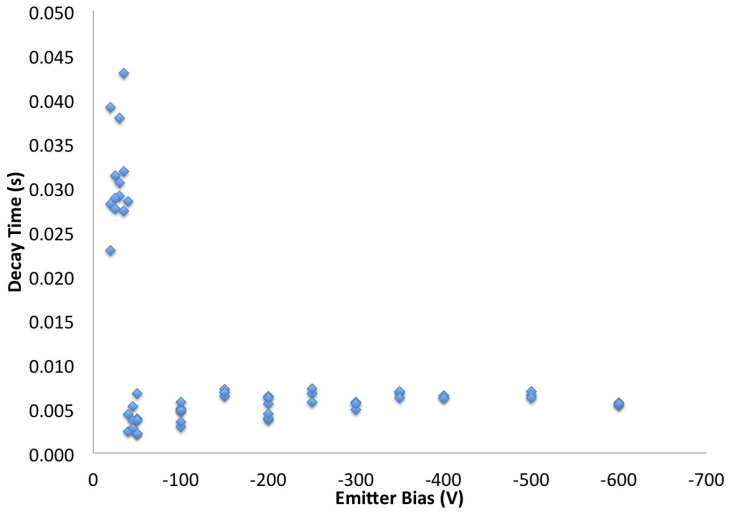

Figure 4.25: Decay time increases abruptly at bias voltages less negative than -40V. This figure includes results with neutral gas pressures of 5 - 7 nTorr and magnetic field strengths between 0.055T and 0.08T. The results more negative than -250V were measured at 5 nTorr and 0.08T while the less negative results were measured at 7 nTorr and 0.055T.

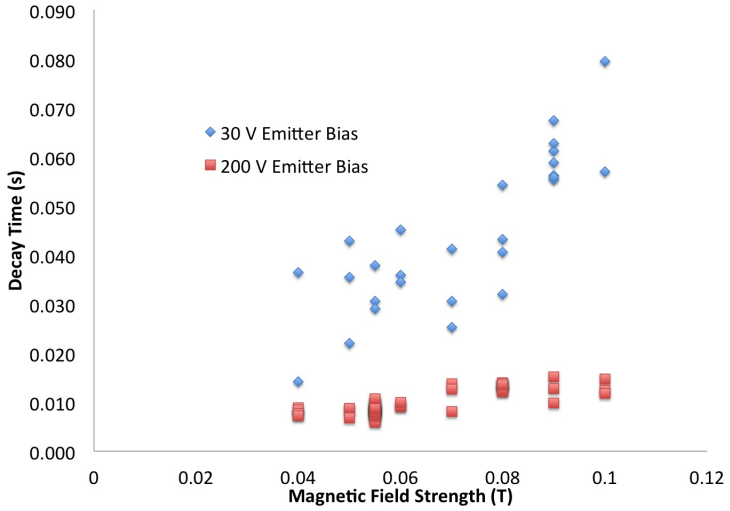

Figure 4.26: The increased decay time shown in figure 4.25 for low emitter bias is consistent across magnetic field strengths. These results are for a neutral gas pressure of 5 nTorr.

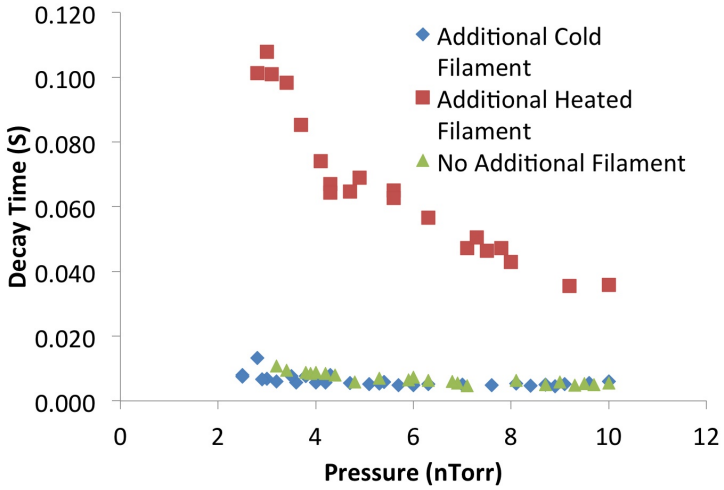

Figure 4.27: The presence of a floating heated filament in the magnetic surfaces after emitter retraction substantially increases measured confinement time. This figure shows a comparison between experiments with a cold filament in the plasma after retraction, a heated filament in the plasma after retraction, and no additional rod inserted. This suggests that the shorter than expected confinement times measured after retraction for plasmas unperturbed by internal objects are related to the absence of a hot (emissive) filament within the confinement region.

for three different cases. The case where an additional cold filament is left in the plasma after retracting the retractable emitter results in short confinement times. Heating that same filament results in substantially longer confinement times. For comparison the case with no additional rod inserted is also shown. Although the insulated rods act as a sink for ions, the presence of a insulated rod still creates rod driven transport and the rods presence does not result in long confinement times after retraction.

This result could be attributed to the capacitance of the wired filament that allows continued emission after the filament is floated. However, results presented in section 5.6 indicate that heated filaments are also capable of affecting a steady state plasma's distribution function. The ability of an individual small heated filament to have a large effect on global plasma equillibrium may appear surprising. However, a calculation of the rate at which electrons interact with the filament supports the plausibility of this result:

$$\#\frac{e^-}{s} = A \times \Gamma = L_{filament} W_{filament} n_{electrons} v_{thermal} \sim 6 \times 10^{12} \frac{e^-}{s} \tag{4.3}$$

This is for a $6 \times 10^{-6}\, m^2$ effective filament area, an electron density of $10^{12}\, m^{-3}$, and an electron temperature of 3 eV. This result means that the entire 3×10^{11} electron inventory could interact with a single heated filament in 50 ms. We have offered one plausible explanation for the improved confinement times with a heated filament by suggesting that the filament is able to lower the overall plasma temperature by collecting hot electrons and re-emiting cold ones. In this assumption the hot electrons would interact with the filament even faster than the relatively colder 3 eV electrons used for this calculation. Thus it is quite reasonable that a single filament could have a substantial impact on electron distribution function and therefore the decay time.

However our ability to design experiments to test whether a heated filament that produces no net emission can affect decay time as described is hindered because the capacitance of wired filaments does not allow net emission to be quickly halted. One experiment that was performed involves varying the location of an additional heated filament in the confining region and measuring the effect on decay time after emitter retraction. If the effect on decay time is not consistent with the effect of emitting steady state plasmas off axis then an altered distribution function could be evaluated as a possible explanation. Figure 4.28 shows the decay time measured after emitter retraction when the position of the additional heated filament is varied in ψ. These results show that the decay time when the heated filament is near the axis is about half of the value measured when the heated filament is between $0.2 < \psi < 0.8$. Off axis emission experiments by Mike Hahn found a similar increase in confinement time by nearly a factor of two for off axis emission however did not have the resolution in ψ that would be necessary for a full comparison [39]. This theory was not tested further.

4.4 Conclusion

The confinement of plasmas unperturbed by internal objects has been studied using a retractable emitter. External diagnostics were developed for these experiments. Two new

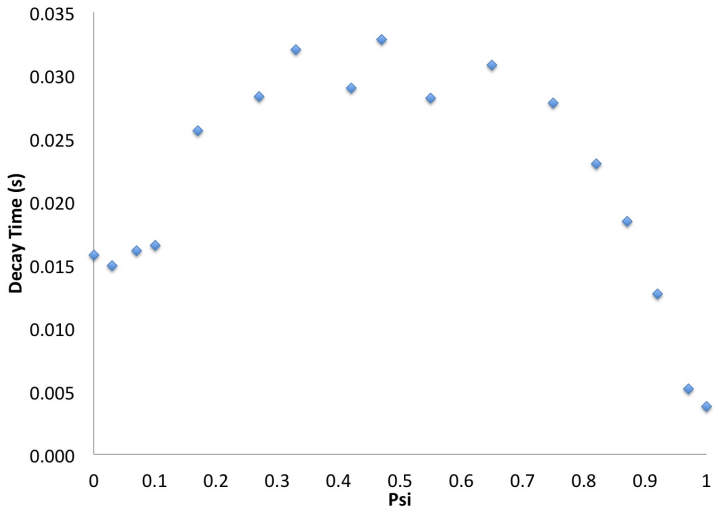

Figure 4.28: Measurements of the decay time when a heated filament is present in the magnetic surfaces after emitter retraction show a decrease in decay time when the filament is near the axis.

diagnostic techniques have been demonstrated to be capable of making measurements in agreement with previous methods. The fixed current probe was studied the most extensively and was successfully used to measure confinement of plasmas after emitter retraction. Plasmas unperturbed by internal objects do not behave as initially predicted. It was expected that these plasmas would behave like steady state plasmas without rod driven transport. Instead measured decay times after retraction are shorter than steady state confinement times. The longest measured decay time after retraction was 92 ms providing a minimum of 3 ms of plasma with short Debye length after the retractable emitter has left the last closed flux surface. 3 ms is long enough to study electron-positron plasmas and that time is expected to increase for lower neutral gas pressures. Decay times after retraction have been measured to change with pressure 10 times faster than steady state plasmas confinement times. We interpret experimental results as indicating that a build up of ions in the confining region results in short decay times. One possible explanation for the fast build up of ions is that the ions are initially created by ionization from energetic electrons in the tail of the Maxwellian distribution. As the ions build up the plasma potential is decreased which allows electrons to accelerate. The increased electron energy results in an increased ionization rate resulting

in a self enhancing process.

Simple calculations confirm that the entire plasma inventory could interact with a heated filament in 50 ms which is on the order of measured confinement times. This supports the theory that a heated filament could cool the plasma and thus reduce ion creation by collecting hot electrons and reemitting electrons at a lower temperature. However, a proper test of this theory could not be performed.

Further studies on this topic will help answer remaining questions. An experiment is currently being designed to operate at lower neutral pressures allowing for the study of plasmas unperturbed by internal objects with longer confinement times. This should allow further opportunity for diagnosing these transient plasmas. Efforts to study the local evolution of plasma potential at various locations in the plasma after retraction should provide more information about how plasma decay evolves. Finally an experimental campaign focused on new methods to create pure electron plasmas without using internal emitters should provide new insights into these results.

Chapter 5

Evaluating The Two Stream Instability

Plasmas are created in CNT by biased emission from a bare heated filament. Electrons leave the filament and travel in opposite directions along a field line to fill a surface. Then, on a slower time scale, cross field transport fills the rest of the confining volume. In this chapter, experimental observations are presented showing that obstructing one side of the filament with a nearby insulator substantially improves confinement. Furthermore, results indicate heating off axis unobstructed filaments significantly reduces that improvement. These observations suggest that a two steam instability could be responsible for the increased transport measured when emitting with an unobstructed filament.

In this chapter results are presented demonstrating the improvement in confinement when emitting with obstructed filaments. Experiments to determine whether a two stream instability is responsible will be discussed. The results of these experiments suggest that the increase in transport is not the result of a two stream instability. Instead, we attribute the difference to the plasma being in a different confinement state as a result of the emitter's interaction with the sheath around it. Results are presented demonstrating multiple confinement states and how perturbations to the sheath of the emitter influence which state the plasma is in. We conclude that the cause of increased transport when emitting with unobstructed filaments is the result of sheath effects and not the two stream instability.

5.1 Introduction

The two stream instability arises when two oppositely directed streams of charged particles pass each other. A density perturbation in one stream will be increased by the force from the bunching of particles in the other stream [17]. These two perturbations will cause each other to grow exponentially, resulting in an instability. The free energy that causes wave growth in the two stream instability results from the distribution function being non-Maxwellian. The mechanism for wave amplification can be thought of as the inverse of Landau damping [96]. In this situation there is a greater number of particles faster than the phase velocity of the wave than there are particles slower than the phase velocity. Thus, the amount of energy gained by slower particles is less than the amount of energy gained by the wave from faster particles.

The conditions for the instability are $k^2 v_0^2 < \omega_p^2$ where v_0 is the velocity of the beam. The instability has a maximum growth rate $\gamma_{max} \approx \omega_p$ and causes the energy of the charged particles to be dissipated as waves [22,33]. The instability conditions indicate that for a given v_0, the plasma is unstable to long wavelength oscillations. It also suggests that for a given k, v_0 needs to be small for the instability to occur. This would not make sense physically for small v_0 because the beam velocity provides energy for the instability. However, Landau damping occurs when $v_0 \lesssim v_{th}$, so no instability is predicted if the beam velocity is not larger than the plasma thermal velocity [19]. Thus Landau damping puts limits on the minimum v_0 for the instability to occur [19].

The two stream instability has been observed and studied in a wide range of plasmas [22]. There has been an interest in the instability as a method for efficiently using electron beams for plasma heating plasmas [32, 95]. In electron beam ion sources the two stream instability can hurt beam efficiency by reducing ion confinement [48, 62]. The Proton Storage Ring at Los Alamos has been troubled by a two stream instabilities from proton beams interacting with electrons trapped in quadrupoles [18]. Further two stream instability studies have investigated semiconductor plasmas [85] and counter rotating galaxies [64] illustrating the diversity of plasmas where the two stream instability may be present.

Plasmas studied in CNT are created by emission from a heated exposed filament held near the magnetic axis. Electrons stream off the filament in both directions along a field line.

These two opposed streams of electrons will pass near each other somewhere on the magnetic surface with similar but oppositely directed velocities. This creates conditions that could result in a two stream instability. Such an instability could affect transport by transferring beam energy into the bulk electrons or providing a means for well confined electrons to get onto poorly confined orbits.

Alternately, the improvement in confinement time could be explained by effects that alter the emitter's sheath and allow the plasma to settle into an equilibrium with decreased transport. Although global factors like magnetic field strength and neutral pressure clearly affect cross field transport in CNT, jumps between multiple stable equilibrium states have been observed [37, 39]. As described in this chapter, experiments indicate that the improvement in confinement time when emitting with an obstructed filament is the result of an improved confinement state as opposed to the reduction or elimination of a two stream instability in CNT. At the same magnetic field strength, neutral pressure, and bias voltage, measurements of states with confinement times varying by a factor of three are presented. We conclude that these confinement states are accessible under similar experimental conditions by altering the sheath between the emitter and the plasma.

5.2 Improved Confinement For Obstructed Emission

Plasmas in CNT are emitted from heated 3mm long coiled tungsten filaments. These filaments are purchased off the shelf as halogen lightbulbs. A vice is used to shatter the bulb and expose this filament. This leaves a bare filament supported by 7mm of glass. The filaments are held in position on the magnetic surfaces by insulating ceramic rods (see figure 2.3 and 5.3). These rods charge negatively resulting in both a local electrostatic perturbation and increased transport by net $E \times B$ flow out of the plasma.

In all experiments described here a steady state plasma is created by emission at the magnetic axis. Confinement time is measured from the total emission current or by the decay of voltage on a probe outside the last closed flux surface after emission has ceased. Experiments are done at low pressures ($p < 10$ nTorr) unless otherwise noted so the ion fraction is less than 1%.

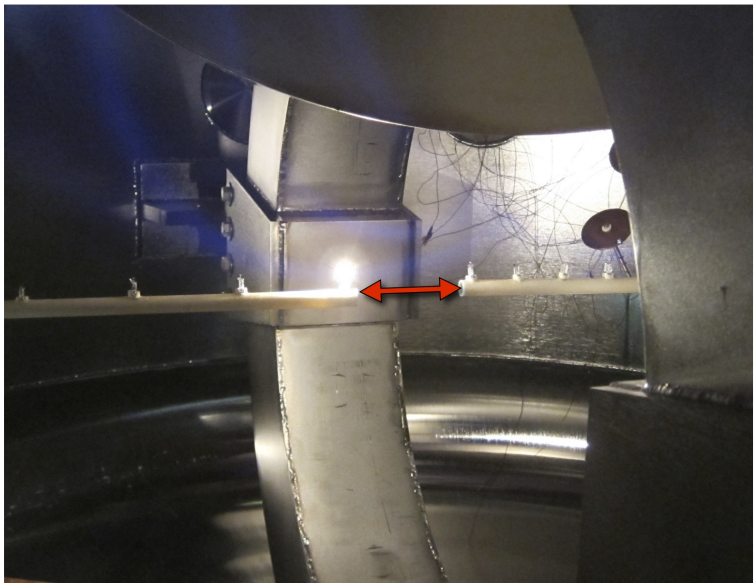

Figure 5.1: This image illustrates the experiment reported in figure 5.2. At 0 cm the two rods are very close to each other and aligned to the axis. A measurement of the red arrow shown in this image would yield the "Second Rod Distance From Axis" reported on the plot. Actual measurements were taken by measuring probe positions as described in section 2.3.2.

5.2.1 Obstructed Emission Experiments

Placing an insulating ceramic rod near the emissive filament creating the plasma results in increased confinement time. Figure 5.2 shows the confinement time when emitting from a filament held on axis by the four probe array as the position of the eight probe array is varied. The ceramic rods of the probe arrays are known to charge negatively with respect to the plasma resulting in increased transport. It was expected that pulling the eight probe array away from the axis would result in a steady increase in confinement time as the perturbation due to the rod is reduced. Instead figure 5.2 shows a steady decrease in confinement time followed by a sudden drop when the eight probe array is approximately 2 cm from the axis. The expected increase in confinement time from removing the rod does not begin until it is 5 cm out.

Specialized filaments with only half of the glass bulb removed were created to study this unexpected behavior. Figure 5.3 shows a comparison of the specially made filament to the

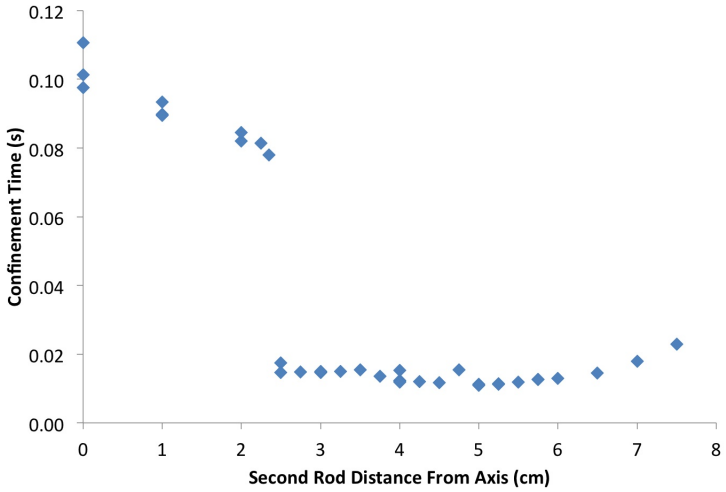

Figure 5.2: Confinement time improves when a second rod is inserted near to the on axis emitter.

standard bare filament commonly used for creating and diagnosing CNT plasmas. These partially blocked filaments substantially improve confinement time relative to bare filament emission (Figure 5.4) and were used when measuring the current record confinement time of 337 ms as shown in figure 5.5. The record confinement time was not measured at the best neutral pressure and magnetic field achievable in CNT. If linear scalings are assumed then a confinement time of approximately 500 ms can be expected for at the best currently achievable CNT parameters (magnetic field strength of 0.2T and 1.1 nTorr neutral pressure).

The confinement results for obstructed emission shown thus far have all been measured via the emission current and assuming no change in the total inventory. Confinement times were also measured by the decay of potential at the plasma edge. The two methods measure a similar trend (figure 5.6); however, confinement times measured with the edge voltage probe are on average 30% longer than those measured from the emission current. This difference is small relative to the change for obstructed versus bare filament emission and is likely the previously mentioned capacitance in the filament which allows continued emission. Floating potential profiles were measured using the fixed current probe as described in section 4.2.1. These measurements required movement of the charged rod holding the probe.

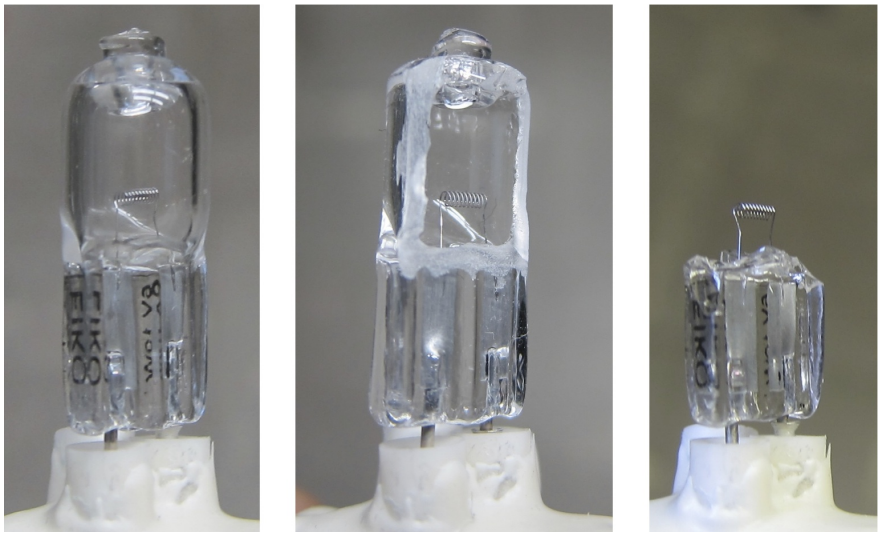

Figure 5.3: This figure shows the filaments used for electron emission in CNT. On the left is a picture of the the off the shelf light bulbs before modification. In the middle is an example of the specially made partially blocked filaments with half of the glass bulb removed. On the right is the standard bare filaments commonly used for creating and diagnosing CNT plasmas.

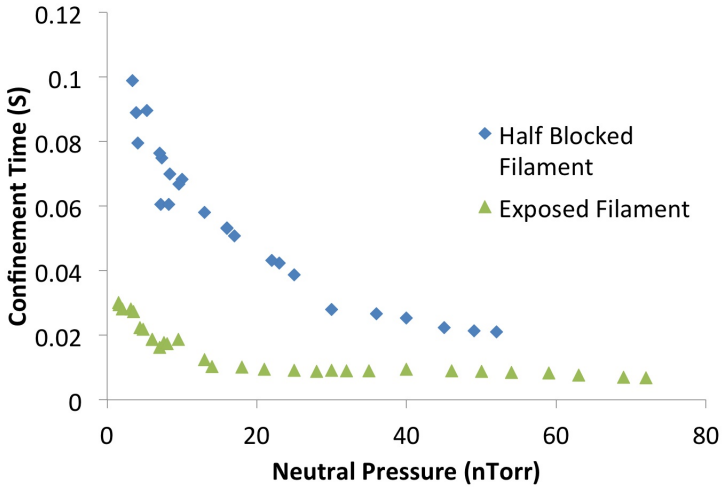

Figure 5.4: Confinement time is substantially improved when emitting from the partially blocked filament shown in figure 5.3.

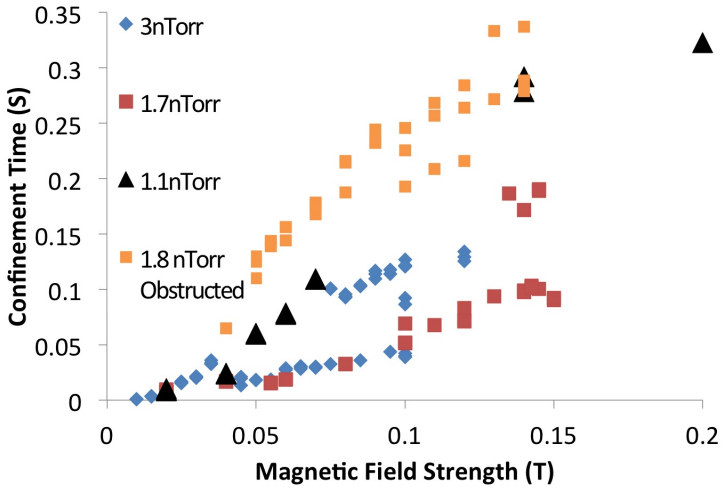

Figure 5.5: The current record confinement time measured in CNT was measured while emitting from an obstructed filament (labeled as 1.8 nTorr Obstructed).

Measurements with other filaments confirm that changing the position of the rods perturbation does not effect the potential profile. Figure 5.7 shows the similarities in potential profiles measured for obstructed and unobstructed emission further indicating the similarity in total electron inventory.

Finally it was found that heating off axis filaments substantially reduces confinement time when emitting from an obstructed filament (figure 5.8) while heating obstructed off axis filaments does not result in a similar effect. Heating off axis bare filaments also increases transport when emitting from a bare filament. However, the effect is much smaller. The results presented in this section motivated the investigation of whether this change in confinement time could be explained as the result of a two stream instability in CNT. The hypothesis was that obstructed emission blocked one stream of emission and limited the transport caused by a two stream instability resulting in the improved confinement time. An unobstructed heated off axis floating filament collects electrons and reemits in both directions on a field line and thus could cause a two stream instability.

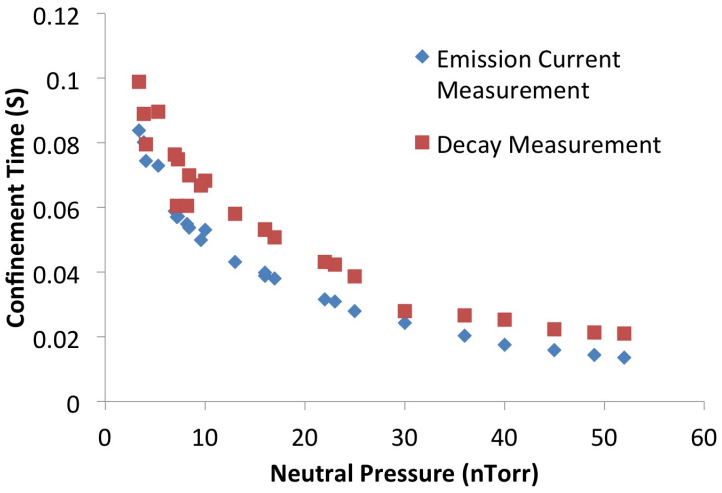

Figure 5.6: A comparison of confinement times measured via emission current and decay of the potential at the edge. These measurements were taken with 0.055 T magnetic field strength and -200V emitter bias.

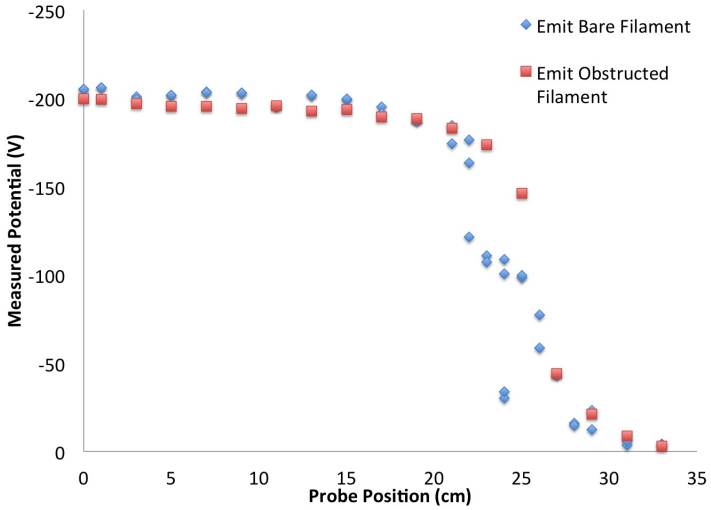

Figure 5.7: Voltage profiles are very similar for emission with and without obstructions.

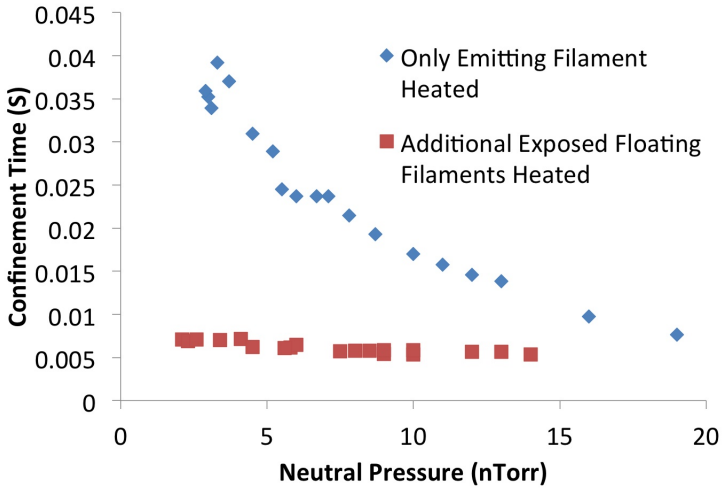

Figure 5.8: When emitting with an obstructed filament confinement time is substantially reduced when additional floating off axis filaments are heated. The off axis filaments emit no net current. These measurements were taken with 0.055 T magnetic field strength and -200V emitter bias.

5.3 Experimental Results

Emitting with an obstructed filament results in a consistent and measurable improvement of confinement time as compared to emitting from a bare filament. A two stream instability has been presented as one hypothesis that could explain these results. To evaluate this hypothesis the following questions were investigated:

- **Beams:** Can a beam of electrons be measured in the plasma (Section 5.4)?
- **Directional Emission:** Does emitting in one direction improve confinement or are methods to block the second stream causing the improvement (Section 5.5)?
- **Off Axis Filaments:** How does heating off axis filaments drive transport (Section 5.6)?

Although efforts were made to directly measure the two stream instability, no conclusive results were found. Attempts to measure oscillations near the plasma frequency (between 10-100 MHz) suffered from hardware limitations. CNT's data acquisition cards are not fast

enough to measure the plasma frequency and measurements with a lab oscilloscope were unsuccessful due to noise pick up near 16 MHz regardless of the presence of the plasma. This measurement was not pursued further as a result of the evidence presented below which indicates that a two stream instability is not responsible for the observed change in confinement time.

5.4 Beams

Experiments were performed to measure whether an observable beam of electrons is present in CNT plasmas. Electrons leave an emitting bare filament traveling in both directions along a field line. It is possible that these electrons continue traveling together as a beam. However, it has been previously shown that electrons in CNT are in thermal equilibrium even when confinement time is on the order of collision times [8, 54, 55]. This implies that electrons are thermalized quickly and may not travel as beams in the plasma. Furthermore, simulations done by Benoit Durand de Gevigney predict that a single stream of electrons from an obstructed emitter would eventually reach the perturbation from the charged insulating rod and be turned around. This prediction suggests that if beams are present in CNT then blocking one beam at the emitter would still result in beams traveling in two directions.

To study the presence of beams in the bulk plasma a bare cold filament was used as a Langmuir probe to study the distribution function. This can be done by sweeping the probe voltage, measuring the IV curve, and comparing it to the results given from a simulated distribution function. For these studies two distribution functions were considered. A bulk distribution representing a plasma without beams:

$$f(v) = \frac{n_{total}}{\sqrt{\pi/2}v_{thbulk}} \exp\left(-\frac{v^2}{2v_{thbulk}^2}\right) \tag{5.1}$$

and a bulk plus beam distribution:

$$f(v) = \frac{n_{bulk}}{\sqrt{\pi/2}v_{thbulk}} \exp\left(-\frac{v^2}{2v_{thbulk}^2}\right) + \frac{n_{beam}}{\sqrt{\pi/2}v_{thbeam}} \exp\left(-\frac{(v+v_{beam})^2}{2v_{thbeam}^2}\right) \tag{5.2}$$

Where $v_{th} \equiv (T/m)^{1/2}$ when T is in units of energy. For these simulations measured CNT parameters were used for total density, bulk temperature, and plasma potential. Beam

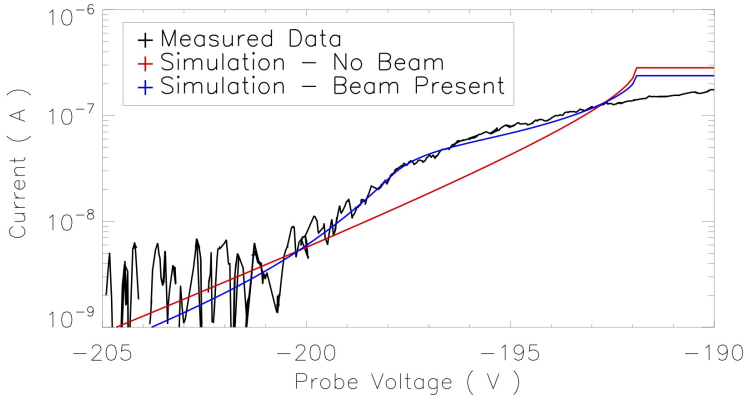

Figure 5.9: An example of a poorly fit Langmuir probe trace. Here the measured knee is actually the result of electron saturation and not from a beam. This fit is for a beam density 30 percent of the total density, a 6eV beam with 1ev thermal velocity, and a 3eV bulk temperature.

thermal temperature is not known so values between 0.4 and 1 eV were used. Beam densities up to half of the bulk density were considered. An electron beam would gain energy as it is accelerated through the sheath from the negatively biased emitter thus considered beam velocities were limited to values that could be achieved with the difference between emitter and plasma potential.

Initial fits misinterpreted the physics observed in IV curves in CNT as shown in figure 5.9. In this case the knee that was fit to actually occurs because of electron saturation. As the probe becomes more negative it begins to deplete the electrons in the surface that the probe sits on. The collection rate at a fixed voltage is then limited by cross field transport. Figures 5.10 and 5.11 demonstrate the dependence on cross field transport with larger collected currents in electron saturation for low magnetic field strength and high pressure respectively. The simulated IV trace shown in figure 5.9 does not include cross field transport and instead is flat in saturation.

The measurements in figures 5.9, 5.10, and 5.11 were performed off axis and do not show indications of a beam population. Next, Visualizations were used to align the probe to the same surface as the emitter as shown in figure 5.12. Any beam originating from the emissive filament should present the largest measurable signal at this location. However, figures 5.13

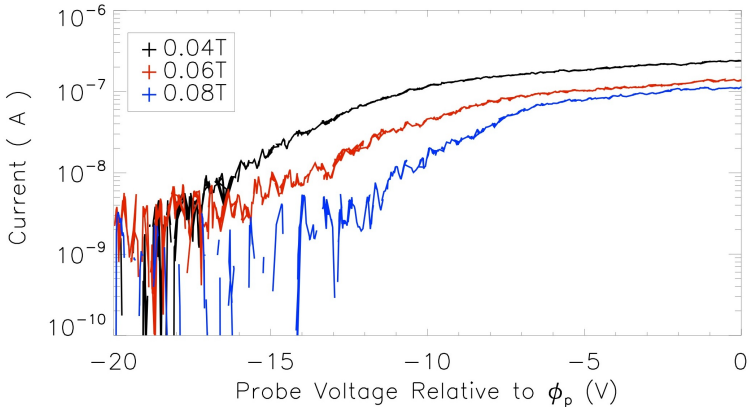

Figure 5.10: Langmuir probe current-voltage characteristics at a fixed 1.6nTorr pressure demonstrate that decreasing magnetic field strength increases electron saturation current as a result of increased cross field transport.

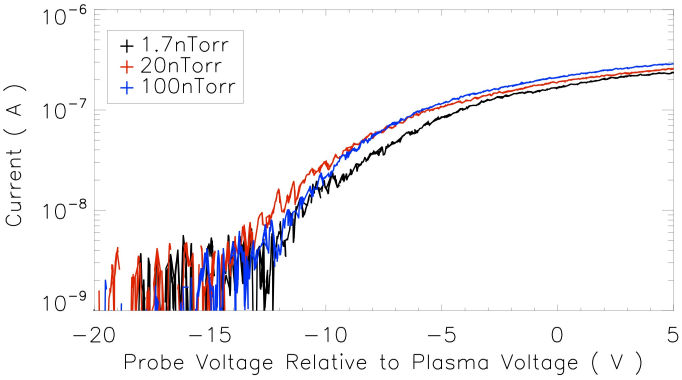

Figure 5.11: Langmuir probe IV characteristics at 0.08T magnetic field strength demonstrate that increased cross field transport increases electron saturation current as shown by increasing neutral pressure. The plasma potential varies decreases by 2V at 100 nTorr so collected current is plotted against relative voltage.

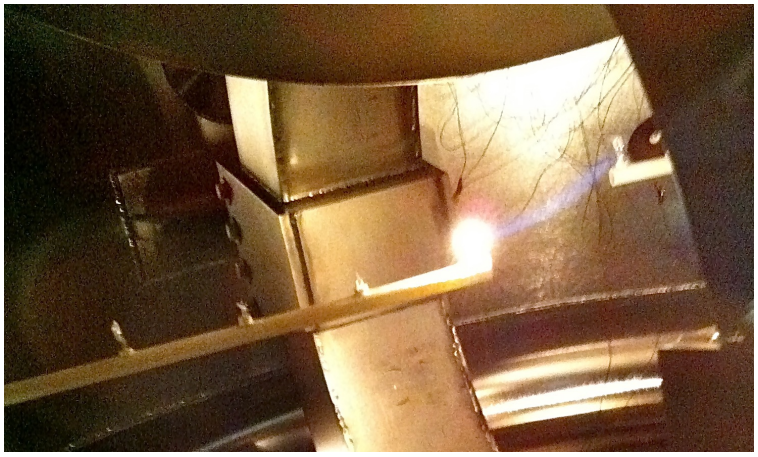

Figure 5.12: When investigating the distribution function for the presence of beams a langmuir probe was aligned to the same field line as an emitter using visualizations. In this picture a glowing field line connects the probe and emitter.

and 5.14 again show no indication of a beam population in the measured IV characteristic. A small knee when the probe is -211 V was evaluated to rule out the possibility of a beam signal. Figure 5.15 shows the best case fit to that knee. For this fit a 10 eV beam with a 1eV thermal velocity and 5% of total density was used. Not only is a 10 eV unlikely with a plasma potential of -199 V and emitter bias of -200 V, but it was not possible to account for the sharpness of the knee while maintaining the slope of the IV curve for lower voltages.

These results can be used to put limits on the density of a beam population that could be present without being measured. By adding noise to the simulated data and analyzing using the same methods applied to measured results it is possible to evaluate the beam density that this diagnostic is capable of measuring. It was found that for a beam with 1 eV thermal velocity and 6 eV velocity 2% of total density is the minimum density that a beam would need to be measurable over noise. Thus these measurements place an upper limit on the size of beams that could be present in CNT.

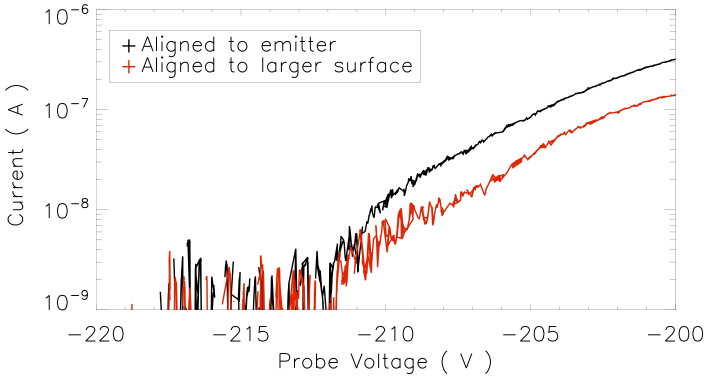

Figure 5.13: A comparison of measured IV characteristics with the langmuir probe aligned to the emitter on axis (black) and off axis (black) does not show a measurable beam in either case. These traces were measured with a -200V emitter bias and 0.06T magnetic field.

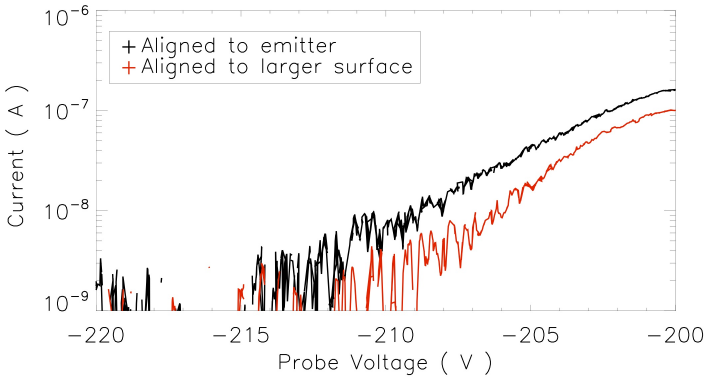

Figure 5.14: A comparison similar to figure 5.13 but with a 0.08T magnetic field still shows no beams.

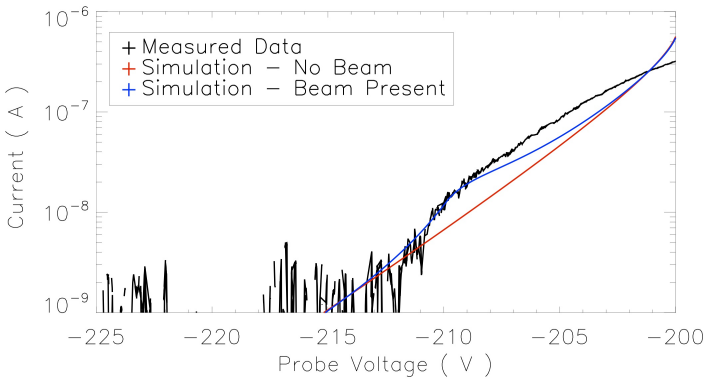

Figure 5.15: A comparison of a simulated beam (blue) to measured results (black).

5.5 Directional Emission

To investigate the presence of a two stream instability in CNT, plasmas created by emission in one or both directions were compared. Two direction emission has been used to create the majority of plasmas studied in CNT and is achieved with a bare heated and biased filament. To limit one stream of electrons plasmas were created with an obstruction blocking emission from one side of the filament. For these experiments three methods were used to obstruct beams: back to back emitting filaments separated by an insulator, back to back filaments separated by a biasable plate, and a biasable plate aligned to the axis but 12 cm from the emitting filament.

5.5.1 Directional Emitter With Insulator

A directional emitter was designed to study the differences between plasmas created with a unidirectional filament versus plasmas created with the standard bare filament (figure 5.16). The probe uses two obstructed filaments placed back to back. If properly aligned, such that the filaments both emit on the same magnetic surface, it is possible to quickly switch between one and two directional emission. However the two filaments could not be exactly aligned. The 3mm long filaments are capable of emitting currents thousands of times greater than the microamps emitted in these experiments, so it is likely that only a sub-milimeter portion of the filament actually emits. Properly aligning two filaments to a field line with sub-

Figure 5.16: Picture of the directional emitter with back to back obstructed emitters.

millimeter tolerances was not within the scope of this experiment. However, a two stream effect would be expected even with streams on slightly different surfaces.

Instead the filament on the magnetic surface closest to the axis dominates emission while the further out filament did not emit. Figure 5.17 shows four cases of emission from the directional probe. In all four cases the filament facing the positive B direction is heated and biased to -200 V. The filament facing the negative direction is cold and floating in the first case (Emit +B Cold -B), heated and floating in the second case (Emit +B Heated -B), heated and biased to -200 V in the third case (Heated +B Heated/Biased -B), and heated and biased to -210 V in the fourth case (Simultaneous Emission). It was found that only the filament facing in the positive B direction would emit for the first three cases and simultaneous emission required the negative B filament to be set 10 volts more negative. Simultaneous emission was very sensitive to this voltage difference. If the negative B filament was -208 V it would not emit and if it was -212 V it would dominate emission. Even when the voltages are properly set emission between the two filaments is unstable. Figure 5.19 shows an example of this unstable emission. The bias voltage on the two filaments is stable from 5 seconds to 18 seconds but the filament facing the positive B direction jumps between emitting $0\mu A$ and $2\mu A$. Reported simultaneous emission is the sum of the the emission from both

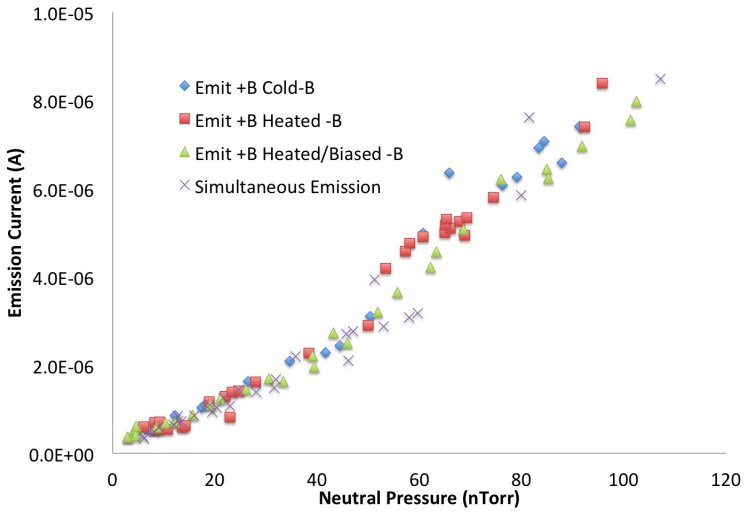

Figure 5.17: Emission with the directional emitter shows no significant difference in loss rate (as measured by emission current) when emitting when emitting in one or both directions. These results were measured with a 0.08T magnetic field strength.

filaments. For comparison figure 5.18 includes emission measurements for emission from a bare filament, emission from the directional probe remains much smaller than emission from a bare filament in all cases.

5.5.2 Directional Emitter With Bias Plate

The same probe shown in figure 5.16 was modified by replacing the obstructed filaments with bare filaments and placing a biasable metal plate between two filaments. The plate was designed to be the same size as the glass obstruction used in secion 5.5.1. The plate can be used to simulate the perturbation created by the charged glass of the obstructed filaments. If the confinement improvement when emitting with obstructed filaments is the result of blocking one of the electron streams then biasing the plate more negative relative to the emitter should not decrease emission current once the plate collects no current. Figure 5.20 shows the first experiment with this emitter demonstrating that making the plate more negative relative to the emitter decreases emission current steadily. Inserting an additional rod partial increases emission current until the plate is 90 V more negative than the emitter

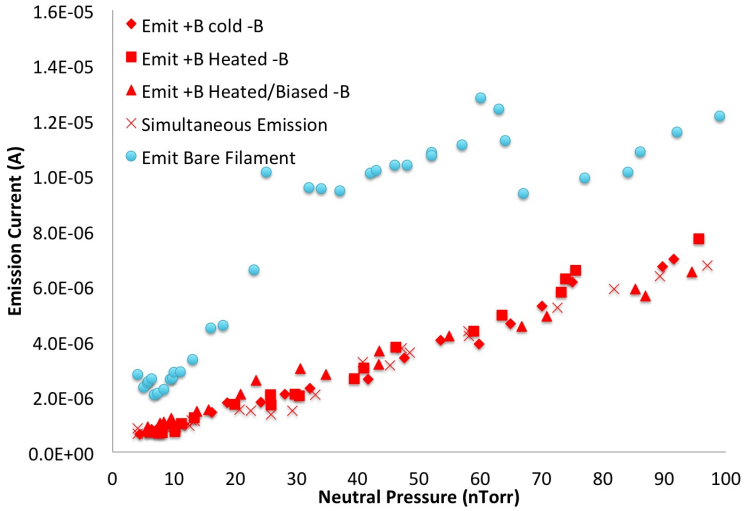

Figure 5.18: These results are similar to figure 5.17 but include a comparison to bare filament emission and were measured at 0.04T.

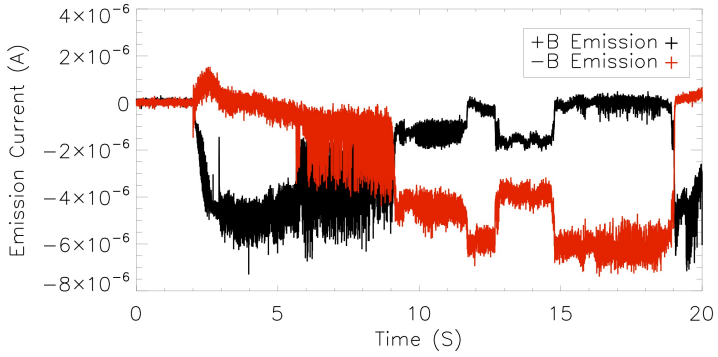

Figure 5.19: Sample simultaneous emission current measurement at 6 ntorr base pressure and 0.02T magnetic field strength shows that simultaneously emitting from two emitters can result in emission switching between the two filaments. Here negative current represents emission and positive current represents collection.

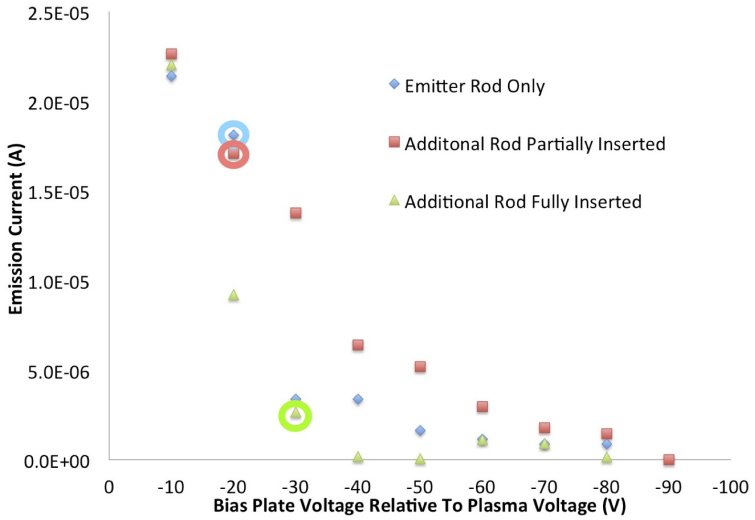

Figure 5.20: Shows that adding a second rod still decreases loss rate even when emitting with the back to back probe with a bias plate in between filaments.

so, for values less negative than this amount the emission current still depends on plasma characteristics. Inserting the additional rod to the axis results in the same decreased emission current first shown in figure 5.2. The point at which the bias plate no longer collects current is circled for each case. A comparison with the results in section 5.5.1 indicates that the insulating glass on the obstructed filaments charges 30 V more negative than the emitter.

Figure 5.21 shows that heating off axis filaments in this configuration still increases transport indicating again that global effects still affect emission current until the bias plate is 90 volts more negative than the emitter. For this plot points are only shown where the bias plate collects no current. The drop in emission current with increasing plate bias after the plate stops collecting indicates that confinement improvements with obstructed emission are not the result of a two stream instability.

5.5.3 Spatially Separated Bias Plate

A third experiment was performed to further establish that the measured improvement in confinement time for obstructed emission is not the result of blocking one stream of electrons. A 7 cm by 8 cm biasable metal plate was aligned via visualizations to intercept the axis while

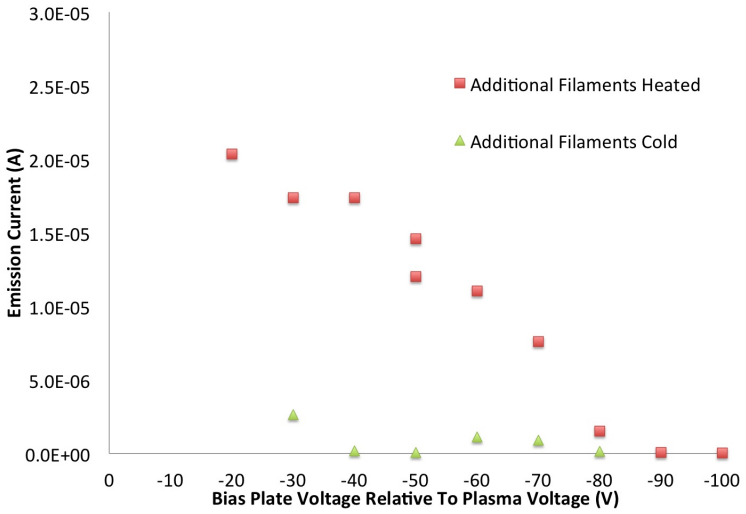

Figure 5.21: Heating additional off axis filaments increases loss rate until the bias plate voltage completely limits emission. Points are only shown for voltages that resulted in no collected current by the biasing plate.

positioned 12 cm away from the emitting filament. This plate is shown in figure 5.22 before it was aligned to the axis. At this location the plate can easily block one stream coming from a filament without creating a potential perturbation at the filament. Figure 5.23 shows the results when emitting from various emitters on the eight probe array. Filaments one and two were visually confirmed as blocked by the plate, filament three was blocked after multiple transits, and filament four was confirmed to be unblocked.

Although emission current from filament one decreases as the voltage on the bias plate increases it never drops to the very low levels characteristic of obstructed emission and demonstrated by the emission measured from filament two. The measured emission current for filament four still follows a trend similar to the other filaments despite not being blocked. These results combined with the result reported early demonstrate that the improvement in confinement time when emitting with an obstruction is not the result of blocking a two stream instability. This result is further supported by previous experiments where the insulating rod of the retractable emitter was positioned to intersect the axis while plasma was created by on axis emission from the eight probe array. In this case the position of the retractable emitter only decreased confinement times with no indication of any improvement from blocking the

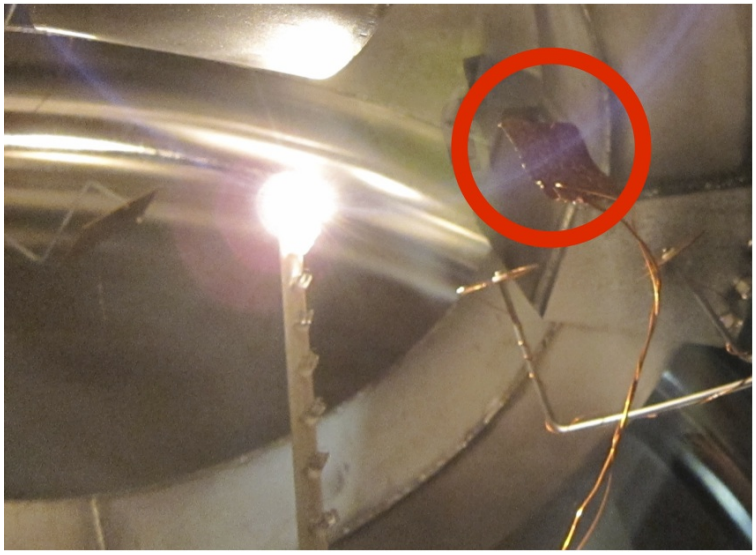

Figure 5.22: The bias plate is 12 cm from the on axis emitter. This picture shows the plate before it has been properly aligned to the axis. The plate is circled in red to distinguish it from the circular probes used to study ion instabilities.

on axis electron streams.

5.6 Off Axis Filaments

The experiments reported above indicate that the blocking of a two stream instability is not responsible for the confinement improvement with obstructed emission. The improvement instead appears to be the result of a local effect near the emitter. The remaining question is why heating off axis floating filaments results in a significant increase in transport? Electron temperature measurements were made at various positions in the plasma using a Langmuir probe. Results for obstructed emission show that heating additional off axis filaments increases the electron temperature (figure 5.24) while results for unobstructed emission show that heating off axis filaments decreases the electron temperature (figure 5.25). These results are summarized in figure 5.26 with raw results reported in figure 5.27.

A decrease in electron temperature when heating off axis filaments was expected for both cases. These heated filaments are floating and can produce no net emission. When a hot

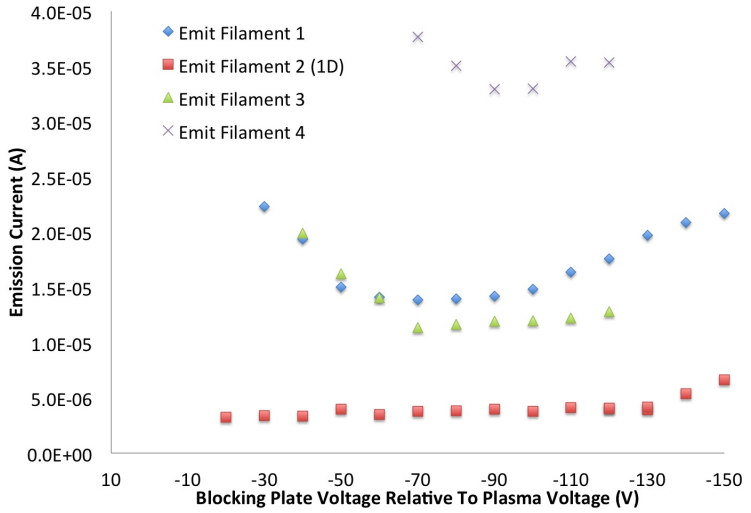

Figure 5.23: Loss rate versus voltage on blocking plate

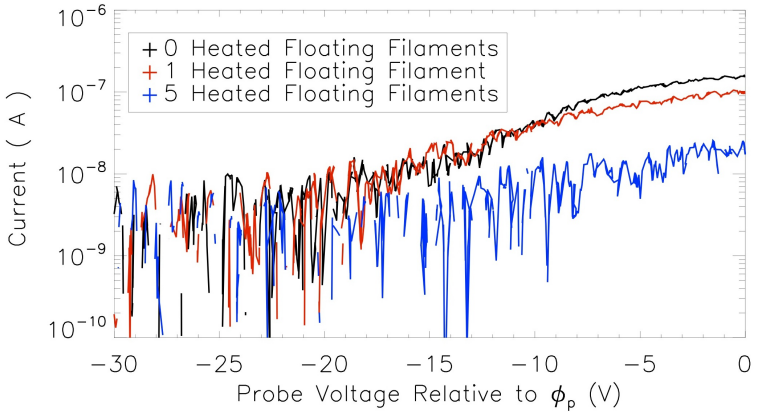

Figure 5.24: Langmuir probe IV characteristics show an increase in electron temperature when heating additional off axis filaments and emitting from an obstructed filament.

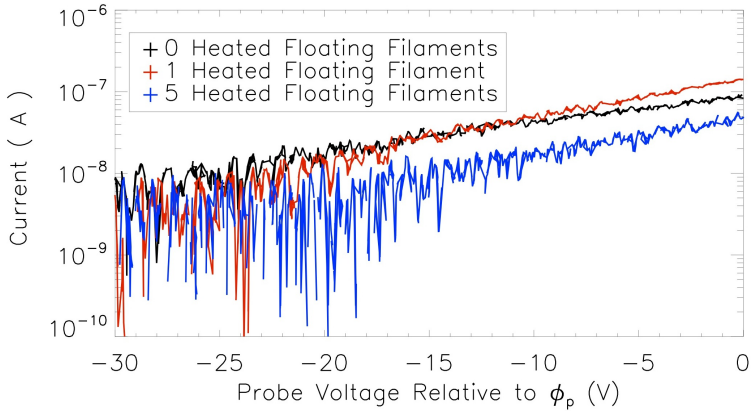

Figure 5.25: In contrast to the results presented in figure 5.24 Langmuir probe IV characteristics show a slight decrease in electron temperature when emitting from a bare unobstructed filament.

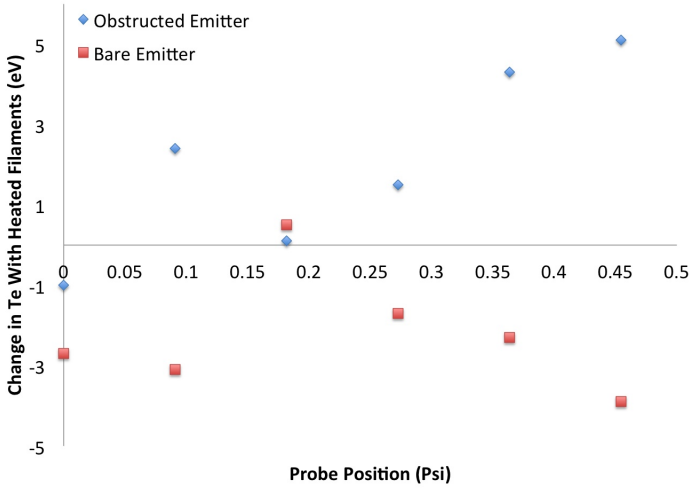

Figure 5.26: A comparison of the effect on electron temperature when heating additional off axis filaments shows an increase in temperature when emitting from an obstructed filament and a decrease when emitting from a bare filament.

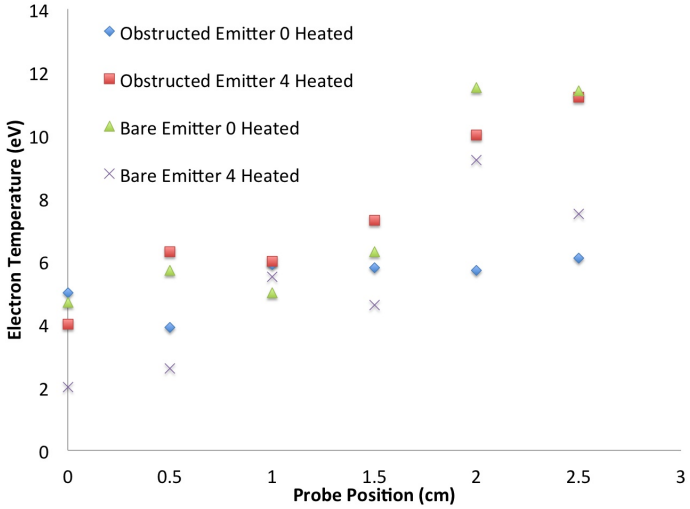

Figure 5.27: Electron temperature measurements from figure 5.26. Here measured temperatures are shown for cases with and without four off axis filaments heated and floating (in addition to the on axis biased emissive filament). The case for obstructed emission with heated filaments and unobstructed emission without heated filaments are in relatively good agreement.

electron in the plasma encounter the filament it can be collected. The filament will then reemit an electron to remain neutral. Reemitted electrons can be lower energy than collected fast moving electrons resulting in a cooling effect. The results in figure 5.27 show this behavior for unobstructed behavior. Surprisingly, this is not the case for obstructed emission where heating off axis filaments increases the temperature into agreement with the "unobstructed emission without additional heated filaments" results. This change in temperature is consistent with the drop of obstructed emission confinement times to unobstructed levels when heating off axis filaments. Although it is not clear why the temperature increase occurs, this provides a reasonable alternative to the two stream instability as an explanation for decreased confinement time.

5.7 Sheath Effects

The evidence presented in this chapter demonstrates that the increase in confinement time when creating plasmas with an obstructed emitter is not the result of reducing a two stream instability. Instead the improvement is a local effect resulting from the the obstructions perturbation of the emitter's sheath. Large changes in transport resulting from emitter-sheath effects have been observed before in CNT in the form of transport jumps [37, 39]. In those experiments it was found that filaments that exceeded a critical emission current would create cathode instabilities that resulted in increased transport. Figure 5.5 has shown that equilibrium can be achieved at multiple stable confinement states in CNT. For the 3 nTorr results, two different confinement times are observed under the same conditions between 0.07 T and 0.1 T. For obstructed emission, however, only results in the highest confinement state have been observed.

Experiments were performed to study the effect of a potential perturbation on the multiple observable confinement states. In these experiments sectors of the conducting boundary temporarily biased to -100 V and then returned to ground. When the segment nearest to the emitter was biased the emission current dropped and then stayed in the improved confinement state after the bias on the mesh was returned to 0. This experiment is shown in figure 5.28 and the resulting increase in confinement time matches well with times in the higher confinement state observed without a perturbation above 0.13 T. It appears that

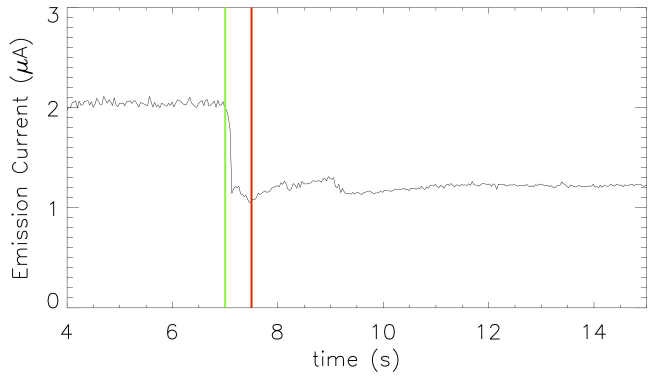

Figure 5.28: During steady state emission the potential on a sector of the conducting boundary is changed from 0 to -100V (green) and then returned to zero (red). This perturbation switches the plasma to an improved confinement state.

decreasing the emission current via a potential perturbation allows the plasma to remain in a steady state improved confinement equilibrium after the perturbation has been removed. The improved confinement times for obstructed emission are believed to result from a similar effect via the potential perturbation created by charging up the obstruction. This is further supported by the agreement of confinement times measured at 0.14 T at 1.1 nTorr and 1.8 nTorr obstructed in figure 5.5. The 1.1 nTorr confinement times measured at 0.14 T are substantially higher than those measured at 1.7 nTorr despite a relatively small improvement in neutral pressure. This instead suggests that these points were measured in an improved confinement state that corresponds to the state measured with obstructed emission.

5.8 Conclusions

Improved confinement times are observed when emitting with an obstruction blocking one stream of electrons. This improvement is observed whether the obstruction is a nearby insulated rod, an insulator less than 1 cm away from the emissive filament, or a negatively biased metal plate located a few millimeters from the filament. Heating off axis floating filaments removes this improvement even though the floating filaments produce no net emission. These

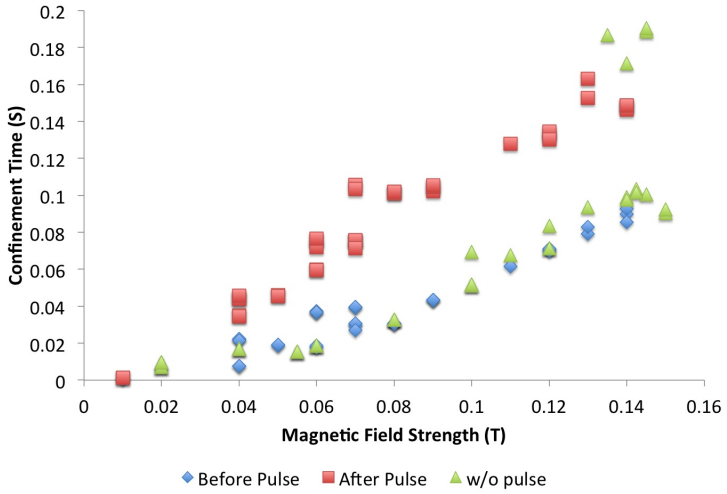

Figure 5.29: The perturbation demonstrated in figure 5.28 causes the plasma to switch from a low confinement state to a higher confinement state.

observations initially were believed to be the result of a two stream instability.

However, on further investigation the two stream instability was ruled out. No beams were successfully measured in the plasma using Langmuir probes capable of measuring beams as small as 2% of the total electron population. Emitting with two back-to-back filaments with an insulating obstruction in between resulted in improved confinement despite the simultaneous emission in opposed direction. Emitting with two back-to-back filaments with a biasable obstruction in between indicates that an insulating obstruction was charging to 30 V more negative than the emitter. Finally a biasable blocking plate aligned to the axis but 12 cm from the emitting filament was not able to create the large improvement in confinement time observed with the near by obstructions. This indicates that the confinement improvement is the result of effects local to the emitter. The decrease in confinement time that results from heating off axis filaments was observed to be the result of an increase in electron temperature.

The cause of the improved confinement time when emitting with an obstruction near the emitter is believed to be the result of altering the emitter's sheath to allow steady state equilibrium in an improved confinement state. The limiting effect is induced by a sufficiently negatively charged nearby obstruction. These improved states have been observed before in

CNT, are influenced by potential perturbations, and are in agreement with some confinement times measured for obstructed emission.

Further studies on this topic are necessary for a better understanding of the underlying physics. Clearly steady state confinement in CNT depends more on the interaction of the heated filaments with the sheath than initially predicted. Even larger confinement improvements may be possible with a research program dedicated to studying the physics of the interaction between the emissive filament, the sheath, and the bulk plasma in CNT. These experiments also show the importance of the method used to create plasmas in CNT. Experiments with different plasma creation techniques may result in significantly improved confinement times with otherwise similar equilibrium conditions.

Chapter 6

Conclusions

This thesis describes experimental studies of the confinement of non-neutral plasmas on magnetic surfaces. A highlighted conclusion from each section is listed here with more detail below:

- Improving the match between equipotential and magnetic surfaces results in improved orbit quality and increased confinement time.
- Ion accumulation limits the decay time in plasmas unperturbed by internal objects. Confined plasmas have been measured with decay times as long as 92 ms after the retractable emitter has left the last closed flux surface.
- Increased confinement times when emitting from a partially obstructed filament are the result of local alterations to the sheath of the emitting filament which allow the plasma to reach an equilibrium state with improved confinement.

Improved Confinement With A Conducting Boundary

Record confinement time was improved by a factor of 16, to 337 ms, after the installation of a conducting boundary. The boundary was designed to conform to the the last closed magnetic flux surface (LCFS) so that an equipotential could be enforced at the LCFS. Numerical simulations predicted that this would improve orbit quality in CNT by decreasing the mismatch between equipotential and magnetic surfaces within the plasma. More than a

factor of 10 improvement to confinement time was predicted [24] however measurements of electron-neutral transport indicate that only a factor of two improvement can be attributed to improved orbit quality. This is likely due to the experimentally verified fact that the conducting boundary intersects a significant volume of the outer magnetic surfaces ($\psi > 0.7$). Therefore, the boundary reduces the confined volume and does not properly establish an equipotential at the last closed flux surface.

The remaining improvements can be attributed to a factor of approximately 3-4 reduction in rod driven transport with the conducting boundary installed and improved operating parameters. With the boundary installed, electron density increased compared to plasmas with the same central potential without a conducting boundary. The increase in density without a change in electron temperature results in a smaller Debye length. This decreased Debye length reduces the size of the sheath around the insulated rods. Therefore the rod transport, which occurs primarily in the rod sheath, is smaller. The magnetic field strength was also doubled and the neutral pressure decreased by a factor of four resulting in expected improvements toconfinement.

Techniques were also developed to align the boundary to the complex geometry of the magnetic surfaces. Field line visualization was the most used technique for aligning the conducting boundary as a result of its ability to quickly provide information about the three dimensional shape of the magnetic surfaces. These field line visualizations have since been regularly used when aligning probes in the magnetic surfaces.

Confinement Of Plasmas Unperturbed By Internal Objects

The confinement of plasmas unperturbed by internal objects has been studied using a retractable emitter. It was expected that these plasmas would behave like steady state plasmas without rod driven transport. Instead, the longest measured decay time after retraction was 92 ms. Decay times after retraction have been measured to change with pressure 10 times faster than steady state plasmas confinement times. Experimental results show longer confinement times when the background neutral gas is dominated by a gas with a high ionization energy (helium) as opposed to lower ionization energy (nitrogen). We interpret these results as indicating that a build up of ions in the confining region results in short decay times. The

fast build up of ions is attributed to a self enhancing ionization process.

Simple calculations indicate that the entire plasma inventory could interact with a heated filament in 50 ms which is on the order of measured confinement times. This supports the theory that a heated filament could cool the plasma and thus reduce ion creation by collecting hot electrons and reemitting electrons at a lower temperature. However, a proper test of this theory could not be performed.

Evaluating The Two Stream Instability

Improved confinement times are observed when emitting with an obstruction blocking one stream of electrons. Heating off axis floating filaments removes this improvement even though the floating filaments produce no net emission. These observations motivated experiments to study whether the change in confinement is the result of a two stream instability.

Further investigation indicates that the change in confinement is not the result of a two stream instability. No beams were successfully measured in the plasma. Emitting with two obstructed filaments back-to-back resulted in improved confinement despite the simultaneous emission in opposite directions. Emitting with two back-to-back filaments with a conducting biased obstruction in between indicates that the insulated obstruction was charging to 30 V more negative than the emitter. Finally a biased conducting blocking plate aligned to the axis while spatially separated from the emitting filament was not able to create the large improvement in confinement time observed with the near by obstructions. This indicates that the confinement improvement is the result of effects local to the emitter. The decrease in confinement time resulting from heating off axis filaments was observed to be the result of an increase in electron temperature resulting from the filaments.

The cause of the improved confinement time when emitting with an obstruction near the emitter is believed to be the result of altering the sheath of the emitter. This results in steady state equilibrium in an improved confinement state. The limiting effect is induced by a sufficiently negatively charged nearby obstruction. These improved states have been observed before in CNT, are influenced by potential perturbations, and are in agreement with some confinement times measured for obstructed emission.

Chapter 7

Possible Future Studies

This thesis has presented significant progress toward understanding and improving the confinement of non-neutral plasmas confined on magnetic surfaces. Further studies could be performed to extend our understanding. Ideas for possible future experiments are presented below.

- **Improved Conducting Boundary** Future experiments studying non-neutral plasmas confined on magnetic surfaces should be designed to minimize equipotential and magnetic surface mismatch through careful control of the electrostatic boundary conditions. Results with the conducting boundary were encouraging. However, misalignments meant that the full benefit from the installation of the conducting boundary could not be realized. With a few design enhancements a conforming conducting boundary should be able to provide a full test of the improvement from well matched equipotential and magnetic surfaces. This boundary could then be used with the full diagnostic capabilities previously described for capacitive sector probes. A well aligned conducting boundary could also be used to open trajectories by which positrons could be injected [25].

  The conducting boundary installed in CNT was designed as a proof of principle. During the installation and alignment process, design improvements were identified which should be incorporated into any boundaries installed on future experiments. A next generation conducting boundary should include:

  - Structurally rigid connections between segments that maintain electrical isolation
  - Adjustable sections to study the effect of misalignments and easily fix any that may occur during installation
  - Increased spatial resolution achieved by attaching multiple electrically isolated plates to each sector
  - Space for adequate limiters

  Also, designs that allow the conducting boundary to be larger than the last closed flux surface should be evaluated. These would assure that good surfaces are not cut off in the event of misalignments and allow more space for limiters. Metrology techniques, such as the use of a roamer arm, should also be incorporated in the installation/alignment process.

- **Retractable Emitter Studies At Lower Neutral Pressures** The plasmas that remain after emitter retraction show a strong dependence on neutral pressure. At 10 nTorr these plasmas were not confined long enough to be measured (< 5 ms) while confinement times as long as 92 ms were measured at 1.5 nTorr. Experiments capable of studying these plasmas at lower neutral pressures should allow investigation into the transport mechanisms that are drive losses when not limited by ion accumulation.

  Efforts to study the local evolution of plasma potential at various locations in the plasma should provide more information about how plasma decay evolves after retraction. This could be achieved with an enhanced version of the fixed voltage probe (diagnostic method III). A cold filament biased much more negatively than the local plasma potential will not collect electrons. The probe should not be perturbed by the retraction of the emitter when the probe bias is chosen to be more negative than the emitter. After retraction the probes bias could be ramped down on a time scale fast compared to the confinement time. The voltage and time when the probe begins collecting electrons will provide information about the local potential at a given time after retraction. With this data it should be possible to develop an understanding of the density profile evolution after retraction.

  Further studies of the behavior of plasmas without heated filaments present could be

done without a retractable emitter. For example, materials capable of laser induced emission could be employed to quickly halt emission without moving the emitter.

- **Plasma Creation Methods** An experimental campaign focused on new methods to create pure electron plasmas without using internal emitters should provide further insights into the results measured with the retractable emitter. Electron guns have been studied previously on CNT and result in high temperature plasmas with large Debye lengths [39]. Methods to open trajectories into the magnetic surfaces with potential perturbations at the edge could also be pursued [25]. The ionization of neutral beams has also been considered. A beam of heavy atoms could be directed at the confining region and then laser ionized at the magnetic axis. The momentum of the poorly magnetized heavy ions would carry them out of the surfaces while the relatively light electrons would be well confined.

- **Sheath-Filament Effects On Plasma Equilibrium** Observations have shown that the local physics around the emissive filaments plays a substantial roll in global plasma equilibrium. Although experiments in this thesis and Michael Hahn's thesis have begun to explore this interaction a dedicated experimental campaign should provide a greater understanding of the underlying physics. One proposed idea is to surround the emitting filament with a bias-able cap to provide greater control of the sheath. This cap would need to be insulated on the outside to avoid perturbing the plasma. Grounding the cap would result in electron gun plasmas which are expected to have high temperatures and long Debye lengths. However, studies with the cap biased near to the emitter bias will provide valuable information about the role of sheath-filament interaction for establishing global equilibrium.

- **Debye Shielding In Non-neutral Plasmas** Debye shielding is a characteristic of quasineutral plasmas so fundamental that it is often among the first topics taught to new students [19]. In early treatments of non-neutral plasma Debye shielding the main difference from the quasineutral case was that the resulting $\delta\Phi$ from a perturbation was superimposed on potential resulting from the non-neutral plasma's space charge. These derivations started by relating density and potential through the Boltzmann

relation such that

$$n(r) = N(r)exp\left[\frac{e\Phi(r)}{T_e}\right] \tag{7.1}$$

The potential perturbation is defined as the the perturbation created by inserting an object into the plasma minus the unperturbed potential $\delta\Phi \equiv \tilde{\Phi} - \Phi$ resulting in

$$\frac{\epsilon_0}{e}\nabla^2\delta\Phi = n(r)\left[exp\left(\frac{e\delta\Phi}{T_e}\right) - 1\right] \tag{7.2}$$

Linearization then can be used in the case where $\frac{e\delta\Phi}{T_e} \ll 1$ to recover the familiar exponential shielding over characteristic distanct λ_D.

However, the failure of textbook Debye shieldinging in single component plasmas has recently been shown both experimentally and theoretically. A striking example is the the experimental observation of antishielding [41]. Although it is possible to show that a plasma does not need to be Maxwellianized for shielding to occur [72] in collisionless one-dimensional pure electron plasmas shielding requires trapped electrons to occur [42]. In the case without trapped electrons a positive potential perturbation would cause electrons to accelerate towards the perturbation. Flux conservation then results in a decreased electron density causing the perturbation to be surrounded by a net positively charged plasma.

Furthermore, it is possible to solve equation 7.2 without making the $\frac{e\delta\Phi}{T_e} \ll 1$ assumption by using a composite solution [25]. The composite solution provides good agreement with simulation results while the classic textbook approach fails to reproduce the exact potential near the sheath.

An experimental study of shielding in CNT would provide a test of proposed theories for shielding in non-neutral 3 dimensional plasmas while offering a better understanding of experimental results. Previous experiments have shown perturbations from charged rods and biased boundary sectors penetrating deeper than expected by textbook Debye length predictions. This could be achieved by measuring the potential perturbation in the plasma due to biased plates outside the last closed flux surface. A probe designed

to measure the plasma potential with good two dimensional resolution could be used to find how much the curvature of the potential changes when the perturbation is applied. From these measurements that electron density could be found and conclusions could be drawn about shielding.

Bibliography

[1] M. Amoretti, C. Amsler, and G. Bonomi et al. Production and detection of cold antihydrogen atoms. *Nature*, 419(456), 2002.

[2] M. Amoretti, G. Bettega, F. Cavaliere, M. Cavenago, F. De Luca, R. Pozzoli, and M. Romé. Cylindrical penning trap for the study of electron plasmas. *Review of Scientific Instruments*, 74(9):3991–3997, 2003.

[3] M. Amoretti, G. Bonomi, A. Bouchta, P.D. Bowe, C. Carraro, C.L. Cesar, M. Charlton, M. Doser, A. Fontana, M.C. Fujiwara, R. Funakoshi, P. Genova, J.S. Hangst, R.S. Hayano, L.V. Jorgensen, V. Lagomarsino, R. Landua, E. Lodi Rizzini, M. Macri, N. Madsen, G. Manuzio, G. Testera, A. Variola, and D.P. van der Werf. Complete nondestructive diagnostic of nonneutral plasmas based on the detection of electrostatic modes. *Physics of Plasmas*, 10(8):3056–3064, 2003.

[4] F. Anderegg, E. M. Hollmann, and C. F. Driscoll. Rotating field confinement of pure electron plasmas using Trivelpiece-Gould modes. *Phys. Rev. Lett.*, 81(22):4875–4878, Nov 1998.

[5] K. Avinash. On toroidal equilibrium of non-neutral plasma. *Phys. Fluids B*, 3(12), 1991.

[6] John W Berkery and Allen H Boozer. The effect of the electric field on the confinement of electron plasmas on magnetic surfaces. *Phys. Plasmas*, 14(10):104503, 2007.

[7] J.W. Berkery, Q.R. Marksteiner, T. Sunn Pedersen, J.P. Kremer, and R.G. Lefrancois. Ion accumulation in a pure electron plasma confined on magnetic surfaces. *Physics of Plasmas*, 14:084505, 2007.

[8] J.W. Berkery, T. Sunn Pedersen, J.P. Kremer, Q.R. Marksteiner, R.G. Lefrancois, M.S. Hahn, and Paul Wesley Brenner. Confinement of pure electron plasmas in the Columbia Non-neutral Torus. *Physics of Plasmas*, 14(6), 2007.

[9] J.W. Berkery, T. Sunn Pedersen, and L. Sampedro. A retractable electron emitter for the creation of unperturbed pure electron plasmas. *Review of Scientific Instruments*, 78(1):013504, 2007.

[10] S.N. Bhattacharyya and K. Avinash. Equilibrium of non-neutral plasma in toroidal geometry with applied electric field. *Physics of Fluids B*, 4(7):1702–1707, 1992.

[11] Allen H. Boozer. What is a stellarator? *Physics of Plasmas*, 5(5):1647–1655, 1998.

[12] Allen H. Boozer. Physics of magnetically confined plasmas. *Rev. Mod. Phys.*, 76(4):1071–1141, Jan 2005.

[13] P. W. Brenner, T. S. Pedersen, X. Sarasola, and M. S. Hahn. Confinement studies in the Columbia Non-neutral Torus. *Contributions to Plasma Physics*, 50(6-7):678–682, 2010.

[14] P. W. Brenner, T. Sunn Pedersen, M. Hahn, J. W. Berkery, R. G. Lefrancois, and Q. R. Marksteiner. Studies of enhanced confinement in the Columbia Non-neutral Torus. In *NON-NEUTRAL PLASMA PHYSICS VII: Workshop on Non-Neutral Plasmas 2008*, volume 1114, pages 75–80. AIP, 2009.

[15] P.W. Brenner, T.S. Pedersen, J.W. Berkery, Q.R. Marksteiner, and M.S. Hahn. Magnetic surface visualizations in the Columbia Non-neutral Torus. *Plasma Science, IEEE Transactions on*, 36(4):1108–1109, Aug. 2008.

[16] Leon Brillouin. A theorem of larmor and its importance for electrons in magnetic fields. *Phys. Rev.*, 67(7-8):260–266, Apr 1945.

[17] O. Buneman. Instability, turbulence, and conductivity in current-carrying plasma. *Phys. Rev. Lett.*, 1(1):8–9, Jul 1958.

[18] P J Channell. Two-stream instability model with electrons trapped in quadrupoles. *Journal of Instrumentation*, 4(08):P08008, 2009.

[19] Francis F. Chen. *Introduction to Plasma Physics and Controlled Fusion*. Springer, New York, 2006.

[20] C. D. Child. Discharge from hot CaO. *Phys. Rev. (Series I)*, 32(5):492–511, May 1911.

[21] J. D. Daugherty, J. E. Eninger, and G. S. Janes. Experiments on the injection and containment of electron clouds in a toroidal apparatus. *Phys. Fluids*, 12(12):2677, 1969.

[22] R. C. Davidson. *Physics of Nonneutral Plasmas*. Imperial College Press and World Scientific Publishing, London, UK, Second edition, 2001.

[23] Benoit Durand de Gevigney. *Theoretical and Numerical Investigation of Transport in the Columbia Non-neutral Torus*. PhD thesis, Columbia University, 2010.

[24] Benoit Durand de Gevigney, Thomas Sunn Pedersen, and Allen H. Boozer. Numerical investigation of electron trajectories in the Columbia Non-neutral Torus. *Physics of Plasmas*, 16(12):122502, 2009.

[25] Benoit Durand de Gevigney, Thomas Sunn Pedersen, and Allen H. Boozer. Debye screening and injection of positrons across the magnetic surfaces of a pure electron plasma in a stellarator. *Physics of Plasmas*, 18(1):013508, 2011.

[26] A.G. Dikii, V.M. Zalkind, G.G. Lesnyakov, O.S. Pavlichenko, A.V. Pashchenko, V.K. Pashnev, D.P. Pogozhev, and V.M. Tonkopryad. New method for studying the vacuum magnetic configuration in a stellarator. *Soviet Journal of Plasma Physics*, 14(3):160–164, 1988.

[27] Daniel H. E. Dubin and T. M. O'Neil. Two-dimensional bounce-averaged collisional particle transport in a single species non-neutral plasma. *Physics of Plasmas*, 5(5):1305–1314, 1998.

[28] T. Estrada et al. Electron internal transport barrier formation and dynamics in the plasma core of the TJ-II stellarator. *Plasma Phys. Control. Fusion*, 46:277, 2004.

[29] G. Gabrielse, N. S. Bowden, and P. Oxley et al. Background-free observation of cold antihydrogen with field-ionization analysis of its states. *Phys. Rev. Lett.*, 89(21):213401, Oct 2002.

[30] A. A. Galeev, R. Z. Sagdeev, and G. P. Fewers. Plasma diffusion in a toroidal stellarator. *Journal of Applied Mechanics and Technical Physics*, 9:617–625, 1968. 10.1007/BF00912861.

[31] R.F. Gandy, M.A. Henderson, J.D. Hanson, G.J. Hartwell, and D.G. Swanson. Magnetic surface mapping with an emissive filament technique on the Auburn Torsatron. *Review of Scientific Instruments*, 58(4):509–515, 1987.

[32] G. C. Goldenbaum, W. F. Dove, K. A. Gerber, and B. G. Logan. Plasma heating by intense, relativistic electron beams. *Phys. Rev. Lett.*, 32(15):830–833, Apr 1974.

[33] R. J. Goldston and P H Rutherford. *Introduction to Plasma Physics*. Taylor and Francis Group, New York, 1995.

[34] R. G. Greaves and C. M. Surko. An electron-positron beam-plasma experiment. *Phys. Rev. Lett.*, 75(21):3846–3849, Nov 1995.

[35] R. G. Greaves and C. M. Surko. Antimatter plasmas and antihydrogen. In *The 38th annual meeting of the Division of Plasma Physics (DPP) of the American Physical Society*, volume 4, pages 1528–1543. AIP, 1997.

[36] R.G. Greaves, M.D. Tinkle, and C.M. Surko. Modes of a pure ion plasma at the brillouin limit. *Physical Review Letters*, 74(1):90–93, 1995.

[37] M. Hahn, T. Sunn Pedersen, P. W. Brenner, and Q Marksteinner. Confinement jumps in a non-neutral plasma. *Physics of Plasmas*, 16:022105, 2009.

[38] M. Hahn, T. Sunn Pedersen, Q. Marksteiner, and J. W. Berkery. Confirmation of a large density variation along the magnetic axis of the Columbia Non-neutral Torus. *Phys. Plasmas*, 15:020701, 2008.

[39] Michael Hahn. *Pure Electron Plasma Equilibrium and Transport Jumps in The Columbia Non-neutral Torus*. PhD thesis, Columbia University, 2009.

[40] Takateru Hamada, Tokuhiro Obiki, Tohru Mizuuchi, Fumimichi Sano, and Masahiko Nakasuga. A physical model of the beam impedance method within ideal nested magnetic surfaces. *Review of Scientific Instruments*, 71(5):2062–2067, 2000.

[41] C. Hansen and J. Fajans. Dynamic and Debye shielding and antishielding in magnetized, collisionless plasmas. *Phys. Rev. Lett.*, 74(21):4209–4212, May 1995.

[42] C. Hansen, A. B. Reimann, and J. Fajans. Dynamic and Debye shielding and antishielding. *Physics of Plasmas*, 3(5):1820–1826, 1996.

[43] H. Himura, H. Wakabayashi, M. Fukao, M. Isobe, S. Okamura, and H. Yamada. Production of helical non-neutral plasmas by collisionless electron penetration. *J. Plasma Fusion Res.*, 6:756, 2004.

[44] H. Himura, H. Wakabayashi, M. Fukao, and the CHS group. Experimental investigation of helical non-neutral plasmas. In *Non-neutral Plasma Physics V*, volume 692 of *AIP Conf. Proceedings*, page 293. AIP, New York, 2003.

[45] H. Himura, H. Wakabayashi, M. Fukao, Z. Yoshida, M. Isobe, S. Okamura, C. Suzuki, S. Nishimura, K.Matsuoka, K.Toi, and H. Yamada. Observation of collisionless inward propagation of electrons into helical vacuum magnetic surfaces via stochastic magnetic fields. *Phys. Plasmas*, 11(2):492, 2004.

[46] H. Himura, H. Wakabayashi, Y. Yamamoto, M. Isobe, S. Okamura, K. Matsuoka, A. Sanpei, and S. Masamune. Experimental verification of nonconstant potential and density on magnetic surfaces of helical nonneutral plasmas. *Phys. Plasmas*, 14:022507–1, 2007.

[47] Y. Itikawa. Cross sections for electron collisions with nitrogen molecules. *Journal of Physical and Chemical Reference Data*, 35(1):31–53, 2006.

[48] L. Jacquet and M. Tagger. Ion-electron two-stream instability in EBIS ion sources. *Nuclear Instruments and Methods in Physics Research Section A: Accelerators, Spectrometers, Detectors and Associated Equipment*, 369(1):1 – 10, 1996.

[49] R. Jaenicke, E. Ascasibar, P. Grigull, I. Lakicevic, A. Weller, M. Zippe, H. Hailer, and K. Schworer. Detailed investigation of the vacuum magnetic surfaces on the W7-AS stellarator. *Nuclear Fusion*, 33(5):687–704, 1993.

[50] A. A. Kabantsev and C. F. Driscoll. Trapped-particle modes and asymmetry-induced transport in single-species plasmas. *Phys. Rev. Lett.*, 89(24):245001, Nov 2002.

[51] A. A. Kabantsev, J. H. Yu, R. B. Lynch, and C. F. Driscoll. Trapped particles and asymmetry-induced transport. *Physics of Plasmas*, 10(5):1628–1635, 2003.

[52] S.S. Khirwadkar, P.I. John, K. Avinash, A.K. Agarwal, and P.K. Kaw. Steady state formation of a toroidal electron cloud. *Physical Review Letters*, 71(26):4334–4337, 1993.

[53] Jin Joong Kim and Nackchin Sung. Stimulated emission in optically pumped atomic-copper vapor. *Opt. Lett.*, 12(11):885–887, Nov 1987.

[54] Jason P. Kremer, T. Sunn Pedersen, Quinn R. Marksteiner, and Remi G. Lefrancois. Diagnosing pure-electron plasmas with internal particle flux probes. *Review of Scientific Instruments*, 78(1):013503, 2006.

[55] J.P. Kremer. *The Creation and First Studies of Electron Plasmas in the Columbia Non-neutral Torus*. PhD thesis, Columbia University, 2006.

[56] J.P. Kremer, T. Sunn Pedersen, Q. Marksteiner, and R.G. Lefrancois. Experimental confirmation of stable, small Debye length pure electron plasma equilibria in a stellarator. *Physical Review Letters*, 97, 2006.

[57] Irving Langmuir. The effect of space charge and initial velocities on the potential distribution and thermionic current between parallel plane electrodes. *Phys. Rev.*, 21(4):419–435, Apr 1923.

[58] Remi G. Lefrancois, Thomas Sunn Pedersen, Allen H. Boozer, and Jason P. Kremer. Numerical investigation of three-dimensional single-species plasma equilibria on magnetic surfaces. *Physics of Plasmas*, 12(7):072105, 2005.

[59] Remi Guy Lefrancois. *The Equilibrium of Electron Plasmas Confined on Magnetic Surfaces*. PhD thesis, Columbia University, 2007.

[60] G.G. Lesnyakov and E.D. Volkov. Toroidal stellarator diode: Discharge features and electron transport. *Plasma Devices and Operations*, 14(2):111–136, 2006.

[61] G.G. Lesnyakov, E.D. Volkov, A.V. Georgievskij, V.M. Zalkind, Yu.K. Kuznetsov, F.I. Ozherel'ev, O.S. Pavlichenko, D.P. Pogozhev, K. Schworer, and H. Hailer. Study of the magnetic configuration of an l=3 torsatron by the triode and the luminescent rod methods. *Nuclear Fusion*, 32(12):2157, 1992.

[62] Morton A. Levine, R.E. Marrs, and Robert W. Schmieder. Measurement of instabilities and ion heating in an electron beam ion source. *Nuclear Instruments and Methods in Physics Research Section A: Accelerators, Spectrometers, Detectors and Associated Equipment*, 237(3):429 – 440, 1985.

[63] H. Lin, R.F. Gandy, S.F. Knowlton, G.J. Hartwell, D. Prichard, G. Sassar, and E. Thomas. Electron transport studies in stochastic magnetic fields on the Compact Auburn Torsatron. *Physics of Plasmas*, 2(6):2026–2032, 1995.

[64] R. V. E. Lovelace, K. P. Jore, and M. P. Haynes. Two-stream instability of counterrotating galaxies. *The Astrophysical Journal*, 475(1):83, 1997.

[65] J. H. Malmberg and J. S. deGrassie. Properties of nonneutral plasmas. *Phys. Rev. Lett.*, 35:577–580, 1975.

[66] J. H. Malmberg and C. F. Driscoll. Long-time containment of a pure electron plasma. *Phys. Rev. Lett.*, 44(10):654–657, Mar 1980.

[67] Q.R. Marksteiner, T. Sunn Pedersen, J.W. Berkery, M.S. Hahn, J.M. Mendez, B. Durand de Gevigney, and H. Himura. Observations of an ion driven instability in non-

neutral plasmas confined on magnetic surfaces. *Physical Review Letters*, 100(6):065002, 2008.

[68] Quinn Robert Marksteiner. *Studies of Non-neutral Ion Electron Plasmas Confined on Magnetic Surfaces*. PhD thesis, Columbia University, 2008.

[69] J. P. Marler and M. R. Stoneking. Confinement time exceeding one second for a toroidal electron plasma. *Phys. Rev. Lett.*, 100:155001, 2008.

[70] Xabier Sarasola Martin. *Plasmas of arbitrary neutrality*. PhD thesis, Columbia University, 2011.

[71] H. Matsuura, A. Okitsu, and M. Numano. Modeling of the mapping experiments based on the diffusion process. *Journal of the Physical Society of Japan*, 65(10):3215–3219, 1996.

[72] Nicole Meyer-Vernet. Aspects of Debye shielding. *American Journal of Physics*, 61(3):249–257, 1993.

[73] A. Mohri, H. Higaki, H. Tanaka, Y. Yamazawa, M. Aoyagi, T. Yuyama, and T. Michishita. Confinement of nonneutral spheroidal plasmas in multi-ring electrode traps. *Japanese Journal of Applied Physics*, 37(1):664–6701, 1998.

[74] A. Mohri, T. Yuyama, Y. Kiwamoto, Y. Yamazawa, and T. Michishita. Confinement of nonneutral plasmas in a trap composed of a cusped magnetic field and an electrostatic octopole field. *Japanese Journal of Applied Physics*, 37(12B):1553–1555, 1998.

[75] K.A. Morrison, S.F. Paul, and R.C. Davidson. Electron plasma expansion rate studies on the Electron Diffusion Gauge experimental device. *Physics of Plasmas*, 12:072310, 2005.

[76] Eiji Nakamura, Sumio Kitajima, Masakazu Takayama, Shigeru Inagaki, Takeo Yoshida, and Hiroshige Watanabe. Particle transport study with an electron beam in the Tohoku University Heliac. *Japanese Journal of Applied Physics*, 36(Part 1, No. 2):889–895, 1997.

[77] T. M. O'Neil. A confinement theorem for nonneutral plasmas. *Phys. Fluids*, 23:2217, 1980.

[78] T. M. O'Neil and C. F. Driscoll. Transport to thermal equilibrium of a pure electron plasma. *Phys. Rev. Lett.*, 22:266, 1979.

[79] T. S. Pedersen. *New Developments in Nuclear Fusion Research.* Nova Science, New York, 2005.

[80] T. Sunn Pedersen and A.H. Boozer. Confinement of noneutral plasmas on magnetic surfaces. *Physical Review Letters*, 88(20):205002, 2002.

[81] T. Sunn Pedersen, A.H. Boozer, W Dorland, J.P. Kremer, and R. Schmitt. Prospects for the creation of positron-electron plasmas in a non-neutral stellarator. *Journal of Physics B*, 36:1029–1039, 2003.

[82] T. Sunn Pedersen, A.H. Boozer, J.P. Kremer, R.G. Lefrancois, W.T. Reiersen, F. Dahlgreen, and N. Pomphrey. The Columbia Nonneutral Torus: A new experiment to confine nonneutral and positron-electron plasmas in a stellarator. *Fusion Science and Technology*, 46:200–208, 2004.

[83] T. Sunn Pedersen, J.P. Kremer, R.G. Lefrancois, Q. Marksteiner, N. Pomphrey, W.T. Reiersen, F. Dahlgreen, and X. Sarasola. Construction and initial operation of the Columbia Nonneutral Torus. *Fusion Science and Technology*, 50:372–381, 2006.

[84] T. Sunn Pedersen, J.P. Kremer, R.G. Lefrancois, Q. Marksteiner, X. Sarasola, and N. Ahmad. Experimental demonstration of a compact stellarator magnetic trap using four circular coils. *Physics of Plasmas*, 13:012502, 2006.

[85] B. B. Robinson and G. A. Swartz. Two stream instability in semiconductor plasmas. *Journal of Applied Physics*, 38(6):2461 –2465, May 1967.

[86] H. Saitoh, Z. Yoshida, C. Nakashima, H. Himura, J. Morikawa, and M. Fukao. Confinement of pure-electron plasmas in a toroidal magnetic-surface configuration. *Physical Review Letters*, 92(25):255005, 2004.

[87] H. Saitoh, Z. Yoshida, and S. Watanabe. Stable confinement of toroidal electron plasmas in an internal conductor device Prototype-Ring Trap. *Phys. Plasmas*, 12:092102, 2005.

[88] Haruhiko Saitoh, Zensho Yoshida, Junji Morikawa, Sho Watanabe, Yoshihisa Yano, and Junko Suzuki. Long-lived pure electron plasma in Ring Trap-1. *Plasma and Fusion Research*, 2:045–045, 2007.

[89] X. Sarasola, T. S. Pedersen, P. W. Brenner, and M. S. Hahn. First observations of partially neutralized and quasineutral plasmas in the Columbia Non-neutral Torus. *Contributions to Plasma Physics*, 50(6-7):673–677, 2010.

[90] M.G. Shats, D.L. Rudakov, B.D. Blackwell, L.E. Sharp, R. Tumlos, S.M. Hamberger, and O.I. Fedyanin. Experimental investigation of the magnetic structure in the H-1 heliac. *Nuclear Fusion*, 34(12):1653, 1994.

[91] L Spitzer. The Stellarator Concept. *Physics of Fluids*, 1(4):253–264, 1958.

[92] M. R. Stoneking, P. W. Fontana, R. L. Sampson, and D. J. Thuecks. Electron plasmas in a "partial" torus. *Phys. Plasmas*, 9(3):766, 2002.

[93] M.R. Stoneking, M.A. Growdon, M.L. Milne, and R.T. Peterson. Poloidal e x b drift used as an effective rotational transform to achieve long confinement times in a toroidal electron plasma. *Physical Review Letters*, 92(9), 2004.

[94] Ryukichi Takahashi, Osamu Motojima, Tokuhiro Obiki, Masahiko Nakasuga, Tooru Mizuuchi, and Atuo Iiyoshi. An experimental study of the vacuum magnetic surfaces of Heliotron E. *Japanese Journal of Applied Physics*, 28(Part 1, No. 12):2604–2609, 1989.

[95] L. E. Thode and R. N. Sudan. Two-stream instability heating of plasmas by relativistic electron beams. *Phys. Rev. Lett.*, 30(16):732–735, Apr 1973.

[96] Bruce T. Tsurutani and Gurbax S. Lakhina. Some basic concepts of wave-particle interactions in collisionless plasmas. *Rev. Geophys.*, 35(1):491–501, Jul 1997.

[97] Kōji Uo. The confinement of plasma by the heliotron magnetic field. *Journal of the Physical Society of Japan*, 16(7):1380–1395, 1961.

[98] Z. Yoshida et al. Toroidal magnetic confinement of non-neutral plasmas. In *Non-Neutral Plasma Physics III*, volume 498 of *AIP Conf. Proceedings*, page 397. AIP, New York, 1999.

[99] Puravi Zaveri, P. I. John, K. Avinash, and P. K. Kaw. Low-aspect-ratio toroidal equilibria of electron clouds. *Phys. Rev. Lett.*, 68(22):3295, 1992.